Surfactant Mediated Acid-Base Particle Charging in Apolar Media

Matthew Gacek

A dissertation submitted in partial fulfillment

of the requirements for the degree of

Doctor of Philosophy

University of Washington

2015

Reading Committee:

John C. Berg, Chair

Rene M Overney

Brian Hayes

Program Authorized to Offer Degree:

Department of Chemical Engineering

University of Washington

Abstract

Surfactant Mediated Acid-Base Particle Charging in Apolar Media

Matthew Gacek

Chair of the Supervisory Committee:

Professor John C. Berg

Department of Chemical Engineering

The creation and stabilization of electric charge in apolar environments (dielectric constant ≈ 2) has been an area of interest dating back to when an explanation was sought for the occurrence of what are now known as electrokinetic explosions during the pumping of fuels. More recently attention has focused on the charging of suspended particles in such media, underlying such applications as electrophoretic displays (e.g., the Amazon Kindle® reader) and new printing devices (e.g., the HP Indigo® Digital Press). The endeavor has been challenging owing to the complexity of the systems involved and the large number of factors that appear to be important. A number of different, and sometimes conflicting, theories for particle surface charging have been advanced, but most observations obtained in the authors' laboratory, as well as others, appear to be explainable in terms of an acid-base mechanism. Adducts formed between chemical functional groups on the particle surface and monomers of reverse micelle-forming surfactants dissociate, leaving charged groups on the surface, while the counter-charges formed are sequestered in the reverse micelles. For a series of mineral oxides in a given medium with a given surfactant, surface charging (as quantified by the maximum electrophoretic mobility or zeta potential obtained as surfactant concentration is varied) was found to scale linearly with the

aqueous PZC (or IEP) values of the oxides. Different surfactants, with the same oxide series, yielded similar behavior, but with different PZC crossover points between negative and positive particle charging, and different slopes of charge vs. PZC. Thus the oxide series could be used as a yardstick to characterize the acid-base properties of the surfactants. This has led directly to the study of other materials, including surface-modified oxides, carbon blacks, pigments (charge transfer complexes), and polymer latices. This dissertation focuses on the acid-base mechanism of particle charging in the context of the many other factors that are important to the phenomenon, including the presence of water, of other components (e.g., synergists, contaminants, etc.), and of electric field effects. The goal is the construction of a road map describing the anticipated particle charging behavior in a wide variety of systems, assisting in the choice or development of materials for specific applications.

Table of Contents

List of Figures

List of Tables

Acknowledgements

The first and most important person that needs to be thanked is Professor John C. Berg. I cannot express how much his guidance and mentorship has had an impact on my life. Thank you.

Secondly, I want to thank all of the other researchers, undergraduate and graduate, that have helped me conduct these experiments. Specifically, Dr. Saran Poovarodom's research and guidance was a tremendous help to me when I was first getting started. Galen Brooks was instrumental in conducting the initial mineral oxide charging series. David Bergsman helped me conduct the water content study and surface treating silica particles. Max Kaganyuk was a great help in characterizing the charging behavior of carbon black. I also want to thank Ed Michor, whose parallel work on reverse micelle charging provided insight into some of the intricacies of particle charging in apolar media. In addition, I want thank Kyle Caldwell and Dr. Prasad Bhosale for their helpful discussions and feedback.

Lastly, I would like to thank the Xerox Corporation for partially funding this work, and for providing me with an internship. This research was also funded by the University of Washington Center for Surfaces, Polymers, and Colloids.

Dedication

To my lovely wife, Courtney, and our faithful pup, Sancho.

Chapter 1

Overview of acid-base charging in apolar media

1.1. Introduction

There are a number of key factors that must be accounted for in the study of particle charging in apolar media, but none as important as the mechanism by which particles obtain charge. Identifying and understanding the nature of particle charging in these systems has been of central focus in this area of study for decades and it appears that a unifying mechanism has emerged: that of acid-base interactions. It appears that, for most systems, the magnitude and polarity of charge is dependent on the relative acid-base properties of the surfactant and the particle surface, the "hard" or "soft" nature of the surfactant head group, and the ability for the surfactant to stabilize charges in reverse micelles. Exploring the recent research in this area and the validity of the acid-base mechanism is the main focus of the current work.

The study of charge generation in nonpolar systems has remained an active area of interest over 100 years after it was initially investigated [1–3]. Interest in the subject was sporadic until the 1950s as the control of conductivity became important for preventing electrokinetic explosions in the petroleum industry [4]. Over time, the idea of generating and manipulating charge on particle surfaces has been applied to a number of different applications [5], particularly as it applies to electrostatic particle stabilization in media of low dielectric constant [6–12]. Some specific applications include the stabilization of carbon particles in motor oil [13–16], stabilization of pigment in paints and inks [5], electrophoretic displays [17–20], and full color "digital press" electronic lithographic printers (http://www8.hp.com/us/en/commercial-

printers/indigo-presses/overview.html). For many applications it is desirable for the medium to be insulating, limiting power consumption and providing long battery life in many of the e-reader devices available today. Such applications have helped drive research to better understand the phenomena of stabilizing charge in apolar (dielectric constant of approximately 2 or lower) fluids.

The generation of stable charge in apolar systems is less probable than in aqueous systems due to the low dielectric constant of the medium. A simplistic energetic explanation of this is the Bjerrum length (λ_B) which is defined as the ratio of the force of coulombic attraction to the thermal energy in the system:

$$\lambda_B = e^2/4\pi\varepsilon\varepsilon_0 k_B T \tag{1.1}$$

where e is the elementary charge, ε is the dielectric constant of the medium, ε_0 is the permittivity of free space, k_B is the Boltsmann constant, and T is the absolute temperature. In essence, λ_B characterizes the effective distance of separation needed for charges to be stable. In room temperature water λ_B is only about 0.7 nm. This is of the order of the size of a hydration sheath of water molecules, allowing most ions to freely dissociate. In an apolar environment of a dielectric constant of 2.0 the Bjerrum length is of the order of 28 nm, preventing free dissociation of most ions. Some level of spontaneous dissociation can be achieved for very large organic ions [21]. More commonly, charge stabilization is achieved through the addition of surfactants that form reverse micelles or similar aggregates. A reverse micelle has a polar core of large dielectric surrounded by a shell of the hydrophobic surfactant tail groups. The high dielectric core is a region that is more energetically favorable to house charge. An interesting aspect of reverse micelles is that the critical micelle concentration (CMC) does not appear always to be a distinct

concentration as it is in aqueous systems [22,23]. There may be surfactant doublets, triplets, and "pre-micellar" aggregates that form near the CMC [24], and it has been suggested that the presence of some water may be required for reverse micelles to form at all [25–27]. Reverse micelles are believed to be capable of acquiring charge through the process of disproportionation, where two neutral micelles collide and exchange charge to yield a positively charged micelle and a negatively charged micelle, as opposed to a single micelle expelling an ion via dissociation [5,28–32]. The reason for this is that it is more energetically favorable for both the positive and negative ion to be housed in a reverse micelle as opposed to one bare ion being in the apolar medium. The charging of reverse micelles has been studied extensively using transient current measurements [32–37]. In addition, there is some evidence that near the CMC pre-micellar aggregates may engage in some amount of dissociation as the concentration of micelles is not large enough to engage in disproportionation. This is demonstrated by conductivity measurements of solutions of dioctyl sodium sulfosuccinate, more commonly known as Aerosol OT (AOT), in hexadecane as shown in Figure 1.1 [31].

The presence of reverse micelles is also generally believed to be necessary to stabilize charge on particle surfaces in apolar media. It is assumed that the system is net neutral in charge. Therefore, when a particle surface acquires charge, the counter charge must be stabilized elsewhere (presumably in reverse micelles). This is repeatedly demonstrated in the literature in that particles have little to no charge below the detected surfactant CMC and suddenly begin to charge once that concentration is reached [6,38–40]. As research has progressed, there have been a number of mechanisms put forth and debated at length in the literature. Many of these mechanisms appear to be highly system dependent, making it difficult to apply them to apolar systems in any general way. The proposed mechanisms include but are not limited to the

adsorption of bare ions produced from micelle dissociation [40,41], ionization of groups on the particle surface [8,42,43], preferential adsorption of charged micelles or hemi-micelles [41,44–47], and acid-base charge transfer [14,15,39,48–50].

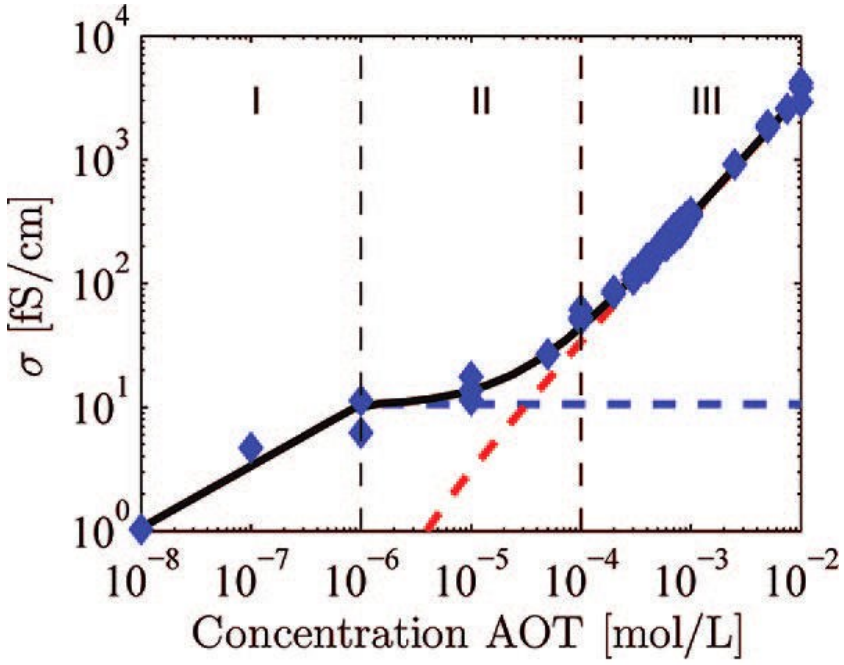

Figure 1.1. Conductivity of AOT/hexadecane solutions without particles. Symbols indicate measurements. Red dashed line indicates reverse micelle contribution to conductivity. Reprinted with permission from [Sainis, S.K.; Merrill, J.W.; Dufresne, E.R.; Langmuir 2008, 24, 13334–13337]. Copyright [2008] American Chemical Society.

In recent years there has been growing evidence to support the theory of acid-base charge transfer being the dominant mechanism for a variety of apolar systems. The acid-base mechanism, originally put forth by Fowkes [14,15,48], proposes that the polarity and magnitude of charge is strongly dictated by the relative acidity or basicity of both the surfactant and the particle surface functionality. This theory has been shown to be applicable for a number of different types of surfactants as well as a wide variety of particles, as discussed in more detail in Section 1.3. It has previously been established for non-aqueous systems of intermediate dielectric

constant, otherwise known as “leaky” dielectric fluids, that acid-base properties play an important role in determining the polarity and magnitude of charge [51–57], but the scope of this review is confined to apolar systems of low dielectric constant, where reverse micelles are necessary to stabilize charge. One of the main challenges of validating the acid-base charging mechanism is first identifying and characterizing the acid-base properties of both the surfactant molecules and the particle surfaces, and some of the common techniques used are summarized in Section 1.2.

Studying the behavior of charge generation and stabilization in these systems is difficult due to the inherent complexity of such systems, even in an ideal laboratory setting. There are a number of key variables that need to be taken into consideration at all times. One of the most commonly identified variables is surfactant concentration. As previously mentioned, a certain concentration of surfactant is required to form reverse micelles, above which particles will obtain charge. However, it is also commonly observed that once the surfactant concentration reaches a certain point, the particle charge decreases with increasing surfactant [31,38–40,58–60]. It is believed that this occurs due to charge screening or neutralization cause by charged reverse micelles [29,31,61,62]. At large surfactant concentrations, more charge is generated in the bulk solution due to micelle-micelle charging, increasing this effect. The size of the polar cores of the reverse micelles and the amount of trace water in the system, to which it contributes, are also significant factors for both micelle and particle charging (discussed further in Sections 1.4 and 1.5). Another important factor that is often overlooked is the effect of the applied electric field used during particle electrophoretic mobility measurements. It has been repeatedly shown that a significant amount of charge can be induced on particles in the presence of a strong electric field [49,61–65], and is a recurring issue in electrophoretic mobility studies. These effects appear to

be particularly strong near the surfactant CMC. To account for this, measurements should be conducted at several different applied electric field strengths, and the electrophoretic mobility should be extrapolated back to zero applied field strength to ascertain the inherent particle surface charge. One must be aware of this when considering the results of any study that does not account for these effects. Because of the complexity of these systems, it is the purpose of this review to explore in detail some of the major factors that affect particle charging in apolar media. The goal is to shed some light on what is currently understood about these systems so that more targeted and refined studies may be conducted in this fascinating area of research.

1.2. Characterizing acid and base properties for fluids and solids

Before one can analyze the validity of an acid-base charging mechanism for particles dispersed in apolar media it is important to review how acids and bases are defined and characterized. There have been a number of other reviews that have focused solely on this topic [66,67], and those ideas will be summarized in this section. Of particular interest is the issue of applying the characterization of acids and bases to apolar systems, since acid-base interactions are traditionally defined in the context of aqueous systems. An example of this is the classic interpretation of acids and bases that was put forth by Arrhenius in 1887 [68]. In his definition acids are identified as anything that increases the hydronium ion concentration, and bases are anything that increases the hydroxyl ion concentration of the solution. In this definition, an acid-base reaction was one that yielded a salt and water upon neutralization of the acid and base as shown in equation (1.2).

$$HCl\ (acid) + NaOH\ (base) \rightarrow NaCl\ (salt) + H_2O \qquad (1.2)$$

1.2.1. Brønsted-Lowry and Lewis acid-base theories

While the Arrhenius theory was a significant first step toward modern acid-base theory, it was limited by the fact that acids and bases are defined by their relationship with water. In 1923 this definition was independently broadened by Brønsted [69] and Lowry [70]. An acid was something that could act as a proton donor and a base was a proton acceptor. While this definition retained the idea that a proton is transferred during an acid-base reaction, water was no longer required to take part in the reaction. Since a proton cannot exist on its own, there must be a base present to accept the proton. When this happens, the acid that donates a proton becomes a conjugate base of the acid, and a base that accepts a proton becomes a conjugate acid of the base. This is depicted in the reversible reaction in equation (1.3).

$$HA\ (acid) + B\ (base) \rightleftharpoons A^{-}\ (conjugate\ base) + HB^{+}\ (conjugate\ acid) \qquad (1.3)$$

An important aspect of the Brønsted-Lowry theory is that most all substances have the capability of being both acidic and basic. Defining something as an acid or a base becomes a matter of the relative acidity or basicity of a substance. Therefore, one can rank the acidic strength of a series of materials relative to a common base or the basicity of materials relative to a common acid. This theory can also be applied to functional groups on a solid surface.

A more comprehensive definition for acids and bases was put forth at the same time by Lewis [71]. This definition removes the restriction of acid-base reactions requiring the transfer of a proton to encapsulate a broader understanding of possible interactions. A Lewis base is defined as a substance that can donate an electron pair, whereas a Lewis acid is something that can accept an electron pair [72]. Therefore, an acid-base reaction results in the formation of a dative

bond between the acid and base, where the electrons are furnished solely by the base, and such a formation is referred to as an acid base adduct as shown in equation (1.4).

$$A + B \rightleftharpoons A{:}\,B \tag{1.4}$$

In addition, acid-base adducts can undergo displacement reactions. These occur when the acid-base components of an adduct are transferred between different species in a solution as shown in equation (1.5).

$$A{:}\,B + A'{:}\,B' \rightleftharpoons A'{:}\,B + A{:}\,B' \tag{1.5}$$

It is important to note that equation (1.5) takes the same form as the Brønsted-Lowry acid-base reaction depicted in equation (1.3). The implication is that Brønsted-Lowry acids can be Lewis adducts with the acidic portion being H^+. In addition, all Brønsted-Lowry bases are also Lewis bases. Therefore, the Lewis definition of acid-base reaction is more universally applicable, but in aqueous solutions the Brønsted-Lowry description is usually a more convenient approach.

1.2.2. Characterizing and ranking acids and bases

A common aspect of Brønsted-Lowry theory as well as Lewis acid-base theory is that while molecules can be inert (neither acidic nor basic) or monofunctional acids or bases, most materials are at least somewhat bifunctional or amphoteric, in that they can act as both acids and bases. How a molecule or functional group is classified depends on whether it is a stronger acid or a base. This can often be difficult to determine simply by looking at the molecular structure. Therefore, a number of analytical tests have been employed to create ranking systems for both acidity and basicity, some of which are detailed below.

1.2.2.1. Acid dissociation constant (K_A)

The strength of a Brønsted-Lowry acid or base can be described by the acid dissociation constant (K_A) and base dissociation constant (K_B), respectively. These terms describe the tendency for an acid to donate a proton or a conjugate base to accept a proton. In theory, this can be done regardless of solvent effects by the following equations [67]:

$$K_A = \frac{[A^-]a_H}{[HA]} \tag{1.6}$$

$$K_B = \frac{[HA]}{[A^-]a_H} \tag{1.7}$$

where a_H is the activity of the proton species, $[HA]$ is the concentration of the acid, and $[A^-]$ is the concentration of the conjugate base. Therefore, a strong acid has a weak conjugate base and a weak acid has a strong conjugate base. There are a few practical challenges to determining these values. The first is that K_A and K_B cannot be measured directly because an acid cannot act as a proton donor without the presence of a base to receive it. This means that the acidity of a substance can only be measured with reference to a base by measuring the equilibrium constant (K) of the acid-base reaction depicted in equation (1.3).

$$K = \frac{[A^-][HB^+]}{[HA][B]} = K_{A1}K_{B2} \tag{1.8}$$

This means that comparing the K values of a series of acids with the same reference base (typically water) gives a ranking of the acidity that should be independent of the solvent. Bases may be similarly ranked in reference to a common acid (also typically water). The second obstacle that must be overcome is that the activity of the different species is not dependent on just the concentration, but also the activity coefficient. To account for this, most dissociation

constants are determined in a solution of high ionic strength, where the product of the activity coefficients is assumed to be constant [73]. Overall, the acid dissociation constant represents a convenient and effective means for ranking acidity and basicity for substances that exhibit Brønsted-Lowry type acid-base interactions and are soluble in aqueous solutions.

A common industrial technique used to represent acid-base properties of petroleum products, especially surfactants, is the "acid number" (ASTM D664) [74] and "base number" (ASTM D2896) [75]. The acid number is defined as the number of milligrams of KOH needed to neutralize 1 gram of an acid of interest. The base number is defined as the equivalent basicity of 1 gram of a base of interest defined in terms of the number of milligrams of KOH. There are several different techniques that are used to determine these values, but the most common is potentiometric titration. The acid number is usually obtained through titration of potassium hydroxide in solution with propane-2-ol, and the base number is determined by the titration of perchloric acid.

1.2.2.2. Gutmann donor / acceptor number

Determining the relative strength of Lewis acids and bases requires a different approach than what is used for Brønsted-Lowry acids and bases discussed above. A method of characterizing and ranking Lewis acids and bases was first developed by Gutmann et al. [76,77] and later added to by Fowkes [48]. Gutmann introduced the donor number (*DN*) for quantifying the strength of Lewis bases. It was defined as the molar exothermic heat of reaction with 10^{-3} M antimony pentachloride ($SbCl_5$), a very strong acid, in a neutral solvent (1,2-dichlorothane) [67].

$$DN_B = -\Delta H(SbCl_5 : B) \tag{1.9}$$

Later, the acceptor number (*AN*) was introduced by Gutmann and coworkers, and is defined as the relative ^{31}P NMR downfield shift ($\Delta\delta$) induced in triethyl phosphine when dissolved in the acid of interest. For reference, the neutral solvent hexane was assigned an acceptor number of 0, and $SbCl_5$ was assigned a value of 100. Later, this characterization technique was refined by Riddle and Fowkes [48] when they indicated that the ^{31}P NMR spectrum shift is affected by van der Waals interactions. This would significantly alter a number of the previously reported *AN* values. As an adjustment, the Lifshitz-van der Waals (LW) shift was subtracted from the total shift to yield the acid-base contribution. Riddle and Fowkes showed that the Lifshitz-van der Waals contribution to the spectrum shift ($\Delta\delta^{LW}$) can be correlated to the LW contribution to the liquid surface tension (σ^{LW}) by the following equation

$$\Delta\delta^{LW} = \delta_0 + 7.37 - 0.312\sigma^{LW} \tag{1.10}$$

where δ_0 is ^{31}P NMR peak position for $(C_2H_5)_3PO$ (referenced to diphenylphosphinic chloride, extrapolated to zero concentration, and corrected for volume susceptibility vs n-hexane), as tabulated by Gutmann [78], and σ^{LW} is in units of mJ/m^2. This adjustment greatly enhances the agreement between the *AN* and the expected enthalpy of interaction with a base of known *DN*. This single-parameter ranking of acidity or basicity is convenient in its simplicity and relationship to fundamental system properties. In addition, the *AN* and *DN* allow for materials to be classified as bifunctional acids and bases. However, it does overlook some aspects of Lewis acid-base interactions that are accounted for in Section 1.2.2.3.

1.2.2.3. Drago E and C parameters

Another method for determining the relative strength of Lewis acids was proposed by Drago and Wayland [79]. As the Lewis acid-base interaction is defined by adduct formation, it is

more appropriate to determine the exothermic molar heat of reaction of forming an adduct ($-\Delta H^{AB}$) of the type depicted in equation (1.4). An interesting complication was revealed by the work of Pearson on the "hard and soft" acid-base (HSAB) principle [80] which followed from work done by Mulliken [81] and Edwards [82]. Pearsons suggested that the energy of interaction between Lewis acids and bases is twofold: electrostatic (hard) and covalent (soft). A "hard" acid or base is one that has a small size, low polarizability, high oxidation state, and high positive charge density at the acceptor site (acids) or high negative charge density at the donor site (bases). Conversely, a "soft" acid or base is one that has a large size, high polarizability, low oxidation state, and low charge density at the acceptor (acid) or donor (base) site. Drago and Wayland translated this idea to predicting the enthalpy of acid-base adduct formation in organic liquids:

$$-\Delta H^{AB} = E_A E_B + C_A C_B \tag{1.11}$$

where E_A and E_B represents the "hard" or electrostatic contribution, and C_A and C_B represent the "soft" or covalent contribution to the heat of adduct formation. As equation (1.11) shows, the strongest acid-base interactions will occur when a hard acid interacts with a hard base or when a soft acid interacts with a soft base. Drago *E* and *C* parameters have been compiled for a large number of molecules using calorimetry and other measurements, and they have proven to be a fairly effective predictive tool for Lewis acid-base interactions. The major downside of this classification is that, unlike the *AN* and *DN*, it assumes all materials are either monotonic acids or monotonic bases. To account for this would require two sets of *E* and *C* parameters for each substance (one for acidic properties and one for basic properties).

1.2.3. Acid-base characterizations for solid surfaces

Analyzing the charging behavior of particles requires one to be able to characterize the acid-base properties of a solid surface, typically in contact with a fluid. This is more complicated than it sounds at first glance as a surface is almost always populated by a diverse collection of exposed functional groups. For example, even something as simple as a mineral oxide can be composed of surface oxygen groups with a wide variety of functionality. The following discussion demonstrates the difficulty of finding a reliable set of parameters for describing how a solid surface will interact with a liquid in the context of acidity and basicity.

1.2.3.1. van Oss-Chaudhury-Good correlation

The van Oss-Chaudhury-Good (vOCG) correlation uses the contact angle of several probe liquids to determine the acidity and basicity of the surface. The ability to do this stems from the extension of the geometric combining rule used for short-range interfacial forces put forth by van Oss et al. [83] which allows one to express the acid-base component of the surface tension as

$$\sigma^{AB} = 2\sqrt{\sigma^{+}\sigma^{-}} \tag{1.12}$$

where σ^{+} and σ^{-} are the characteristic acid and base parameters of the material, either solid or liquid. From this, one can express the interfacial tension as

$$\sigma_{12} = \sigma_1 + \sigma_2 - 2\sqrt{\sigma_1^{LW}\sigma_2^{LW}} - 2\sqrt{\sigma_1^{+}\sigma_2^{-}} - 2\sqrt{\sigma_1^{-}\sigma_2^{+}}. \tag{1.13}$$

If applied to a probe liquid in contact with a solid surface of interest, one can combine equation (1.13) with Young's equation:

$$cos\theta = (\sigma_S - \sigma_{SL})/\sigma_L \tag{1.14}$$

where σ_S is the solid surface energy, σ_L is the liquid surface tension, and σ_{SL} is the solid-liquid interfacial tension. The resulting relationship takes the following form

$$\sigma_L(1 + cos\theta) = 2\sqrt{\sigma_S^{LW}\sigma_L^{LW}} + 2\sqrt{\sigma_S^{+}\sigma_L^{-}} + 2\sqrt{\sigma_S^{-}\sigma_L^{+}}. \tag{1.15}$$

Using equation (1.15), one can determine the vOCG acid and base parameters of a solid (σ_S^+ and σ_S^-) by measuring the contact angle of two separate probe liquids of known surface tension and known σ_L^+ and σ_L^-. The LW component of the solid surface can be determined using an inert probe liquid. The main difficulty in implementing this technique is determining the σ_L^+ and σ_L^- of the probe liquids. This problem was addressed by van Oss and coworkers by using water as the first probe liquid, which is known to have a surface tension of 72.8 mN/m (σ^{LW} = 21.8 mN/m and σ^{AB} = 51.0 mN/m at 20 ^{o}C). They then assumed that the acid and base vOCG parameters of water were equal to one another, and this allowed them to solve equation (1.13) to yield a value of 25.5 mN/m for both σ_W^+ and σ_W^-. Once the first probe liquid was fully defined, van Oss and coworkers used a series of presumed monofunctional solids to determine the vOCG parameters of several other reference liquids (glycerol, formamide, and dimethyl sulfoxide).

With these probe liquids characterized it is now, in principle, possible to determine the σ_S^+ and σ_S^- parameters for any solid surface of interest, provided the probe liquids do not wet out the solid. The vOCG correlation is widely used due to the simplicity of the technique, and because it captures the bifunctional nature of the solids. However, it should be noted that these parameters do not take into account any “hard” or “soft” acid-base effects that may take place between the solid and liquid. In addition, the validity of this technique has not been fully justified, as there are a couple of key assumptions that may or may not be valid. The first of

which is that the extension of the geometric mixing rule to acid-base interactions has no theoretical foundation. Secondly, the assumption that $\sigma_W^+ = \sigma_W^-$ is made with no obvious justification. It is observed that almost all solid surfaces appear to be dominantly basic according to the vOCG correlation. In addition, the vOCG parameters for solids cannot be compared to any other thermodynamic parameters such as the Drago or Gutmann parameters as there is no fundamental relationship between these values. Lastly, there appears to be some internal inconsistency with the vOCG model, as demonstrated by Kwok [84]. Kwok tested the model by calculating σ^{LW}, σ^+, and σ^- for fluorocarbon, polystyrene, and poly(methyl methacrylate) using contact angles of different combinations of probe liquids, and found that the calculated values depended significantly on the probe liquids used. Considering all of these factors, the validity of the vOCG correlation is often questioned.

1.2.3.2. Isoelectric point (IEP) and point of zero charge (PZC)

There are a large number of materials that have surface functional groups that will undergo acid-base charge transfer in the presence of water. Examples of this are mineral oxides, which have surface oxygen functionality that is hydroxylated to some extent when in the presence of some moisture (even low levels of water vapor). These surface hydroxyl groups are capable of either accepting a proton when in a solution of low pH

$$MOH + H_3O^+ \rightarrow MOH_2^+ + H_2O \tag{1.16}$$

or donating a proton when in a solution of high pH

$$MOH + OH^- \rightarrow MO^- + H_2O. \tag{1.17}$$

As a result, mineral oxide surfaces will often obtain a net charge when in contact with an aqueous solution. At a specific pH, the net surface charge becomes zero, and this point is known as the point of zero charge (PZC). The PZC will vary from oxide to oxide based on the characteristic acidity or basicity of the surface of the material, as depicted in Figure 1.2. The method for determining the point of zero charge involves performing potentiometric titrations at several different background electrolyte concentrations. When moles of acid or base is plotted against the solution pH there will be a common intersection point for the different background electrolyte concentrations, assuming there is no specific adsorption of ions or chemical alteration of the surface. This intersection point corresponds to the PZC, because it is the only point at which the differences in screening caused by different electrolyte concentrations would be nonexistent. In general, the PZC can apply to any charge determining ions, but for surfaces where the charge determining ions are H_3O^+ and OH^- it is a useful tool for ranking the acidity or basicity of the surface of a material.

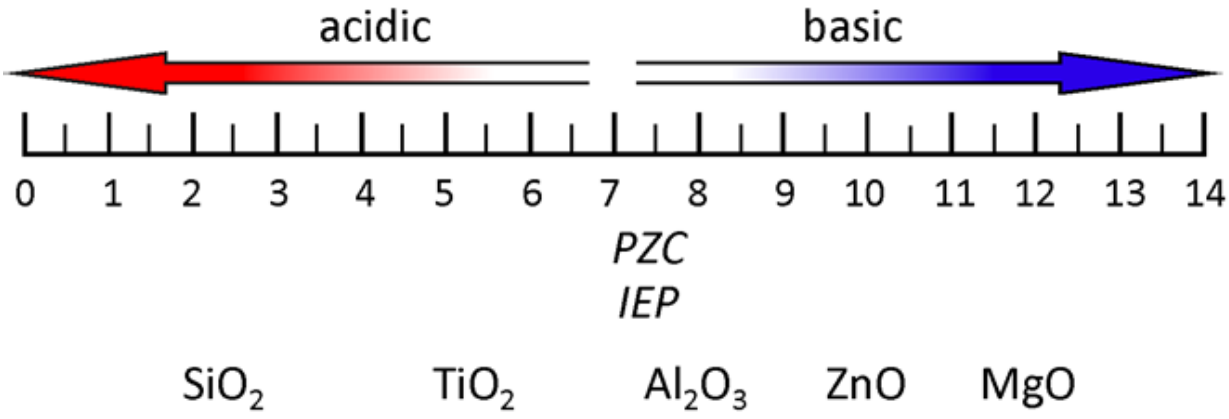

Figure 1.2. A schematic of the PZC or IEP of mineral oxide particles is depicted. The inherent acidity or basicity of mineral oxides is well described by the pH at which the surfaces have net neutral charge when in contact with an aqueous system.

Similarly, the isoelectric point (IEP) is the pH at which the zeta potential, the potential at the plane of shear between the surface and the solution, is zero. The IEP is determined by electrokinetic titration, where the zeta potential is calculated at several different pHs to determine the point at which it is zero. As long as there is no specific adsorption of ions to the particle surface, the IEP will be identical to the PZC.

The IEP and PZC have become the most commonly used scale of solid acid-base properties, especially for salts and oxides. As a result of the convenience and popularity of these techniques IEP and PZC values have been documented for a large number of materials [85,86]. Of course, the material to be probed must be insoluble in water, which somewhat limits the applicability of this technique. It should be noted that the IEP and PZC take into account both Brønsted-Lowry and Lewis type acid-base interactions. As previously mentioned, even though these interactions are conveniently described as proton transfer events, such charge transfer events are captured by the electron transfer description of Lewis acid-base theory.

1.2.3.3. Inverse gas chromatography (IGC)

Inverse gas chromatography (IGC) is one of the most powerful techniques that can be used for probing the surface energy as well as the acid-base properties of a solid surface [87]. The apparatus for IGC is identical to traditional gas chromatography, where one is probing the properties of a gas of interest with a known stationary solid phase. What makes IGC the "inverse" of traditional gas chromatography is that one is probing the properties of a stationary solid of interest with known gas samples. Inverse gas chromatography is typically run in the infinite dilution regime by injecting a small sample of the probe gas into a stream of inert carrier gas (such as nitrogen) which then flows through a column packed with the solid material of

interest. This means that the resulting adsorption onto the solid surface is in the linear "Henry's law" regime. The main parameter that is measured is the relative retention volume (V_N), defined as the volume of the inert carrier gas required to elute the injected probe through the sample. This is determined using the following equation

$$V_N = jF_{col}(t_R - t_{ref}) \tag{1.18}$$

where j is a correction factor to account for the pressure drop across the length of the column, F_{col} is the volumetric flow rate of the carrier gas, t_R is the retention time of the probe gas, and t_{ref} is the retention time for the nonadsorbing carrier gas (typically this is probed with methane). When in the "Henry's law" regime, the retention volume relates to the surface energy and acid-base properties by the following equation

$$RTln(V_N) = 2a_{mol}\sqrt{\sigma_S^{LW}\sigma_L^{LW}} - \Delta G_{ads}^{AB} + C \tag{1.19}$$

where R is the ideal gas constant, T is the absolute temperature, a_{mol} is the molar area of the adsorbate on the surface, σ_S^{LW} and σ_L^{LW} are the Lifshitz-van der Waals contributions to the surface tension of the solid and the probe, ΔG_{ads}^{AB} is the acid-base contribution to the free energy change of adsorption, and C is a constant that depends on the choice of the reference state. For gas probes that are inert with regard to acid-base properties, such as linear alkanes, the ΔG_{ads}^{AB} term is equal to zero. Therefore, if a series of linear alkanes are used, typically butane through nonane, one can plot $RTln(V_N)$ as a function of $a_{mol}(\sigma_L^{LW})^{1/2}$ and obtain a straight line with a slope of $2(\sigma_S^{LW})^{1/2}$.

Once the LW contribution to adsorption energy is determined, one can inject various acid and base probes. The additional adsorption energy contributed by either a basic probe binding

with an acidic site on the solid surface or an acidic probe binding with a basic site on the solid surface will require a larger V_N to elute the probe than predicted by LW interactions alone. This will cause a vertical shift above the alkane line on the $RTln(V_N)$ vs. $a_{mol}(\sigma_L^{LW})^{1/2}$ plot, which can be taken as $-\Delta G_{ads}^{AB}$ for each probe. A large shift for basic probes indicates a strongly acidic surface, and vice versa for the acidic probes. This type of analysis takes into account the bifunctionality of the surface, but it does not account for any "hard" or "soft" effects. As a result, there are often some small differences in $-\Delta G_{ads}^{AB}$ from one basic probe to another or one acidic probe to another. IGC is, therefore, best used with a variety a probes to give an overall indication of acid-base surface properties, unless one is trying to probe a series of solid surfaces against a specific chemical probe.

1.2.3.4. X-ray photoelectron spectroscopy (XPS)

Whether dealing with Brønsted-Lowry or Lewis acids and bases, an acid-base reaction involves the transfer of electrons or electron density. Therefore, the electron binding energy (E_B) of the surface groups, obtainable through X-ray photoelectron spectroscopy (XPS), can be used to determine the acid-base properties of a material. The binding energy can be used as a measure of Lewis basicity, as a lower E_B means a lower affinity for electrons. XPS is also a powerful tool for identifying the chemical groups, found at the surface of a material, that typically engage in acid-base interactions. The surface analysis aspect of this technique has led to a number of studies that have correlated E_B to acid-base properties of materials. One such study analyzed the uptake of sodium cations (a Lewis acid) by a series of basic polymers [88]. There have also been a number of studies that have attempted to correlate the E_B of mineral oxides with their IEP, with varying degrees of success [89,90]. As Delamar suggested, the difficulty in correlating these values is that the IEP is based on the competition of acidity and basicity of oxygen groups [90].

Therefore, one needs to introduce a pair of empirical parameters to account for this competition before correlating to IEP values.

1.2.3.5. Calorimetry

The relationship between acid-base interactions and the exothermic molar heat of adduct formation ($-\Delta H^{AB}$) has been mentioned repeatedly in the above sections. It is only logical that the direct measurement of the heat of reaction would be a good technique for evaluating the acid-base properties of a material. The primary drawback with such a test method is that it is a relatively time-consuming and tedious process. Therefore, the enthalpy of adduct formation is often obtained using correlations to other properties such as infrared (IR) spectral shift [91]. Regardless of this, the $-\Delta H^{AB}$ can be directly measured via sensitive calorimetry. In doing so, one must take into account the LW interactions between the acid or base probe and the material of interest and from the lateral interactions between the adsorbed probe molecules. Despite these obstacles, a ranking of the acid-base properties of a series of materials can still be made using a single acid or base as a reference probe molecule. An example of this is a study of the acid-base properties of a series of 20 oxides performed by Auroux and Gervasini [92]. While individual enthalpies of both CO_2 (acid probe) and NH_3 (base probe) could be readily calculated for the series of oxides, neither ranking correlated with the IEP of the oxides. This again demonstrates the competitive nature of acidic and basic sites that comprises the IEP value of an oxide.

1.3. Acid-base charging in apolar media

As mentioned previously, the mechanism by which particles obtain charge in apolar systems is the most important aspect of determining the polarity and magnitude of that charge. Significant evidence has been reported in the literature to suggest that the dominant mechanism

is acid-base charging. It is believed that surfactant monomers will adsorb in a "head down" manner (polar group adsorbs to the surface with the nonpolar tail protruding into the fluid) in apolar systems. An adsorbed monomer may then form an acid-base adduct with a particle surface group. When this adduct separates, there is a finite possibility that charge will transfer between the monomer and the particle surface, and the direction of charge transfer is dependent on the acid-base properties of both the particle and the surfactant, as depicted schematically in Figure 1.3. However, the probability of the charged monomer escaping into the bulk on its own is very small, and most charging events are neutralized at the particle surface. The monomer counter-charge is far more probable to escape the particle surface if it can be incorporated into a nearby reverse micelle.

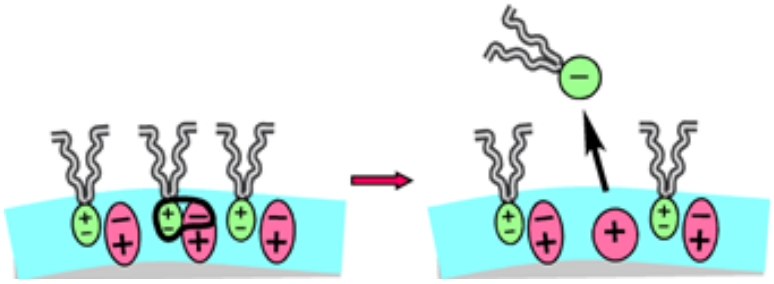

Figure 1.3. A generic scheme of acid-base charging is depicted above. An adsorbed monomer forms an acid-base adduct with a surface functional group. When the adduct is broken and the monomer desorbs, there is a certain probability that charge will be exchanged. The charged monomer is then incorporated into a nearby reverse micelle.

The difficulty in practically applying this idea is in properly characterizing the acid-base properties of the surfactant and the particle. As discussed in Section 1.2, there is no single technique that captures the complete picture of acid-base interactions. The subject becomes more challenging when one attempts to translate acid-base behavior from aqueous systems to apolar ones. Typically, one must first attempt to characterize the acid-base strength of both the

surfactant and the particle surface using one or more techniques in different media. Once these characterizations are made, one can attempt to interpret the particle charging that occurs when these individual components are dispersed together in an apolar environment. This kind of experiment has been conducted for a number of different surfactant and particle systems: ionic and nonionic surfactants, and mineral oxide, polymer, organic pigments, and hydrophobic particles are all discussed in this section.

1.3.1. Mineral oxides

Mineral oxides have been widely used in apolar charging studies for a number of reasons. Firstly, they are an abundant material commonly used in industrial applications, making their charging behavior of great interest. Secondly, their acid-base properties have been extensively studied in aqueous media and are well characterized by their PZC and IEP [43,85–87]. This includes thermodynamic studies that have shown that there is a linear connection between the enthalpy of proton adsorption and the PZC of the oxide [93]. Mineral oxides have also been used as early evidence of acid-base interactions in non-aqueous fluids of moderate dielectric constant [51–54]. Another enticing aspect of mineral oxides is that their surfaces can be chemically modified to alter their hydrophilic/hydrophobic and acid-base properties. Most of the studies conducted on mineral oxides have been of single oxide and surfactant systems. Due to the variability in water content, surface functionality from supplier to supplier, and measurement technique it is often difficult to correlate the results in a meaningful way. This section will therefore focus on some of the more systematic studies of mineral oxide charging.

An example of the tunable nature of mineral oxides is a study conducted by Poovaradom and Berg [39] in which silica particles were modified to be either basic or acidic. The treatments

used were a silanization of the surface hydroxyl groups with either aminopropyltriethoxysilane (APS) to make the particles more basic or with 3-glycidoxypropyltrimethoxysilane (GPS) treated with acid to open the epoxy ring to impart acidic hydroxyl groups on the surface. The effectiveness of these treatments were verified by determining their aqueous IEPs, reported as being at a pH of 3.0 for the silica treated with GPS and 8.5 for the APS treated particles. The particles were then dispersed with the acidic Span 80 and the basic OLOA 11000 surfactants in the apolar solvent Isopar-L. The resulting particle charge is plotted as a function of surfactant concentration as shown in Figure 1.4, reproduced with the authors' permission.

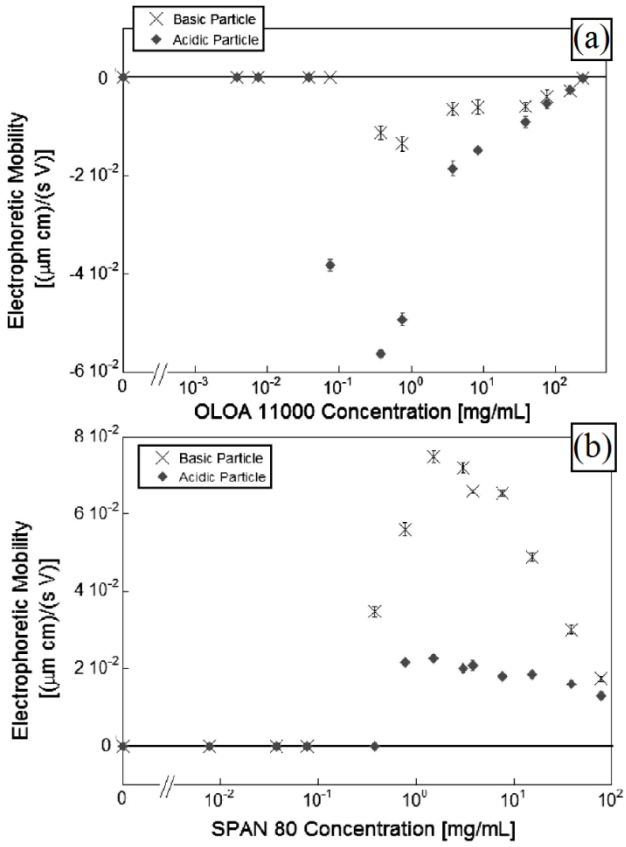

Figure 1.4. Charging of acidic and basic modified silica particles. The electrophoretic mobility of amine (basic) and hydroxyl (acidic) functionalized silica particles in (a) OLOA 11000 and (b) Span 80. Error bars are derived from three measurements. Reprinted from [Poovarodom, S.; Berg, J.C.; J. Colloid Interface Sci. 2010, 346, 370–377], copyright (2010), with permission from Elsevier.

Both particles obtained a negative charge when dispersed with OLOA 11000, and both particles charged positively when dispersed with Span 80. However, the magnitude of the particle charge varied significantly depending on the particle surface treatment. Also of note is that the magnitude of charge varies as a function of surfactant concentration, with a maximum charge occurring at an intermediate concentration. As discussed previously, this is a commonly observed trend and the decrease in charge at large surfactant concentration is attributed to neutralization or screening. The polarity and magnitude of charge can both be explained by acid-base charge transfer. The basic surfactant (OLOA 11000) acts as a proton acceptor or electron donor when interacting with the particle surface, resulting in a negative particle charge. Conversely, the acidic surfactant (Span 80) acts as a proton donor or electron acceptor, imparting a positive charge on to the particle surface. The magnitude of charge is dependent on the acidity or basicity of the particle surface (i.e. its ability to accept or donate protons or electrons). As expected, the magnitude of charge is maximized when an acidic surfactant interacts with a basic particle or when a basic particle interacts with an acidic surfactant. What remained unclear from this research was whether or not the polarity of charge was determined solely by the surfactant or by a combination of the surfactant and particle acid-base properties.

In an attempt to delve deeper into the relationship between acid-base properties and particle charging, the authors of the current review conducted several studies using a series of untreated mineral oxides with IEPs and PZCs that span nearly the entire pH range [50,63]. The IEP and PZC of each mineral oxide were experimentally determined to establish the acid-base properties of each oxide. The mineral oxides were first stabilized in Isopar-L with the anionic surfactant dioctyl sodium sulfosuccinate (AOT) which is commonly used as a charge stabilizer in apolar systems. To account for the fact that the electrophoretic mobility varies with surfactant

concentration, samples were prepared for a range of AOT concentrations and the maximum observed mobility was used for comparison. The maximum particle electrophoretic mobility in Isopar-L was then plotted against the PZC for each mineral oxide, represented by the green line in Figure 1.5.

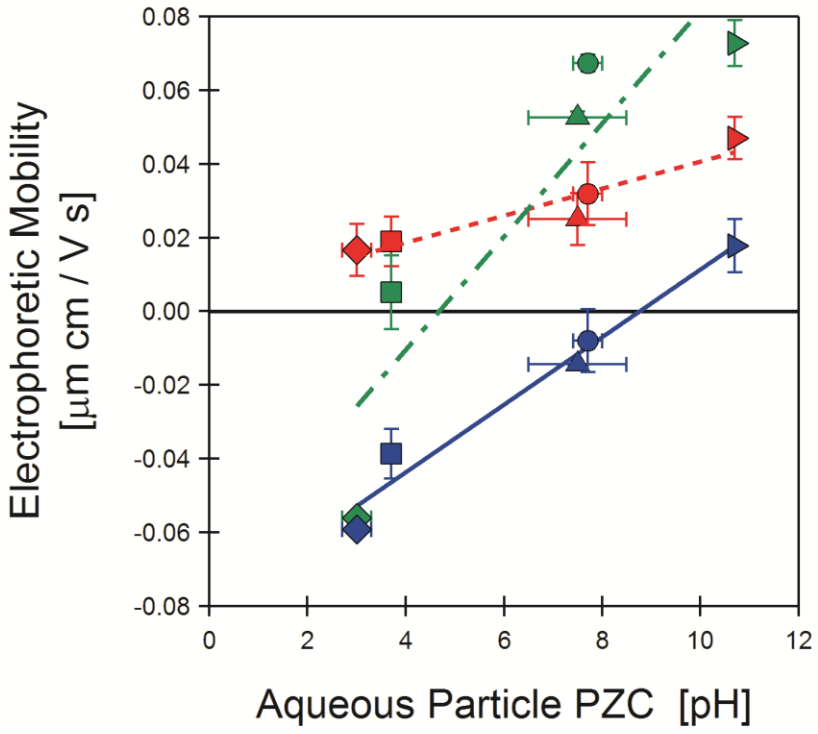

Figure 1.5. Charging of mineral oxide series. The maximum zero-field electrophoretic mobility of silica (◆), titania (■), alumina (▲), zinc oxide (●), and magnesia (▸) particles dispersed in Isopar-L are plotted against their aqueous PZCs. The green symbols (— · —) represent particles dispersed with AOT, the red symbols (- - - -) represent particles dispersed with Span 80, and the blue symbols (—) represent particles dispersed with OLOA 11000. These data were collected in the authors' laboratory in multiple published studies [50,63].

It was observed that AOT was capable of charging particles either positively or negatively. More importantly, the polarity and magnitude of particle charge correlated directly with the PZC of the oxide. The most acidic particle, silica, obtained a negative surface charge. The polarity of charge became positive and increased in magnitude with increasing particle

basicity. This behavior is precisely what is expected according to acid-base charging theory. It is observed that the magnitude and polarity of charge is dictated by the relative acidity of *both* the particle and the surfactant. If the particle is more acidic than the surfactant, the surfactant acts as a proton acceptor or electron donor resulting in a negative particle charge, as depicted schematically in Figure 1.6. Conversely, if the particle is more basic than the surfactant, the surfactant acts as a proton donor or electron receiver resulting in a positive particle charge. The charging behavior observed in this study mirrors the behavior of oxide charging in aqueous studies as well as moderate dielectric constant non-aqueous media.

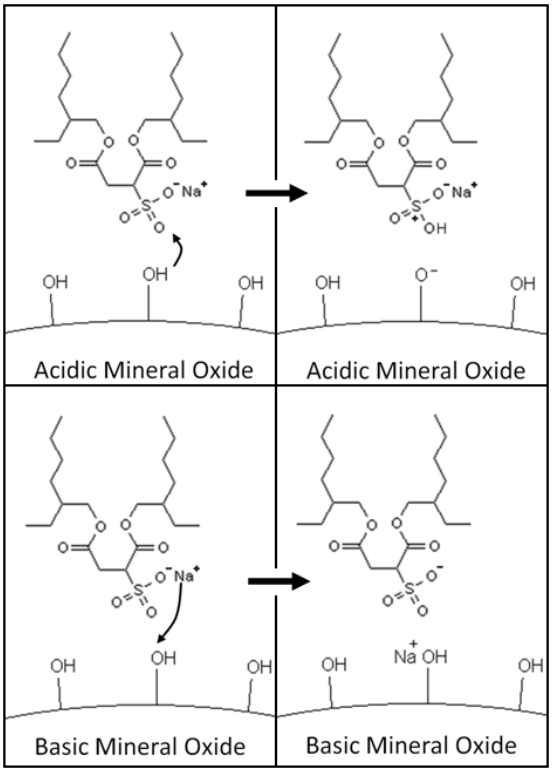

Figure 1.6. Schematic representation of the proposed acid-base charging mechanism for AOT and mineral oxides. In the case where the particle surface is more acidic than the AOT monomer (top), a proton is removed from the surface by an adsorbed monomer and the particle is charged negatively. In the case where the particle is more basic than the AOT monomer (bottom), the particle surface adsorbs the sodium ion from the AOT monomer and the particle is charged positively. In both cases the charged monomer is stabilized in the bulk solution by becoming incorporated in a reverse micelle. Reprinted with permission from [Gacek, M.; Brooks, G.; Berg, J.C. Langmuir 2012, 28, 3032-3036]. Copyright [2012] American Chemical Society.

The important difference is that in apolar media it is the acid-base properties of the surfactant that determine the particle charge as opposed to the acid-base properties of the medium. The implication of this apolar study is that a series of mineral oxides can be used as a means of directly characterizing the acid-base properties of the surfactant. The point of charge reversal is an indicator of the relative acid-base properties of the surfactant in terms of the pH of the oxide PZC. For AOT the charge reversal point occurs at a pH of approximately 5, indicating the surfactant acts as a weak acid in apolar systems.

The study with the series of mineral oxides was repeated for the acidic surfactant Span 80 and the basic surfactant OLOA 11000, shown in Figure 1.5. A similar correlation was observed for both surfactants in that the acidic particles charged more negatively or less positively than the basic particles. The biggest difference between the results for Span 80, OLOA 11000, and AOT is that the point of charge reversal was shifted from one surfactant to the next. For OLOA 11000, the point of charge reversal was at a pH of approximately 9, confirming that it is a basic surfactant. Span 80 charged every particle positively, and if one extrapolates the data to low pH it appears that the point of charge reversal would be approximately at a pH of 0. Another interesting aspect of these plots is that the slope of the mineral oxide electrophoretic mobility vs PZC curve varies from surfactant to surfactant. This indicates that while the relative acid-base properties of the particle and the surfactant are a critical factor in determining the polarity and magnitude of particle charge, there appear to be other influences involved. One possible explanation is that the ability for the surfactant reverse micelles to stabilize charge will impact the slope of the curves shown in Figure 1.5; this is explored in more detail in Section 1.5.

As a test for this surfactant characterization technique, the data from the modified silica study conducted by Poovaradom and Berg [39] are compared to the untreated mineral oxide

mobility vs PZC curves, as shown in Figure 1.7. It is found that good agreement is observed for all of the data. The magnitude of the mobility of the basic treated silica in the presence of Span 80 is larger than expected, but the polarity is properly predicted by acid-base charging. This demonstrates that if the acid-base properties of the particle and surfactant are known, one can predict both the polarity and magnitude of particle charge.

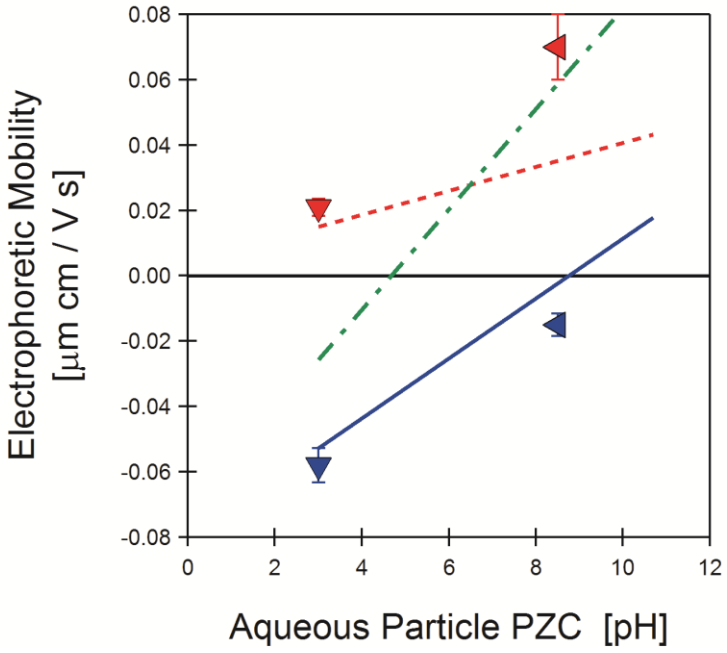

Figure 1.7. The maximum zero-field electrophoretic mobility of surface modified silica from Poovaradom and Berg [39] is overlaid on the plot of untreated mineral oxides from Figure 1.5. Acid treated (▼) and basic treated (◀) silica is plotted in blue and red symbols for particles dispersed with OLOA 11000 and Span 80, respectively.

1.3.2. Carbon black particles

The charging behavior of carbon black in apolar media has been of interest for decades, as additives in motor oil are specifically designed to stabilize carbon black from accumulating on engine parts. More recently, carbon black has been used in apolar ink formulations, and the charge obtained has a direct effect on the particle stability. One of the first systems used to

suggest surfactant mediated acid-base charging was carbon black and OLOA 11000, put forth by Fowkes [13–16]. Even though carbon black is a hydrophobic material, the surface is populated by oxygen containing groups, typically carboxylic acid. Fowkes suggested that the basic OLOA 11000 would adsorb to the particle surface, engage in an acid-base charge transfer with these acidic groups, and then desorb carrying a positive charge with the surfactant and leaving a negative charge on the particle surface. This mechanism is the foundation for many of the cases of acid-base charging discussed in the previous sections.

Characterizing the acid-base properties of carbon black can be challenging, because when carbon black is in contact with water it is believed that hydroxide ions will strongly adsorb to the surface. The specific adsorption of hydroxide ions to a hydrophobic interface can be explained by the strong dipole or hydrogen bonding of the hydroxide ions with the hydrogen atoms of the highly ordered interfacial water molecules that form near any hydrophobic surface [94–97]. The specific adsorption of hydroxide ions makes it difficult to obtain an IEP or PZC for carbon black particles. Another complication with carbon black is that there is a tremendous amount of variability in the surface functionality from supplier to supplier (or even from batch to batch within the same supplier). It is, therefore, difficult to directly compare the apolar charging behavior of carbon black in the literature. The authors of the current review conducted electrophoretic mobility measurements, in their laboratory, of four different sources of carbon black particles dispersed in Isopar-L in the presence of OLOA 11000, AOT, and Span 80. All four sources of carbon black were acidic, as verified by IGC. In the presence of AOT and OLOA 11000 the carbon black charged negatively to varying degrees, whereas Span 80 did not significantly charge the particles, as shown in Figure 1.8. These results, currently unpublished, support the acid-base charging mechanism put forth by Fowkes, based on the acid-base

characterization of these three surfactants shown in Figure 1.5. The negative charge of, presumably acidic, carbon black particles is consistently reported in literature [98].

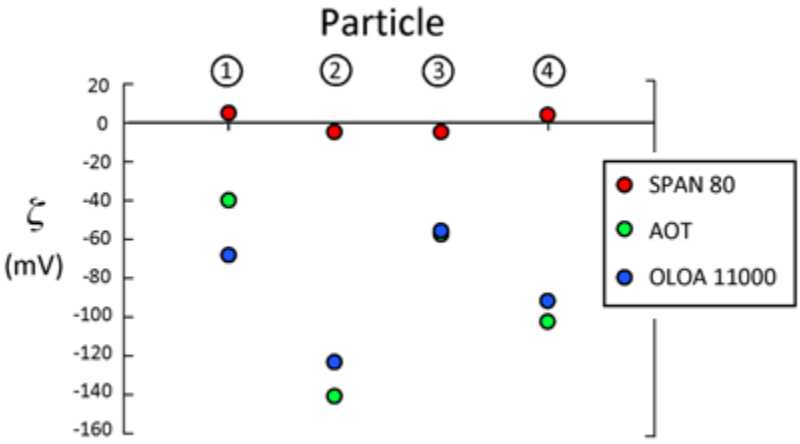

Figure 1.8. The figure shows the particle zeta potential for four different commercially available carbon black samples dispersed in Isopar-L with Span 80, AOT, or OLOA 11000. The figure represents previously unpublished data collected in the authors' laboratory.

1.3.3. Organic pigment particles

In recent years the implementation of organic pigment particles in apolar paints and inks has been an important industry. How these particles charge is not only important to dispersion stability; it has also become a key parameter in inks that take advantage of particle charge to draw particles out of suspension before transferring them to a selected print medium. The surface chemistry of organic pigments is quite different from both polymer particles and mineral oxides, and is often complex. In addition, many pigments used in apolar systems are soluble in water over a wide range of pH, limiting the techniques that can be used to characterize their acid-base properties.

A study was recently conducted by the authors of this review pertaining to two commonly used pigment particles, magenta and cyan [99]. Chemically, the particles were a beta-

oxynapthoic acid pigment lake (magenta) and a copper phthalocyanine blue (cyan). The magenta particles were strongly basic and the cyan particles were amphoteric, as characterized by IGC. These particles were dispersed in *n*-heptane with AOT, Span 80, or OLOA 11000. It was found that the magenta particles charged positively with all three surfactants, with AOT yielding the largest magnitude of charge, as reproduced in Figure 1.9.

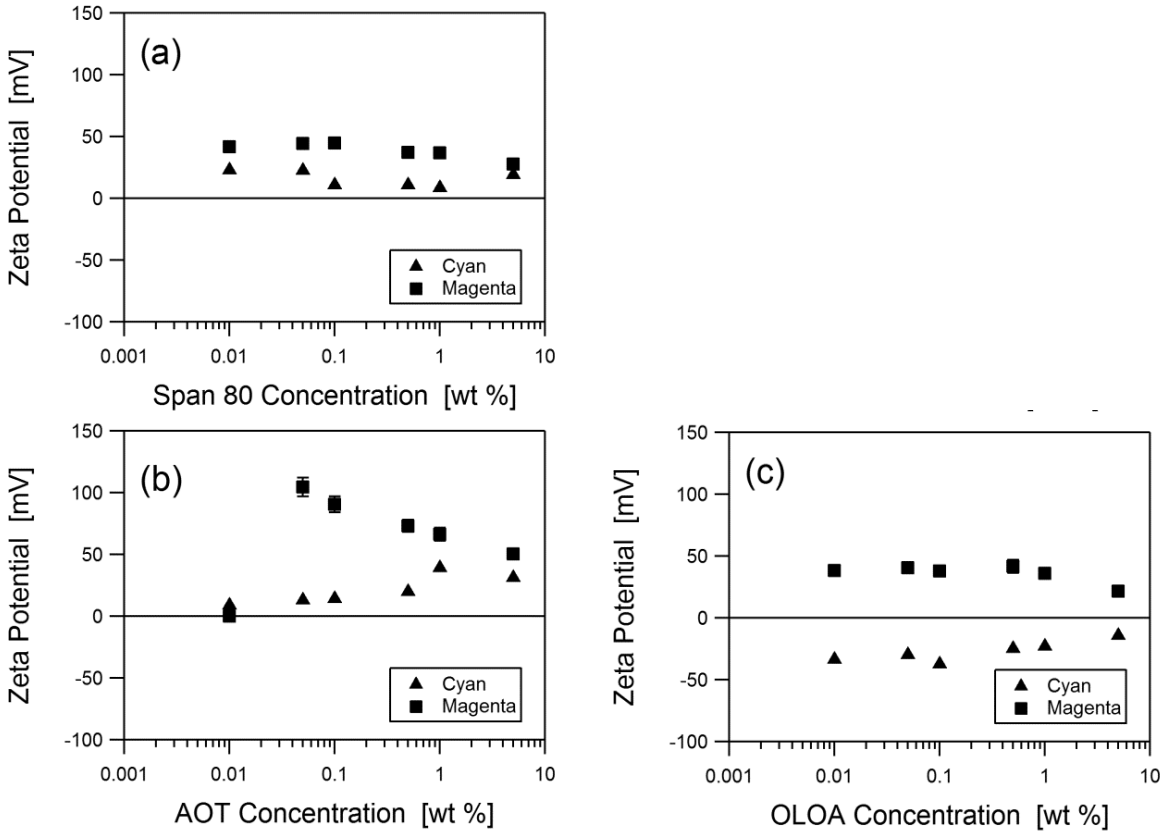

Figure 1.9. The charging behavior of magenta and cyan particles is characterized. The particle zeta potential is plotted as a function of surfactant concentration for dispersions in heptane containing (A) Span 80, (B) AOT, and (C) OLOA 11000. Reprinted with permission from [Gacek, M.M.; Berg, J.C.; Electrophor. 2014, 35, 1766–1772]. Copyright [2014] Wiley-VCH.

The positive charge of magenta is supported by a separate study involving synthesized polyisobutylene succinimide surfactants (OLOA analogues) [58]. The cyan particles charged

positively with both AOT and Span 80, but charged negatively with OLOA 11000. All of these results correlate with the charging behavior predicted by acid-base interactions. The basic magenta acts as a proton acceptor or electron donor in all cases, and the amphoteric cyan acts as a proton or electron donor or acceptor depending on the acidity or basicity of the surfactant. In other studies, cyan has been observed to charge positively in the presence of zirconyl 2-ethyl hexanoate ($ZrO(Oct)_2$) [62,100]. While $ZrO(Oct)_2$ has not been characterized by mineral oxides in the same manner as the other surfactants, the charging is also believed to be the result of an acid-base interaction [100].

A second aspect of the same study analyzed the effect of adding an acidic synergist (a material that is designed to bind to the particle surface and enhance the adsorption of steric stabilizers) to the system. It was observed that synergist added to the magenta surface in the presence of Span 80 resulted in a dramatic decrease of the previously positive particle charge, and the particles quickly aggregated and settled out of suspension. It is likely that the originally basic particle became populated with acidic surface groups, which cannot engage in strong acid-base charge transfer with the acidic Span 80 surfactant. A similar, but less dramatic, effect was observed with the cyan and Span 80 system, because the cyan particles were only marginally positively charged to begin with. In the case of cyan dispersed with AOT, a complete charge reversal from positive to negative was observed upon the addition of synergist. It is believed that the added acidic groups on the particle surfaces are able to act as proton donors or electron acceptors when interacting with the AOT monomers. In the last system studied, it was observed that the addition of synergist to a suspension of cyan and OLOA 11000 caused the magnitude of the negative particle charge to diminish at small surfactant concentrations. This behavior cannot be explained by the adsorption of synergist to the particle surface. It is believed that the acidic

synergist is capable of forming acid-base complexes with the basic OLOA 11000 monomers in solution before they can become adsorbed to the particle surface. The result is that the surfactant monomers are modified to be more acidic. This behavior disappears at larger surfactant concentrations, presumably because there is a smaller ratio of synergist to surfactant in the system. The study demonstrates the importance of using additives for the promotion of surface charge generation in apolar systems as well as the added complexity of competitive interactions between synergists, surfactants, and particles.

1.3.4. Polymeric particles

Particles formed through polymerization reactions are another popular choice for charging studies in apolar media due to the custom chemistries that can be created. Instead of modifying the surfaces as one does with mineral oxides, it is possible to tune the chemistry during particle formulation to have the desired acid-base or hydrophobic/hydrophilic properties. Initial studies of polymer particle charging in apolar media has shown that acid-base interactions may play a key role in determining the particle charge [61].

A systematic study of polymer particle charging in apolar media was conducted by Guo and coworkers [49], where several different functionalized polystyrene (PS) particles as well as a polymethyl methacrylate (PMMA) particle were dispersed in solutions of Span 85 or AOT in decane. The resulting particle charge is compared to how the different particles charge in water as well as characterizing the acid-base properties using van Oss-Chaudhury-Good (vOCG) theory. The PS particles were functionalized with amidine, carboxyl, or sulfate surface groups, and the PMMA particle was functionalized with sulfate groups. In water, the PS particles functionalized with amidine charged positively, the PMMA-sulfate particles charged moderately

negative, and the PS-carboxyl and PS-sulfate particles charged more strongly negative. These results are expected, and show that the acid-base properties of the functional groups are the determining factor regarding charging in an aqueous environment. Based on the results in water one can conclude that the PS-amidine particles are basic, and the remaining particles are acidic to varying degrees. When the particles are dispersed in decane with Span 85 or AOT present the particles display two different charging regimes, as shown in Figure 1.10.

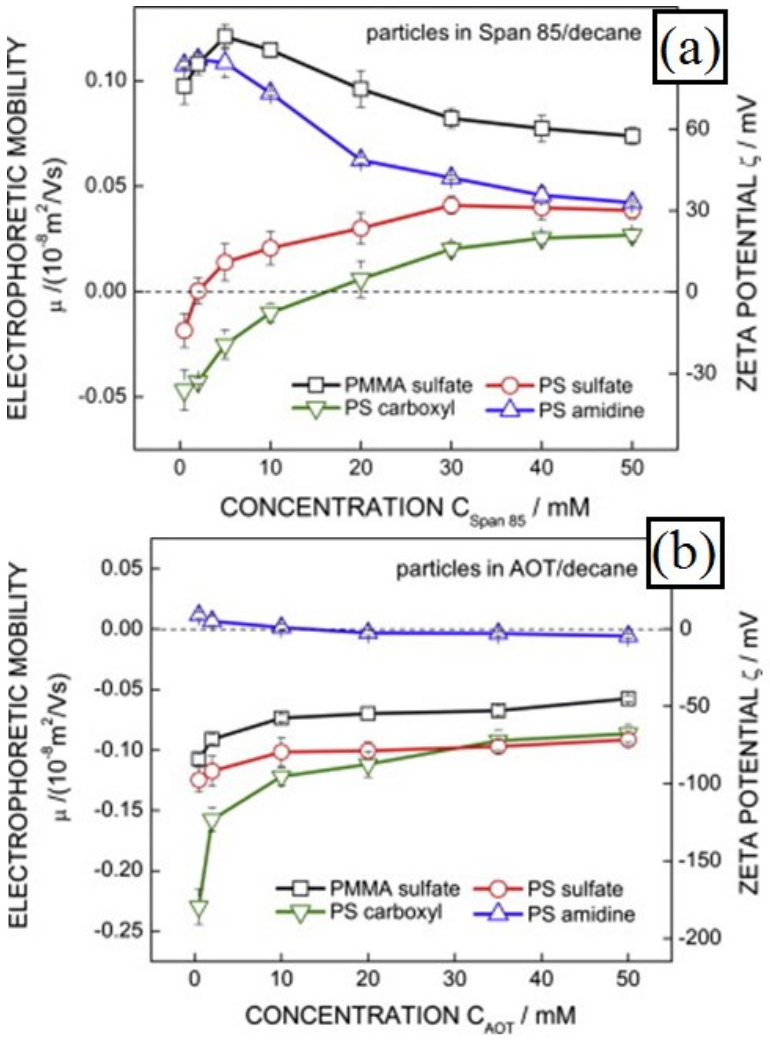

Figure 1.10. Polymer particle charging in apolar media. Zero field electrophoretic mobility and zeta potential (in the Hückel limit) of the different polymer particles in (a) Span 85 and (b) AOT. Reprinted from [Guo, Q.; Lee, J.; Singh, V.; Behrens, S.H.; J. Colloid Interf. Sci. 2013, 392, 83-89], copyright (2013), with permission from Elsevier.

Near the critical micelle concentration (CMC) of approximately 0.2 mM Span 85, the PS-amidine and PMMA-sulfate particles charged significantly positive, while the PS-sulfate and PS-carboxyl particles charged marginally negative. As suggested by Guo et al. [49], this charging shows some dependence on the functional groups of the particles similar to what occurs in water. However, as the surfactant concentration reaches a level well into the micelle regime all of the particles are charged positively. In addition, the magnitude of charge for all of the PS particles are approximately the same at roughly 30 mV zeta potential, and the PMMA particle was significantly larger in magnitude. These results are significantly different than what was observed in water, and are reproduced in Figure 1.10 (a). Behrens and coworkers suggest that this is likely a result of acid-base charge transfer between the Span 85 and the underlying polymer instead of the functional groups. This conclusion is supported by the vOCG characterization of the particles, which shows that PMMA is significantly more basic than the PS particles. The vOCG characterization also showed that all of the particles were monofunctional bases, which is not an uncommon result with vOCG theory as discussed in Section 1.2. These results generate a couple of important questions. Why do some particles appear strongly acidic in water and yet they are all monofunctional bases according to vOCG? Why do the particles charge according to their functional groups in water and charge relative to the underlying polymer in the presence of Span 85? A possible explanation is the "hard" and "soft" nature of water versus the vOCG probes. Hydronium and hydroxide ions are both very hard acids and bases, respectively, and they may be more likely to interact with the presumably harder acid and base functional groups on the particle surface. Based on this hypothesis, Span 85 may be "softer" and interact more with the "softer" polymer groups. This hypothesis might also help to explain the relative inability of Span 85 to charge the "hard" surface hydroxyl groups on mineral oxides

[101]. A more detailed study of these materials would need to be conducted to either confirm or refute this.

The second part of the study dealt with the charging behavior of the same particles in the presence of AOT; these results are reproduced in Figure 1.10 (b). In the AOT/decane system the PS-amidine did not acquire any significant charge, PMMA-sulfate charged moderately negative, and the PS-sulfate and PS-carboxyl particles charged more strongly negative. Based on the vOCG result that all of the particles are monofunctional bases the authors concluded that the particles could not obtain a negative charge via acid-base charging. Therefore, some other mechanism must be occurring, presumably the adsorption of AOT molecules to the particle surface and subsequent dissociation of its polar head group [41,44,45]. However, it is interesting to note that the relative charging exactly mirrored how they charged in water. Another explanation is that AOT, being an ionic surfactant, is presumably "harder" in nature than Span 85. Thus, AOT could more readily engage in acid-base charge transfer with the functional groups on the polymer surfaces, explaining the similarity to the way in which these particles charge in water. This study highlights the complex nature of polymer particle charging due to the more diverse chemistries that are often involved.

1.4. Water content

The water content is the other primary factor influencing the particle charge in apolar systems, second only to the acid-base properties of the surfactant and the particle surface. All of the systems that are described in this review have some trace amount of water in them. Some moisture can be solubilized by the apolar medium itself, often with an upper limit in the 10 to 30 ppm range. Water can also be brought into the system by the hygroscopic components of the

charge stabilizing surfactants, and the particle surfaces often contain some amount of moisture if they have been in contact with ambient air. It has been suggested by some that water is a necessary component for reverse micelles to form and charge to be stabilized in these systems [25–27], and this can have dramatic effects on particle stability [102,103]. To best understand how water affects these systems, one must attempt to separate the effects on both reverse micelle and particle charging.

1.4.1. Effect on reverse micelles

As mentioned in the introduction, reverse micelles or similar aggregates are the key to stabilizing charge in apolar systems. These structures have a polar core with a large dielectric constant surrounded by a low dielectric shell, typically hydrocarbons. According to the idea of micelle disproportionation and charge fluctuation theory the polar core is what houses and stabilizes charge. The system can be modeled as a series of concentric spherical capacitors where the innermost sphere is the ion, the next sphere is the outer edge of the polar core or the reverse micelle, and the outer layer consists of the low dielectric medium extending to infinity [28]. The energy required to place an ion in a reverse myself is expressed by

$$E = \frac{e^2}{8\pi\varepsilon_0\varepsilon_{np}r_c} + \frac{e^2}{8\pi\varepsilon_0\varepsilon_p}\left(\frac{1}{r_i} - \frac{1}{r_c}\right) \tag{1.20}$$

where e is the elementary charge, ε_0 is the permittivity of free space, r_c is the radius of the polar core of the reverse micelle, r_i is the radius of the ion, and ε_{np} and ε_p are the dielectric constants of the nonpolar external medium and the polar core, respectively. It is often assumed that the dielectric constant of the polar core is large enough compared to the nonpolar medium that the second term may be considered negligible. However, it should be noted that this assumption holds true only if the ion radius is rather large. The micelle ionization energy from equation

(1.20) is then used in a Boltzmann relation to represent the fraction of total micelles that are charged at equilibrium (χ) [28].

$$\chi = \frac{(C_+ + C_-)}{C_T} = 2exp\left\{\frac{-Z^2e^2}{8\pi\varepsilon_0 kT}\left[\frac{1}{\varepsilon_{np}r_c} + \frac{1}{\varepsilon_p}\left(\frac{1}{r_i} - \frac{1}{r_c}\right)\right]\right\} \tag{1.21}$$

where C_+ and C_- are the concentration of positively and negatively charged micelles, C_T is the total concentration of micelles, Z is the valence of charge in the micelle (typically assumed to be ± 1), k is the Boltzmann constant, and T is the absolute temperature. Clearly, the size of the polar core is a critical parameter for determining how readily a reverse micelle will stabilize charge: the larger the polar core, the more readily a reverse micelle will charge. All surfactants that form reverse micelles are at least somewhat hygroscopic, and will draw moisture into the polar cores of the reverse micelles, causing them to swell. The amount of moisture in the system, whether drawn in from ambient air or introduced by other means, will dictate how large or small the polar cores are swollen. This theory has been confirmed by several studies correlating water content (which correlates to the reverse micelle polar core size) to the solution conductivity using the following expression

$$\sigma = \frac{e^2\chi C_T}{6\pi\eta R_H} \tag{1.22}$$

where η is the viscosity of the system and R_H is the hydrodynamic radius of the micelles. Good agreement between predicted conductivity and experimental values is found for several different surfactant systems [28].

Another interesting aspect of reverse micelle charging was studied by Guo and coworkers [104]. In the study, the conductivity of both Span 85 and AOT solutions in heptane were

measured as a function of moisture in the system. Interestingly, it was found that the conductivity of the system was not affected by the ionic strength of the water used to swell the micelles (deionized water versus 0.1 M NaCl). The likely explanation for this is that for ions such as sodium or chloride the ionic radius is small enough that the second term in equation (1.20) may contribute a significant amount of energy, making it less favorable for them to become charged. Therefore, one may conclude that either water or some other large ionizable impurity is the likely source of charge in reverse micelles.

1.4.2. Effect on particle charge

Once particles are introduced into the system along with surfactant, a number of complications and questions must be brought to attention. Many particle surfaces, particularly mineral oxides, are hygroscopic and provide an alternate destination for water that is present in the system. Therefore, it is important to determine where the water resides and whether or not this is dependent on how the moisture is introduced to the system. For example, if a hygroscopic particle that has been dried in an oven is dispersed in a surfactant solution, will the particle scavenge water from the reverse micelles? Of ultimate interest is how the presence of moisture in these systems affects particle charging. It has been shown previously that the progressive drying of mineral oxides diminishes their acid-base properties [105]. This would seem to suggest that at least some moisture must be present on the particle surface to facilitate the acid-base charging described in Section 1.3.

A systematic study of water content in solutions containing silica particles dispersed with OLOA 11000 and Isopar-L was carried out in the authors' laboratory to attempt to answer some of these questions [30]. Water was introduced to the system via both the particles and the

surfactant solution, and the location of the water at equilibrium was determined using Karl Fischer titration and centrifugation. It was found that roughly 80 – 90% of the water present in the system was adsorbed at the silica surface. This was true regardless of the surfactant concentration, quantity of water, or how it was introduced to the system. The exception occurred when a very large water amount of water was present in the system, suggesting that the particle surfaces were saturated with water. In addition, the conductivity of the system was compared with and without the presence of particles, after normalizing for the amount of water located in the reverse micelles. It was observed that the conductivity increased upon addition of silica particles, indicating charge was generated as a result of an interaction between the particles and the surfactant solution. The results support the mechanism of acid-base charging discussed in Section 1.3. It should be noted that these results are the opposite of what was observed in a study conducted by Dukhin [40], in which the conductivity of alumina/Span 80/kerosene dispersions were seen to decrease upon addition of particles. One possible explanation for this apparent contradiction is that the alumina particles were dried in an oven before being dispersed in solution to regulate the amount of water in the system. The dry particles likely scavenged some water from the Span 80 reverse micelles once they were introduced to the system, shrinking their polar cores, and decreasing the conductivity of the solution.

The last phase of the study of water in silica/OLOA 11000/Isopar-L dispersions was to examine the effect of water content on the particle electrophoretic mobility, and the results are reproduced in Figure 1.11 [30]. It was observed that for OLOA 11000 concentrations near the CMC an addition of water resulted in increased particle charging, suggesting that added water helped facilitate micelle-particle charging events. Conversely, at OLOA 11000 concentrations well above the CMC the particle electrophoretic mobility decreased with increasing water

content. This is likely because in this regime charge screening or neutralization becomes a strong influence on particle electrophoretic mobility.

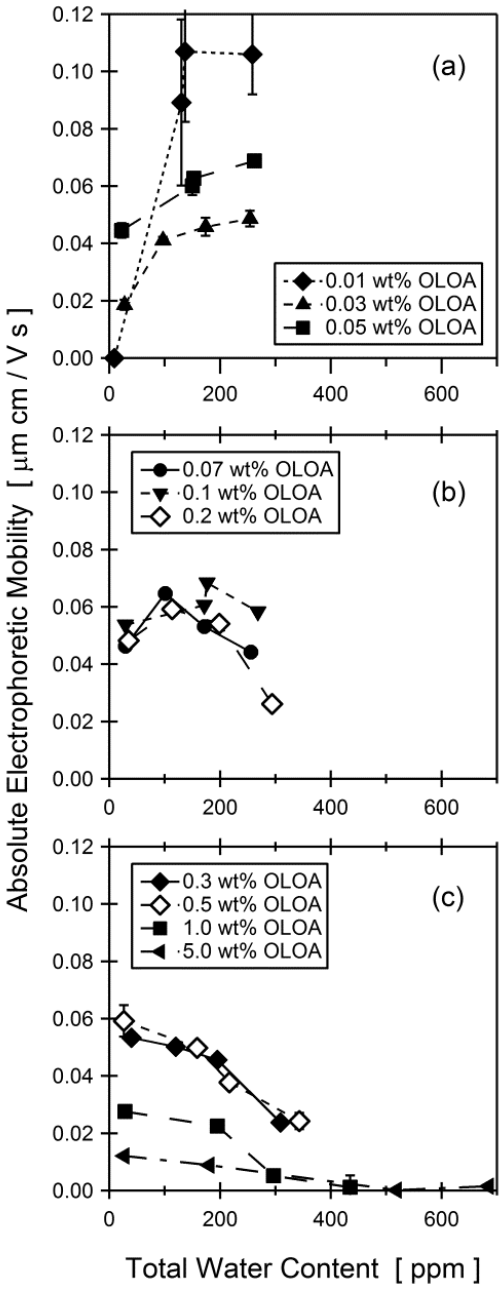

Figure 1.11. Effect of water on silica particle charging. The magnitude of the particle electrophoretic mobility is plotted as a function of total water content for (a) small, (b) intermediate, and (c) large OLOA 11000 concentrations. Error bars are derived from three measurements, and are often smaller than the markers. Reprinted with permission from [Gacek, M.; Bergsman, D.; Michor, E.; Berg, J.C. Langmuir 2012, 28, 11633-11638]. Copyright [2012] American Chemical Society.

Adding water to the system will swell the reverse micelles, enhancing micelle-micelle charging, and increasing the charge in the bulk solution available for screening or neutralizing the particle. It is clear that the presence of trace water in these systems is of critical importance to charge stabilization, and it must be accounted for when studying other aspects of these systems.

1.5. Surfactant structure

Much has already been discussed of the importance of the functionality of the head group in influencing the polarity and magnitude of particle charge. However, of equal importance is the overall structure of the surfactant monomer, the building block for forming reverse micelles. The molecular weight, length, and branching of the nonpolar tail group in relation to the polar head group is of critical importance to the CMC, the packing parameter of the reverse micelles, whether or not the surfactant can form reverse micelles, the solubility of the surfactant in solution, and the steric stability gained from surfactant adsorbed on particle surfaces. The hydrophile-lipophile balance (HLB) number is a simple way to categorize the size of the polar head group relative to the nonpolar tail of surfactants. The HLB number is defined as twenty times the molecular weight of the hydrophilic portion of the surfactant divided by the total molecular weight of the surfactant. While it is not a perfect indicator of all properties, as it does not account for a number of structure-specific effects, it does provide a quick means for classifying surfactants. To study the effects of surfactant structure on charging in apolar systems requires careful, systematic variation of either the head group or the tail group.

One such study was conducted by Parent and coworkers [58], where they studied a series of polyisobutylene succinimide (PIBS) surfactants synthesized with polyamine head groups of various lengths. These surfactants are very similar to the commercially available OLOA

surfactants. In this study, the reverse micelle size and structure was studied as well as the concentration of charged micelles and the charge imparted to magenta particles. It was found that a larger polyamine head group resulted in a larger polar core for the reverse micelle and a larger concentration of micelles that acquired charge. The explanation for this is identical to the explanation for reverse micelles that are swelled with water: the larger the polar core, the more energetically favorable it is to house charge. The magenta particle charging results, reproduced in Figure 1.12, showed an initial spike as a small polyamine was added, but then deceasing particle charge with increasing polyamine head group length.

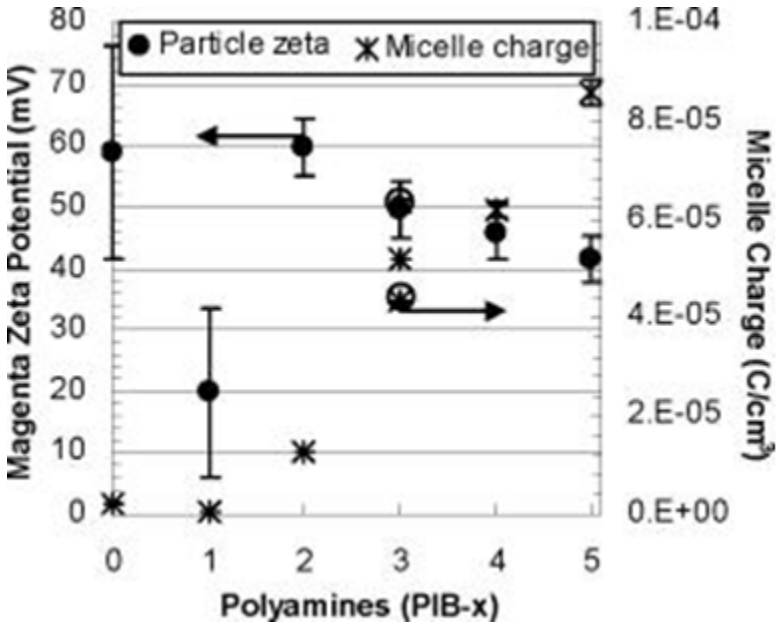

Figure 1.12. (●) Particle zeta potential and (*) surfactant-only solution charge concentration for samples made with PIB-1 through PIB-5 as well as O11k in outlined markers. Reprinted with permission from [Parent, M.E.; Yang, J.; Jeon, Y.; Toney, M.F.; Zhou, Z.L.; Henze, D.; Langmuir 2011, 27, 11845-11851]. Copyright [2011] American Chemical Society.

The explanation for this is that all of the dispersions were prepared at 3 wt % surfactant, which is well above the CMC. It is presumed that at this large concentration of surfactant charge screening or neutralization plays an important role in determining the particle zeta potential. In

this regime, a reverse micelle that is more capable of housing charge will only enhance the screening or neutralization, similar to the effects seen with increasing surfactant concentration [31,39,40,58–60] or micelle swelling [30].

Another systematic study was conducted by Dukhin [40] of commercial surfactants of the sorbitan ester (Span) family in kerosene. It was observed that the HLB value of the different surfactants (HLB values ranged from 1.8 to 8.6) scaled directly with the solution conductivity for any given concentration of surfactant. The results support the same trend as the PIBS study discussed above in that a larger HLB value surfactant will likely form a reverse micelle with a larger polar core. This study was followed up by one from the current authors' laboratory in which the same Span series was used to charge a series of mineral oxides dispersed in Isopar-L [101]. It was discovered that when the maximum particle electrophoretic mobility as a function of surfactant concentration was plotted against the particle PZC (similar to the study on AOT discussed in Section 1.3) the slope of the line increased with increasing HLB, reproduced in Figure 1.13.

The conclusion was that a larger HLB value would make the surfactant reverse micelles more capable of housing charge when interacting with the particle surface, increasing the magnitude of charge that was imparted to the particle. It should be noted that this trend is for the maximum particle charge observed. The Span with the largest HLB displayed significant charge screening/neutralization over a larger range of concentrations. Therefore, the intermediate HLB value Span was the most robust in its ability to impart charge to the mineral oxide particles, which is a similar conclusion to the study by Parent and coworkers [58].

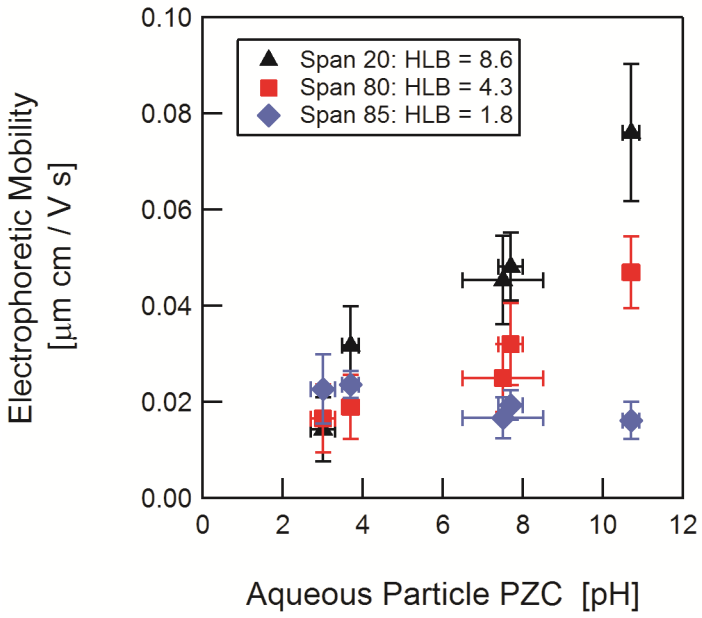

Figure 1.13. The maximum zero-field electrophoretic mobility of silica, titania, alumina, zinc oxide, and magnesia particles dispersed in Isopar-L are plotted against their aqueous PZCs. The particles were dispersed with Span 20 (▲), Span 80 (■), and Span 85 (♦). Reprinted from [Gacek MM, Berg JC, J. Colloid Interface Sci., 2014; DOI: http://dx.doi.org/10.1016/j.jcis.2014.11.075], copyright (2014), with permission from Elsevier.

1.6. Conclusions

How particles obtain charge in apolar environments has continued to be a subject of great interest in the scientific community. After many decades of research, there is much that is still not fully understood about these systems. However, the last twenty years have yielded a number of important breakthroughs in clarifying how and why charge can be stabilized on particles dispersed in apolar systems. Significant charge stabilization is facilitated by the formation of surfactant aggregates that take the form of reverse micelles. It has been shown through a variety of studies that, for surfactants that form reverse micelles, the size of the polar core is the key parameter in determining how readily charge can be stabilized. A larger reverse micelle core will

result in a larger probability of a micelle obtaining charge. The size of the polar core can be manipulated by the surfactant structure or the amount of trace moisture in the system.

Another important aspect of particle charging in these systems is the occurrence of charge screening or neutralization at large surfactant concentrations. In most systems it is observed that at a certain surfactant concentration there is enough charge in the bulk solution generated by micelle-micelle charging to cause the particle zeta potential to diminish with increasing surfactant. The maximum particle charge that can be obtained as well as the concentration at which the maximum occurs is primarily dependent on how chargeable a reverse micelle is (i.e. the polar core size). This competition between micelle-micelle and micelle-particle charging will always be an important factor when attempting to optimize these systems for a particular application. The maximum observed particle charge as a function of surfactant concentration is often used to compare different particle/surfactant systems.

The focus of this review is the role of acid-base effects on charging of dispersed colloidal particles in low dielectric systems. There is significant evidence, with a variety of systems, to suggest that the polarity and magnitude of particle charge is dictated by the relative acid-base properties of the particle surface and the charge-stabilizing surfactant. However, characterizing the relevant acid-base properties can be challenging. One prevailing theory for particle charging is that an acid-base adduct is formed between adsorbed surfactant monomers and the particle surface groups. When the monomer desorbs from the surface, there is a finite probability that it will result in an exchange of charge; where the charged monomer is stabilized in a nearby reverse micelle leaving a net charge on the particle surface. This review highlights several studies that demonstrate the validity of acid-base particle charging for mineral oxide, carbon black, organic pigment, and polymer particles. It is also possible that water must be present on

the particle surface to facilitate this type of acid-base charge transfer. Additionally, the maximum particle charge that can be obtained appears to be limited by how readily a nearby reverse micelle will stabilize the counter charge that is generated at the particle surface.

The goal of this detailed account of factors affecting particle charging in apolar media is to develop a general relationship that can be applied to as many different particle and surfactant systems as possible. The two most important parameters are the relative acidity or basicity of the particle and the surfactant. The particle acidity or basicity is most commonly defined by the point of zero charge (PZC) or the isoelectric point (IEP), yielding a single parameter ranking in terms of pH. However, PZC or IEP tests cannot be performed on some materials because they are soluble in water, are susceptible to specific adsorption of ions, or are chemically modified during the course of the acid-base titration. In these cases, it is necessary to employ inverse gas chromatography or some other technique to assign a relevant "acid-base number" to such particles. The surfactant acidity or basicity can be ranked by using a series of mineral oxides of varying PZCs as probes. Plotting the maximum particle electrophoretic mobility as a function of oxide PZC yields a linear relationship, and the point that the particles reverse polarity from positive to negative can be designated as the "effective pH" or "acid-base number" of the surfactant, as shown in Figure 1.5. With these two parameters, one can establish a general relationship in which the particle zeta potential is proportional to the difference in the "particle pH" and the "surfactant pH".

It is universally observed, for every particle and surfactant mixture studied in the authors' laboratory, that the particle charges positively when it is more basic than the surfactant and the particle charges negatively when it is more acidic than the surfactant. While the polarity of charge is correctly accounted for, the above relationship fails to account for the differences in

magnitude of particle charge that can be stabilized by different types of surfactants. As previously discussed, the size of the polar core of the reverse micelles is an important parameter in determining how readily a reverse micelle can stabilize charge, and it can be affected by the surfactant structure and the amount of trace water in the system. Ideally, one could directly measure the polar core size using small angle neutron scattering (SANS) for every surfactant used at many different water contents. Unfortunately, this would require a large amount of time and resources. A simpler and approximate indicator of reverse micelle core size is the surfactant HLB value, assuming water content is regulated. It was shown in Figure 1.13 that the surfactant HLB value scales directly with the ability for different Span surfactants to stabilize charge on mineral oxide particles. Therefore, it seems appropriate for the present analysis to scale the maximum particle zeta potential with the surfactant HLB value.

$$\zeta \propto HLB_{surfactant}\left(pH_{PZC} - pH_{surfactant}\right) \tag{1.23}$$

where ζ is the maximum particle zeta potential as a function of surfactant concentration, $HLB_{surfactant}$ is the HLB value of the surfactant, pH_{PZC} is the particle point of zero charge (sometimes approximated with inverse gas chromatography comparison), and the $pH_{surfactant}$ is the "effective pH" of the surfactant as determined by a series of mineral oxide probes. To test the effectiveness of this relationship, ζ / $HLB_{surfactant}$ is plotted as a function of $pH_{PZC} - pH_{surfactant}$ (or ΔpH) for every particle and surfactant system studied in the author's laboratory, as shown in Figure 1.14. It should be noted that this relationship is only generally applicable because the water content was maintained at a relatively constant level across all experiments by using an oven to dry the particles and desiccators to store the samples.

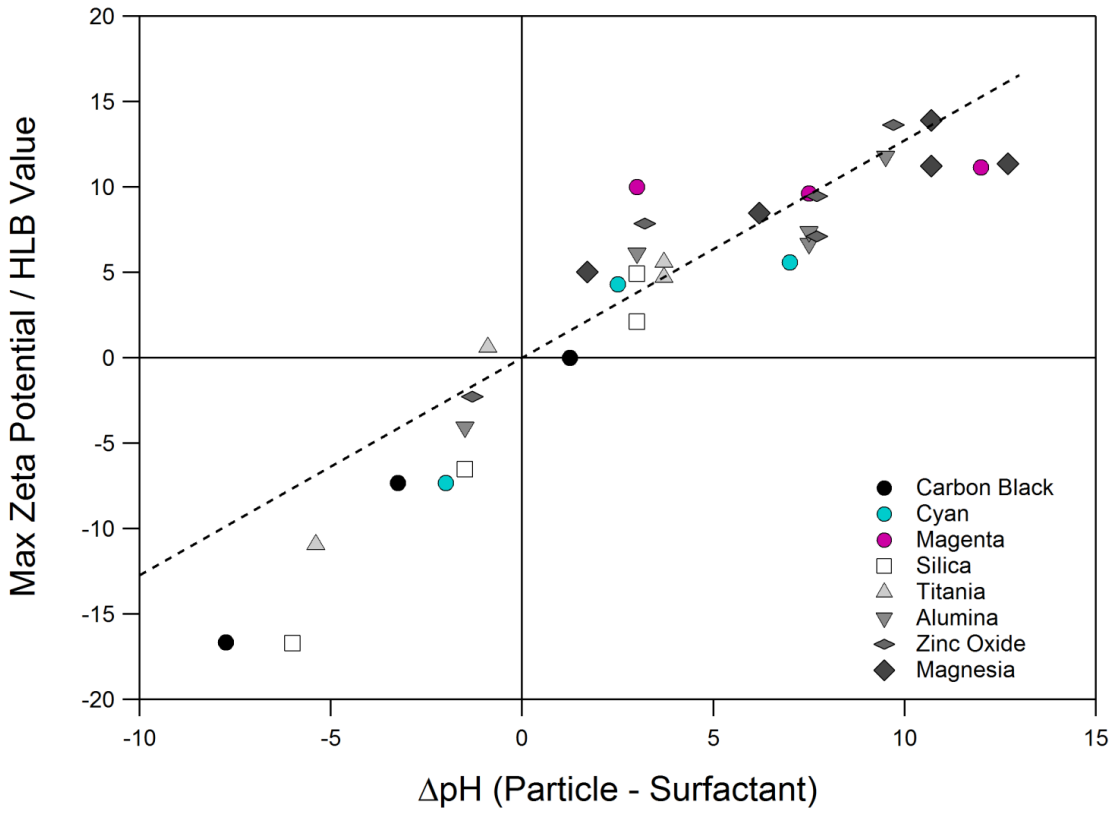

Figure 1.14. Combined charging data for all particle and surfactant systems studied in the author's laboratory. The maximum particle zeta potential scaled by the surfactant HLB value is plotted against the relative acid-base properties of the particle and the surfactant. The particles were dispersed in either Isopar-L or heptane with a range of surfactants including: AOT, OLOA 11000, Span 20, Span 80, and Span 85. Error bars have been omitted for the clarity of the figure, but are often approximately ± 3 – 5 mV/HLB in the y-direction and ± 1 – 2 pH in the x-direction.

It can be observed that, remarkably, nearly every data point falls near a single line. This suggests the broad applicability of the relationship between the relative acid-base properties of particles and surfactants and how particles charge in apolar media. There is obvious room for empirical refinement of this relationship that makes use of micelle core size data and possibly incorporates water content. Another aspect that this relationship does not take into account is the "hard" and "soft" nature of the acid-base interactions of the particle and surfactant. For the present, this represents an important advancement in the understanding of how and why particles charge in apolar media.

Another potentially important factor that was not detailed in this review is the effect of temperature. Many applications that involve particle charging in apolar media operate at elevated temperature, particularly ink jet printers. One would expect that increased temperature would increase the probability that charge is generated in these systems. This could increase the charge on a particle surface, but it might also increase the amount of charge screening or neutralization that is observed at large surfactant concentrations. It is also apparent that the validation of many of the theories of charge stabilization in apolar media requires more studies of the structure of reverse micelles in apolar media, information that can be obtained through careful use of small angle neutron scattering (SANS). It is the hope that a better understanding of the mechanism(s) of charge stabilization in apolar media will lead to better optimization and performance of devices in the future.

1.7. Acknowledgements

This work was supported in part by a gift from the Xerox Corp., and by the Center for Surfaces, Polymers, and Colloids at the University of Washington.

1.8. References

[1] Cady, H.P.; Lichtenwalter, H.O.; *J. Am. Chem. Soc.* **1913**, *35*, 1434–1440.

[2] Cady, H.P.; Baldwin, E.J.; *J. Am. Chem. Soc.* **1921**, *43*, 646–651.

[3] Kahlenberg, L.; Ruhoff, O.E.; *J. Phys. Chem.* **1902**, *7*, 254–258.

[4] Klinkenberg, A.; van der Minne, J.L.; Electrostatics in the petroleum industry: the prevention of explosion hazards; a Royal Dutch/Shell research and development report, *Elsevier*; **1958**.

[5] Morrison, I.; *Colloids Surf. Physicochem. Eng. Asp.* **1993**, *71*, 1–37.

[6] McGown, D.N.L.; Parfitt, G.D.; Willis, E.; *J. Colloid Sci.* **1965**, *20*, 650–664.

[7] Lewis, K.E.; Parfitt, G.D.; *Trans. Faraday Soc.* **1966**, *62*, 1652–1661.

[8] Briscoe, W.H.; Horn, R.G.; *Langmuir* **2002**, *18*, 3945–3956.

[9] Koelmans, H.; Overbeek, J.T.G.; *Discuss. Faraday Soc.* **1954**, *18*, 52–63.

[10] Lyklema, J.; *Adv. Colloid Interface Sci.* **1968**, *2*, 67–114.

[11] Morrison, I.D.; *Langmuir* **1991**, *7*, 192–1922.

[12] Sainis, S.K.; Germain, V.; Mejean, C.O.; Dufresne, E.R.; *Langmuir* **2008**, *24*, 1160–1164.

[13] Pugh, R.J.; Matsunaga, T.; Fowkes, F.M.; *Colloids Surf.* **1983**, *7*, 183–207.

[14] Pugh, R.J.; Fowkes, F.M.; *Colloids Surf.* **1984**, *11*, 423–427.

[15] Pugh, R.J.; Fowkes, F.M.; *Colloids Surf.* **1984**, *9*, 33–46.

[16] Fowkes, F.M.; Pugh, R.J.; *ACS Symp. Ser.* **1984**, *240*, 331-354.

[17] Comiskey, B.; Albert, J.D.; Yoshizawa, H.; Jacobson, J.; *Nature* **1998**, *394*, 253–255.

[18] Chen, Y.; Au, J.; Kazlas, P.; Ritenour, A.; Gates, H.; McCreary, M.; *Nature* **2003**, *423*, 136–136.

[19] Bert, T.; Beunis, F.; Smet, H.; Neyts, K.; *Displays* **2006**, *27*, 35–38.

[20] Murau, P.; Singer, B.; *J. Appl. Phys.* **1978**, *49*, 4820–4829.

[21] Pontiga, F.; Castellanos, A.; *IEEE Trans. Ind. Appl.* **1996**, *32*, 816–824.

[22] Ruckenstein, E.; Nagarajan, R.; *J. Phys. Chem.* **1980**, *84*, 1349–1358.

[23] Shrestha, L.K.; Sato, T.; Aramaki, K.; *Langmuir* **2007**, *23*, 6606–6613.

[24] Eicke, H.-F.; *Top. Curr. Chem.* **1980**, *87*, 85–145.

[25] Barz, D.P.J.; Vogel, M.J.; Steen, P.H.; *Langmuir* **2010**, *26*, 3126–3133.

[26] Alexandridis, P.; Andersson, K.; *J Phys Chem B* **1997**, *101*, 8103–8111.

[27] Eicke, H.-F.; Christen, H.; *Helv. Chim. Acta* **1978**, *61*, 2258–2263.

[28] Michor, E.L.; Berg, J.C.; *Langmuir* **2012**, *28*, 15751–15755.

[29] Hsu, M.F.; Dufresne, E.R.; Weitz, D.A.; *Langmuir* **2005**, *21*, 4881–4887.

[30] Gacek, M.; Bergsman, D.; Michor, E.; Berg, J.C.; *Langmuir* **2012**, *28*, 11633–11638.

[31] Sainis, S.K.; Merrill, J.W.; Dufresne, E.R.; *Langmuir* **2008**, *24*, 13334–13337.

[32] Strubbe, F.; Verschueren, A.R.M.; Schlangen, L.J.M.; Beunis, F.; Neyts, K.; *J. Colloid Interface Sci.* **2006**, *300*, 396–403.

[33] Prieve, D.C.; Hoggard, J.D.; Fu, R.; Sides, P.J.; Bethea, R.; *Langmuir* **2008**, *24*, 1120–1132.

[34] Kornilovitch, P.; Jeon, Y.; *J. Appl. Phys.* **2011**, *109*, 064509.

[35] Jeon, Y.; Kornilovitch, P.; Beck, P.; Zhou, Z.L.; Henze, R.; Koch, T.; *J. Soc. Inf. Disp.* **2011**, *19*, 614–619.

[36] Kim, J.; Anderson, J.L.; Garoff, S.; Schlangen, L.J.M.; *Langmuir* **2005**, *21*, 8620–8629.

[37] Karvar, M.; Strubbe, F.; Beunis, F.; Kemp, R.; Smith, A.; Goulding, M.; Neyts, K.; *Langmuir* **2011**, *27*, 10386–10391.

[38] Kitahara, A.; Amano, M.; Kawasaki, S.; Kon-no, K.; *Colloid Polym. Sci.* **1977**, *255*, 1118–1121.

[39] Poovarodom, S.; Berg, J.C.; *J. Colloid Interface Sci.* **2010**, *346*, 370–377.

[40] Dukhin, A.S.; Goetz, P.J.; *J. Electroanal. Chem.* **2006**, *588*, 44–50.

[41] Kemp, R.; Sanchez, R.; Mutch, K.J.; Bartlett, P.; *Langmuir* **2010**, *26*, 6967–6976.

[42] Strubbe, F.; Beunis, F.; Marescaux, M.; Neyts, K.; *Phys. Rev. E* **2007**, *75*, 031405.

[43] Lyklema, J.; Fundamental of Interface and Colloid Science IV. Particulate Colloids, *Elsevier*; **2005**.

[44] Smith, P.G.; Patel, M.N.; Kim, J.; Milner, T.E.; Johnston, K.P.; *J. Phys. Chem. C* **2007**, *111*, 840–848.

[45] Patel, M.N.; Smith, P.G.; Kim, J.; Milner, T.E.; Johnston, K.P.; *J. Colloid Interface Sci.* **2010**, *345*, 194–199.

[46] Cao, H.Y.; Cheng, Y.J.; Huang, P.W.; Qi, M.; *Nanotechnology* **2011**, *22*, 445709.

[47] Roberts, G.S.; Sanchez, R.; Kemp, R.; Wood, T.; Barlett, P.; *Langmuir* **2008**, *24*, 6530–6541.

[48] Riddle, F.L.; Fowkes, F.M.; *J. Am. Chem. Soc.* **1990**, *112*, 3259–3264.

[49] Guo, Q.; Lee, J.; Singh, V.; Behrens, S.H.; *J. Colloid Interface Sci.* **2013**, *392*, 83–89.

[50] Gacek, M.; Brooks, G.; Berg, J.C.; *Langmuir* **2012**, *28*, 3032–3036.

[51] Labib, M.E.; Williams, R.; *Colloids Polym. Sci.* **1986**, *264*, 533–541.

[52] Labib, M.E.; Williams, R.; *J. Colloid Interface Sci.* **2984**, *97*, 356–357.

[53] Mysko, D.D.; Berg, J.C.; *Ind. Eng. Chem. Res.* **1993**, *32*, 854–858.

[54] Verwey, E.J.W.; *Recl. Trav. Chim. Pays-Bas* **1941**, *60*, 625–633.

[55] Kosmulski, M.; Electrical Interfacial Layer in Nonaqueous Solvents, *Surfactant Sci. Ser.;* **2000**.

[56] Kosmulski, M.; *Colloids Surf. Physicochem. Eng. Asp.* **1999**, *159*, 277–281.

[57] Siffert, B.; Eleli-Letsango, J.; Jada, A.; Papirer, E.; *Colloids Surf. Physicochem. Eng. Asp.* **1994**, *92*, 107.

[58] Parent, M.E.; Yang, J.; Jeon, Y.; Toney, M.F.; Zhou, Z.L.; Henze, D.; *Langmuir* **2011**, *27*, 11845–11851.

[59] Poovarodom, S.; Berg, J.C.; *J. Colloid Interface Sci.* **2011**, *351*, 415–420.

[60] Keir, R.; Suparno; Thomas, J.C.; *Langmuir* **2002**, *18*, 1463–1465.

[61] Espinosa, C.E.; Behrens, S.H.; Guo, Q.; *Langmuir* **2010**, *26*, 16941–16948.

[62] Keir, R.; Quinn, A.; Jenkins, P.; Thomas, J.C.; Ivanova, O.; *J. Imaging Sci. Technol.* **2000**, *44*, 528–533.

[63] Gacek, M.M.; Berg, J.C.; *Langmuir* **2012**, *28*, 17841–17845.

[64] Ohshima, H.; Furusawa, K.; Electrical phenomena at interfaces: fundamentals, measurements, and applications, *M. Dekker*; **1998**.

[65] Bazant, M.Z.; Squires, T.M.; *Curr. Opin. Colloid Interface Sci.* **2010**, *15*, 203–213.

[66] Sun, C.; Berg, J.C.; *Adv. Colloid Interface Sci.* **2003**, *105*, 151–175.

[67] Berg, J.C.; Wettability, *CRC Press*; **1993**.

[68] Arrhenius, S.*Z.; Phys. Chem.* **1887**, *1*, 631.

[69] Bronsted, J.N.; *Recl. Trav. Chim. Pays-Bas* **1923**, *42*, 718–728.

[70] Lowry, T.M.; *J. Soc. Chem. Ind.* **1923**, *42*, 43–47.

[71] Lewis, G.N.; Valence and the structure of atoms and molecules, *The Chemical Catalog Company, Inc.*; **1923**.

[72] Jensen, W.B.; The Lewis acid-base concepts: an overview, *Wiley*; **1979**.

[73] Rossotti, F.J.C.; Rossotti, H.; The determination of stability constants: and other equilibrium constants in solution. *McGraw-Hill*; **1961**.

[74] ASTM D664-11a; Standard Test Method for Acid Number of Petroleum Products by Potentiometric Titration, *ASTM International*; **2011**. DOI: 10.1520/D0664-11A

[75] ASTM D2896-11; Standard Test Method for Base Number of Petroleum Products by Potentiometric Perchloric Acid Titration, *ASTM International*; **2011**. DOI: 10.1520/D2896-11

[76] Gutmann, V.; Steining, A.; Wychera, E.; *Monatshefte Chem. Verwandte Teile Anderer Wiss.* **1966**, *97*, 460.

[77] Mayer, U.; Gutmann, V.; Gerger, W.; *Monatshefte Chem.* **1975**, *106*, 1235–1257.

[78] Gutmann, V.; The donor-acceptor approach to molecular interactions, *Plenum Press;* **1978**.

[79] Drago, R.; Wayland, B.; *J. Am. Chem. Soc.* **1965**, *87*, 3571.

[80] Pearson, R.G.; Hard and soft acids and bases, *Dowden, Hutchinson & Ross*; **1973**.

[81] Mulliken, R.; *J. Phys. Chem.* **1952**, *56*, 801–822.

[82] Edwards, J.O.; *J. Am. Chem. Soc.* **1954**, *76*, 1540–1547.

[83] Vanoss, C.; Chaudhury, M.; Good, R.; *Adv. Colloid Interface Sci.* **1987**, *28*, 35–64.

[84] Kwok, D.Y.; *Colloids Surf. Physicochem. Eng. Asp.* **1999**, *156*, 191–200.

[85] Kosmulski, M.; Chemical properties of material surfaces. Vol. 102, *Marcel Dekker*; **2001**.

[86] Kosmulski, M.; *J. Colloid Interface Sci.* **2011**, *353*, 1–15.

[87] Berg, J.C.; An introduction to interfaces & colloids: the bridge to nanoscience, *World Scientific;* **2010**.

[88] Watts, J.; Chehimi, M.; *J. Adhes.* **1993**, *41*, 81–91.

[89] Mullins, W.; Averbach, B.; *Surf. Sci.* **1988**, *206*, 41–51.

[90] Delamar, M.; *J. Electron Spectrosc. Relat. Phenom.* **1990**, *53*, C11–C14.

[91] Fowkes, F. M. *et al.* Acid-base complexes of polymers. *POL J. Polym. Sci. Polym. Chem. Ed.* 22, 547–566 (1984).

[92] Auroux, A.; Gervasini, A.; *J. Phys. Chem.* **1990**, *94*, 6371–6379.

[93] Lyklema, J.; Fundamentals of Interface and Colloid Science.: Volume II: Solid-Liquid Interfaces, *Academic Press;* **1995**.

[94] Leunissen, M.E.; van Blaaderen, A.; Hollingsworth, A.D.; Sullivan, M.T.; Chaikin, P.M.; *Proc. Natl. Acad. Sci. U.S.A.* **2007**, *104*, 2585–2590.

[95] Marinova, K.G.; Alargova, R.G.; Denkov, N.D.; Velev, O.D.; Petsev, D.N.; Ivanov, I.B.; Borwankar, R.P.; *Langmuir* **1996**, *12*, 2045–2051.

[96] Kreuzer, H.J.; Wang, R.L.C.; Grunze, M.; *J. Am. Chem. Soc.* **2003**, *125*, 8384–8389.

[97] Vacha, R.; Zangi, R.; Engberts, J.B.F.N.; Jungwirth, P.; *J. Phys. Chem. C* **2008**, *112*, 7689–7692.

[98] Basch, A.; Horn, R.; Besenhard, J.O.; *Colloids Surf. Physicochem. Eng. Asp.* **2005**, *253*, 155–161.

[99] Gacek, M.M.; Berg, J.C.; *Electrophor.* **2014**, *35*, 1766–1772.

[100] Basu, S.; *Colloid Polym. Sci.* **1998**, *276*, 420–426.

[101] Gacek, M.M.; Berg, J.C.; *J. Colloid Interface Sci.* **2014**. doi: http://dx.doi.org/10.1016/j.jcis.2014.11.075

[102] Malbrel, C.; Somasundaran, P.; *J. Colloid Interface Sci.* **1989**, *133*, 404–408.

[103] Malbrel, C.; Somasundaran, P.; *Langmuir* **1992**, *8*, 1285–1290.

[104] Guo, Q.; Singh, V.; Behrens, S.H.; *Langmuir* **2010**, *26*, 3203–3207.

[105] Sun, C.; Berg, J.C.; *J. Chromatogr. A* **2002**, *969*, 59–72.

The majority of this chapter has been recently submitted for publication as a review paper to *Advances in Colloid and Interface Science.*

Chapter 2

Investigation of the acid-base charging behavior of mineral oxides dispersed in apolar media in the presence of AOT

2.1. Summary

This chapter presents an investigation of the charging behavior of mineral oxide particles dispersed in apolar media. There are a growing number of applications that seek to use electrostatic effects in apolar media to control particle movement and improve aggregation stability. Progress is limited, however, by incomplete knowledge of the mechanism(s) of particle charging in these systems. It has been shown in a number of cases that the acid-base properties of both the particles and the surfactants used to stabilize charge play key roles. A mechanism for acid-base charging has previously been established for mineral oxides in aqueous systems, where the surface hydroxyl groups act as proton donors or receivers depending on the pH of the surrounding solution. In water, the pH at which the surface charge density is zero, i.e., the point of zero charge (PZC) can be used to characterize the acid-base nature of the mineral oxide particles. The current work explores the possible extension of this charging behavior to apolar systems, with the key difference that the surface hydroxyl groups of the mineral oxides react with the surfactant molecules instead of free ions in solution. The apolar charging behavior is explored by measuring the electrophoretic mobility of a series of mineral oxides dispersed in a solution of Isopar-L and AOT, a neutral surfactant in water. The electrophoretic mobility of the particles is found to scale quantitatively, both with respect to sign and magnitude, with their

aqueous PZC value. This provides support for the theory of acid-base charging in apolar media, and represents a method for predicting and controlling particle charge of mineral oxides dispersed in apolar media.

2.2. Introduction

There are a number of applications that currently make use of charged particles in apolar media. These include electro-photography, various paints and inks, and electrophoretic displays [1,2]. In these systems, the ability to manipulate and control the polarity and magnitude of surface charge is greatly desired. The difficulty in achieving this control stems from the fact that the precise charging mechanism(s) are actively debated, and the role of surface chemistry remains unclear [3,4]. It is, however, clear that the charging behavior in apolar media differs from that in aqueous systems. This is due, at least in part, to the difficulty of achieving charge separation in apolar (low dielectric) media. The separation required to prevent recombination and neutralization of charge is described by the Bjerrum length (λ_B), the distance of separation between opposite charges at which the Coulombic attraction energy is equal to the thermal energy k_BT. It is expressed as

$$\lambda_B = \frac{z^2 e^2}{4\pi\varepsilon\varepsilon_0 k_B T} \tag{2.1}$$

where z is the valence of charge, e is the elementary charge, ε is the dielectric constant of the medium, ε_0 is the permittivity of vacuum, k_B is Boltzmann's constant, and T is temperature. For 1-1 electrolytes, the room temperature Bjerrum length in water ($\varepsilon\approx78$) is about 0.7 nm, and in an apolar medium of dielectric constant 2 the Bjerrum length is about 28 nm. In water, the required charge separation is achieved by the formation of a hydration layer and charges freely dissociate. In apolar media, the charges must be stabilized by a physical barrier such as an inverse micelle,

polymer, or similar structure. It has been well documented over the years that the addition of oil-soluble surfactants allows particles dispersed in apolar fluids to obtain charge and become electrostatically stabilized [5-7].

While the exact mechanism of this charging is actively debated, the proposed mechanisms include: (1) preferential adsorption of charged species [8], (2) charge dissociation of functional groups and subsequent stabilization in inverse micelles [9], and (3) acid-base charge transfer between surface functional groups and adsorbed surfactant molecules, where polarity and magnitude are determined by the relative acidity (or basicity) of the particle and surfactant [10-12]. The third mechanism, proposed by Fowkes and coworkers, appears pertinent when considering the charging of mineral oxides due to the parallel that can be made with the well-established aqueous charging mechanism of oxides. In water, surface hydroxyl groups are charged by acid-base interactions with the surrounding solution, and the polarity and magnitude of charge is determined by the inherent acidity of the oxide and the pH of the solution. The acidity of the particle can then be characterized by the pH at which it has a net zero surface charge, otherwise known as the point of zero charge (PZC). Labib and Williams, in studies of mineral particles suspended in a range of different leaky dielectrics found a dependence of the sign and magnitude of the electrophoretic mobility of any given particle type on the Gutmann donor number of the solvent, and for particles that were mineral oxides, a correlation with their isoelectric points in water [13-15]. Others have found a similar correlation with donor number [16]. However, it remains unclear whether or not an aqueous characterization of oxide particle acidity can be correlated to surface charging in a completely apolar medium.

Previous work has shown that surface functionalizing silica particles to be more acidic or basic had a direct effect on the magnitude of the resulting surface potential [17]. It was

demonstrated that acidic functionalized silica particles obtained a large negative charge when in the presence of OLOA 11000 (a basic surfactant), compared to the relatively small negative charge obtained by basic functionalized silica. Conversely, in the presence of SPAN 80 (an acidic surfactant) the basic silica obtained a large *positive* charge, and the acidic silica exhibited a small positive charge. This was given as support to the acid-base charging mechanism proposed by Fowkes, where the basic surfactant (a proton acceptor or electron donor) carries out an acid-base driven charge transfer, leaving a negative surface charge, and vice versa with the acidic surfactant. In this case, the magnitude of charge was controlled by the relative acidity of the particle compared to the surfactant, but the polarity of charge was always determined by the surfactant. One possible explanation is that the unreacted hydroxyl groups on the surface of the modified silica particles act as bifunctional groups when interacting with the surfactant present in the system. This would explain the marginal positive charge observed on the acidic particles that were in the presence of an acidic surfactant, as well as the marginal negative charge observed on the basic particles in the presence of a basic surfactant. Therefore, the question remains: is the polarity of charge dependent only on the surfactant, or a combination of the surfactant and particle?

The surfactant of interest in the current study is dioctyl sodium sulfosuccinate, more commonly known as "AOT". In water, it is marginally acidic, with a pH of 5-7 observed for 1 wt% solutions [18]. AOT is often used as a "charge control agent" in apolar media, and has been shown to be capable of imparting positive and negative surface charges depending on the particle of interest [9,19,20]. In work done by Smith et al. [9] it was observed that untreated TiO_2 particles (Aeroxide P25) obtained a positive charge in the presence of AOT, whereas TiO_2 particles with octylsilane-treated surfaces (Aeroxide T805) displayed a negative charge. This was

explained by the "preferential partitioning of cations and sulfosuccinate anions" at the particle surface. This partitioning appeared to be governed by the hydrophilicity of the particle surface, in which "hydrophilic" Na^+ ions prefer to adsorb to the bare, hydrophilic TiO_2 surface. Conversely, the "hydrophobic sulfosuccinate ions" preferentially adsorb to the TiO_2 treated with octylsilane (or the cations desorb into "water-swollen" reverse micelles). As noted by Poovarodom [19], this mechanism proves insufficient for explaining the observed negative charge of bare, hydrophilic SiO_2 particles in solutions of Isopar-L and AOT. Therefore, the current work aims to investigate any apparent correlation between the inherent acidity (or basicity) of mineral oxides with their apolar charging behavior. This is carried out by measuring the electrophoretic mobility of a range of unmodified mineral oxides whose aqueous PZCs cover nearly the entire pH range. These particles are dispersed in the apolar Isopar-L solvent and AOT is to be used as the "charge control agent". The apolar electrophoretic mobility can then be plotted against the aqueous particle PZC or isoelectric point (IEP) to determine if there is any correlation.

2.3 Materials and methods

2.3.1. Materials

The apolar solvent chosen was Isopar-L, a commercial isoparaffinic hydrocarbon supplied by Exxon Mobil Chemical (Houston, TX). It consists of C8 to C15 saturated hydrocarbons, with an aromatics content of only 30 ppm, and a dielectric constant of 2.0. It was used as received.

The surfactant used was dioctyl sodium sulfosuccinate more commonly known as Aerosol-OT or AOT, and was obtained from Fisher Scientific (Pittsburgh, PA). AOT has a well-known structure and has been extensively used as a "charge control agent" for apolar dispersions

[3,4,21]. It has been reported by Kotlarchyk et al. that AOT forms spherical inverse micelles with a hydrodynamic diameter of 3.2 nm [22]. AOT is also known to be hygroscopic; therefore, the raw supply and the subsequent solutions were always stored in a desiccator to prevent any additional uptake of water.

The particles used were a series of mineral oxides: silica (SiO_2) from Fiber Optics Center Inc. (New Bedford, MA), titania (TiO_2) from J.T. Baker Chemical Co. (Phillipsburg, NJ), alumina (Al_2O_3) from Baikalox International Corp. (Charlotte, NC), zinc oxide (ZnO) from MK Nano (Mississauga, Ontario), and magnesia (MgO) from MTI Corp. (Richmond, CA). The particles ranged in size from 50 to 500 nm and were selected because their aqueous points of zero charge (PZC) are well documented and span a wide pH range. All particles were supplied in powder form and used as received.

2.3.2. Dispersion preparation

Particles of each type were dried at 120 ^{o}C for 2 hours before being added to solutions of AOT in Isopar-L at various concentrations of AOT. The particle loading in each of the dispersions was 500 ppm by weight. The dispersions were then sonicated for 3 hours and let stand for 24 hours. All dispersions were kept in a desiccator, except during sonication and measurement. Previous work has shown that oxide charging in apolar media can be affected by the amount of water in the system [9]. We anticipate that there was a nontrivial amount of water in our dispersions, considering that the pure Isopar-L had a water content of approximately 20 ppm, and Isopar including 1 wt% AOT registered approximately 300 ppm, as determined by Karl Fischer titration. The final dispersions were not tested, but the procedure outlined above was

designed to limit and regulate the water content in the system so that it would be consistent from sample to sample.

2.3.3. Measurement of electrophoretic mobility

The electrophoretic mobility of the apolar dispersions was measured by dynamic light scattering (DLS) using a Brookhaven Instruments Zeta-PALS. The measurements were conducted using a 200V sinusoidal voltage with a frequency of 2 Hz applied across electrodes spaced 0.5 cm apart. The instrument is theoretically capable of measuring mobilities as low as 0.001 (μm cm)/(s V). It was assumed that the measured mobility was independent of particle size, consistent with the Hückel regime, i.e., where $\kappa a < 0.1$, κ is the Debye parameter, and a is the particle radius. Bartlett and coworkers have shown this to be the case for dodecane with particle sizes and AOT concentrations used in the present study [3].

2.3.4. Aqueous particle charge characterization

The aqueous isoelectric point (IEP) of each particle was determined by electrokinetic titration. The above mentioned Zeta-PALS instrument was used to measure electrophoretic mobility. The pH was controlled with HNO_3 and KOH, and monitored with an Oakton Instruments 510 series pH/conductivity meter. The aqueous point of zero charge (PZC) of each particle was also determined by potentiometric titration using HNO_3 and KOH for pH control, and KNO_3 was used for the background electrolyte in concentrations of 0.001, 0.01, and 0.1 M.

2.4. Results

2.4.1. Aqueous particle charge characterization results

As previously mentioned, all of the particles used in this study are mineral oxides that have been extensively researched regarding their aqueous charging behavior. However, all of the materials exhibit a range of reported values and require experimental determination of their IEP and PZC if comparisons in charging behavior are to be made. Plots of the electrokinetic and potentiometric titrations performed on zinc oxide particles are shown in Figure 2.1 as an example. In many cases, a perfectly clean intersection of the potentiometric titration curves was not observed, as demonstrated in the bottom of Figure 2.1.

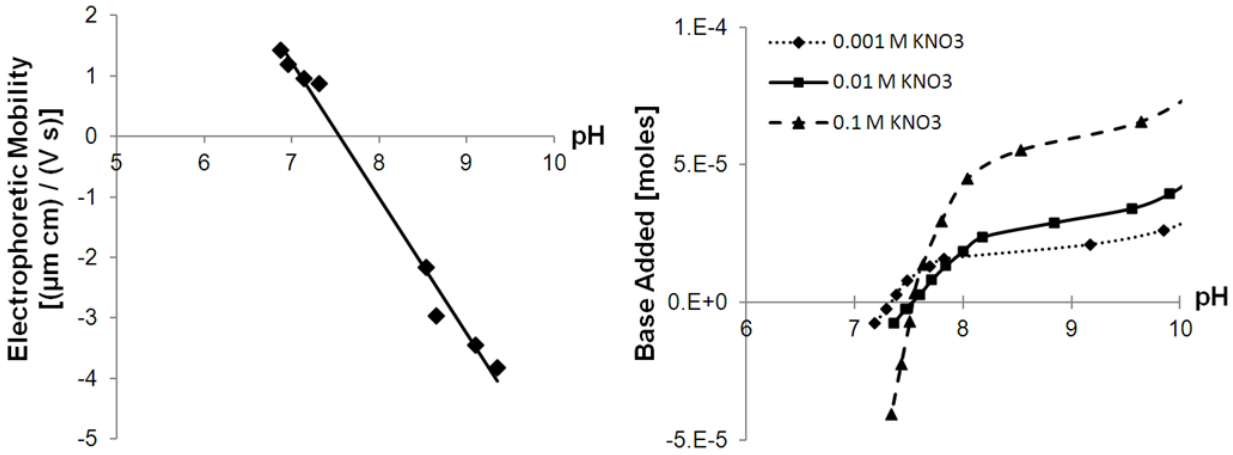

Figure 2.1. Aqueous IEP and PZC determination for zinc oxide particles. The left figure shows the electrokinetic titration results used to determine the zinc oxide aqueous IEP of 7.5 $\pm$ 0.5. The figure on the right shows the potentiometric titration used to determine the aqueous PZC for zinc oxide. No clean intersection of the curves was observed, but the range of intersections was taken as the error to arrive at a value of 7.7 $\pm$ 0.3.

The IEP and PZC results, as well as the reported ranges [23], for the particles are shown in Table 2.1. There were some small discrepancies between the reported values and the experimental results, namely the relatively low values of alumina, zinc oxide, and magnesia.

However, the predicted trend in IEP and PZC values is still observed and the materials chosen still provide a nice range of acid-base functionality. It should also be noted that the materials at the extreme ends of the PZC spectrum, silica and magnesia, are near the limit of what can be resolved without over saturating the system with electrolyte.

Table 2.1. Mineral oxide IEP and PZC data (in terms of pH)

Oxide	**IEP (Exp.)**	**PZC (Exp.)**	**PZC (Lit.)**
Silica	2.1 $\pm$ 0.3	3.0 $\pm$ 0.3	2-3
Titania (rutile)	4.0 $\pm$ 0.2	3.7 $\pm$ 0.2	4-6
Alumina	7.1 $\pm$ 0.3	7.5 $\pm$ 1.0	8-9
Zinc Oxide	7.5 $\pm$ 0.5	7.7 $\pm$ 0.3	9-10
Magnesia	8.5 $\pm$ 0.5	10.7 $\pm$ 0.2	10-12

Shown in this table are experimentally determined values of the IEP and PZC for each type of particle used in the study. The range of reported literature values are shown for comparison [23].

2.4.2. Electrophoretic mobility results in Isopar-L

It has been reported that the electrophoretic mobility of particles in apolar media will vary with surfactant concentration, often exhibiting a maximum [17,24,25]. This dependence on surfactant concentration was observed for all particle systems, with the maximum occurring at approximately 1.0 wt. % AOT in each case. This behavior is demonstrated in Figure 2.2 for silica dispersions. At very low AOT concentrations the measured mobilities were below the resolution of the instrument of 0.001 (μm cm) / (V s) and were therefore reported as zero.

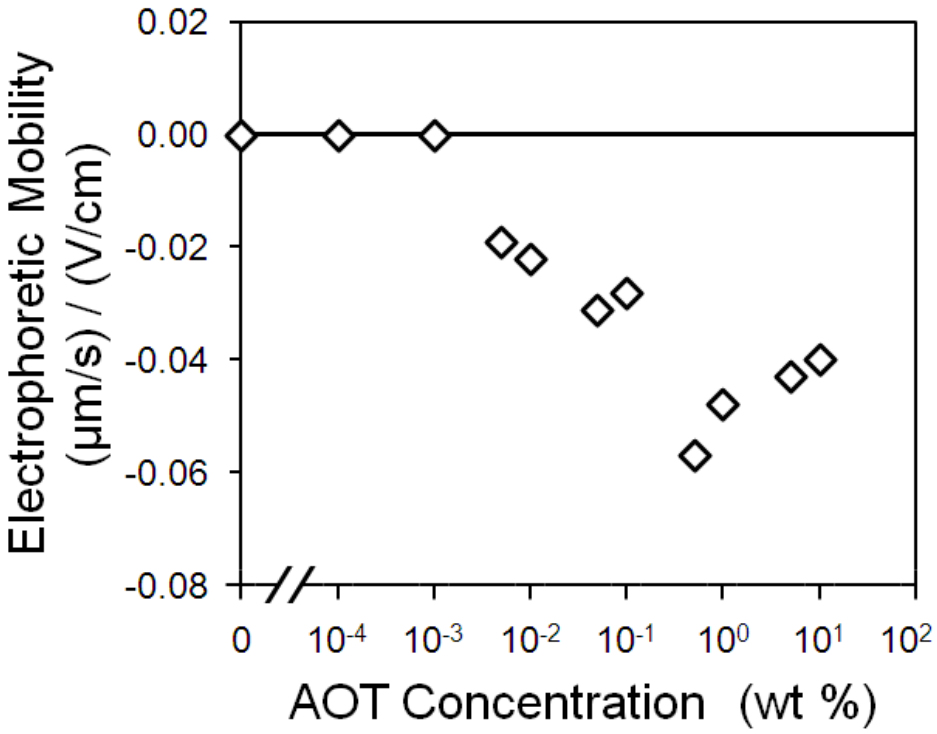

Figure 2.2. Electrophoretic mobility of silica particles dispersed in Isopar-L at various concentrations of AOT. Error bars are derived from 3 measurements and are of the same size or smaller than the data symbols.

The consistent AOT concentration of the maximum mobility from material to material makes it convenient to compare their charging behaviors via these maximum mobilities. In the case of silica, the most acidic, the particles obtained a negative surface charge and the maximum measured value was 0.056 (μm cm) / (V s). Titania did not exhibit much charging at any AOT concentration, with a maximum of positive 0.005 (μm cm) / (V s). The alumina, zinc oxide, and magnesia were all positively charged, with maximum mobilities of 0.053, 0.067, and 0.073 (μm cm) / (V s), respectively. These peak maximum mobilities are plotted against the corresponding aqueous IEP value in Figure 2.3, and they are plotted against the aqueous PZC value in Figure 2.4.

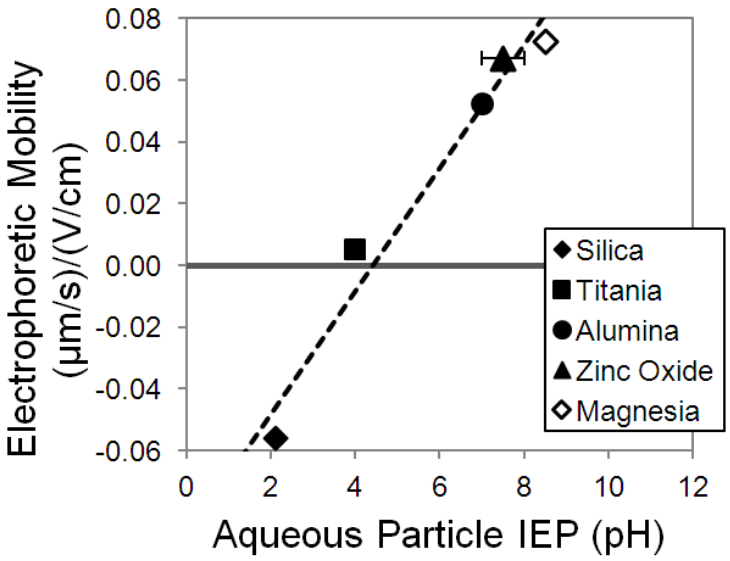

Figure 2.3. Mineral oxide apolar charging behavior (in terms of electrophoretic mobility) plotted against aqueous IEP value. The maximum electrophoretic mobility of the different oxides dispersed in AOT and Isopar-L are plotted against their aqueous isoelectric point (IEP) values. Note the nearly linear correlation between apolar mobility and aqueous IEP. The dashed line is drawn in to guide the eye. Error bars are derived from three measurements, and are equal to or smaller than the data symbols if not clearly visible.

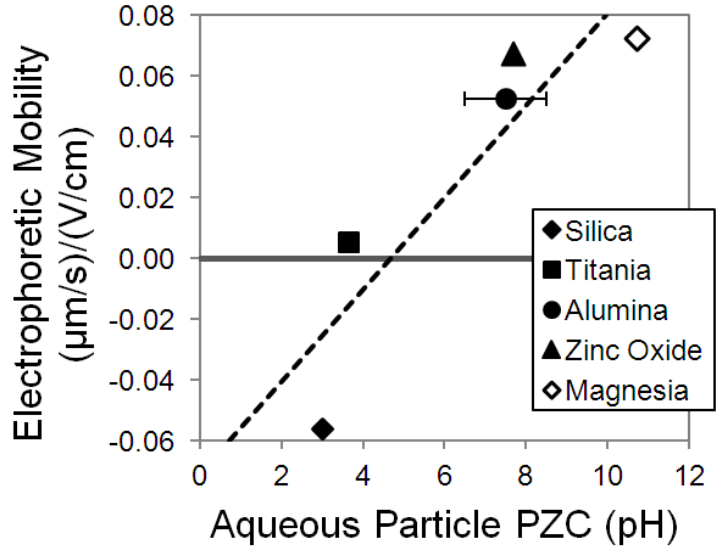

Figure 2.4. Mineral oxide apolar charging behavior (in terms of electrophoretic mobility) plotted against aqueous PZC value. The maximum electrophoretic mobility of the oxides dispersed in solutions of AOT and Isopar-L are plotted against their aqueous point of zero charge (PZC) values. The dashed line is drawn in to guide the eye. Error bars are derived from three measurements, and are equal to or smaller than the data symbols if not clearly visible.

2.4.3. Applied electric field effects

Before discussing the potential implications of these results, an important justification must be made. It has been shown that electric field strength can affect the electrophoretic mobility of apolar dispersions, especially near the surfactant CMC [26]. In this work, the maximum mobilities that are compared were at AOT concentrations well above the CMC, and are therefore not believed to be dependent on electric field strength. A test was done with silica particles dispersed in a solution of 1.0 wt. % AOT in Isopar-L where the electrophoretic mobility was measured at electric field strengths ranging from 20 to 70 kV/m. The results verify that the mobility was statistically independent of field strength over the entire range of applied fields. The remaining materials are assumed to behave similarly, but were not specifically tested at field strengths other than 40 kV/m.

2.5. Discussion

The purpose of this study was to investigate any possible relationship between the apolar charging behavior of unmodified mineral oxides with their relative acidity or basicity (characterized by their aqueous PZC value). The electrophoretic mobility was determined for a range of mineral oxides dispersed in Isopar-L and AOT. The mobility of each type of particle varied with AOT concentration, consistently exhibiting a maximum at approximately 1.0 wt. % AOT, as demonstrated in Figure 2.2. This behavior is consistent with the results of Poovarodom [17,19]. These maximum particle mobilities were then plotted against the aqueous IEP and PZC values of the oxides, as shown in Figures 2.2 and 2.3, respectively. Both figures show a nearly linear correlation between the inherent acidity of the particle and the apolar charging behavior (in both polarity and magnitude of charge). The most acidic, silica, obtained a negative surface

charge, titania exhibited a minimal positive charge, and the other increasingly basic particles exhibited an increasing magnitude of positive charge, respectively. These results provide support for the acid-base charging mechanism proposed by Fowkes and coworkers [10-12], where the polarity and magnitude of charge is determined by the relative acidity (or basicity) of both the surfactant and the particle.

One of the primary difficulties with the proposed mechanism has been the characterization of "acidity" in an apolar system. However, the observed charging behavior of these mineral oxides in AOT and Isopar-L is very similar to what one would observe in an aqueous system with a pH of approximately 5. As such, this could be thought of as an "effective pH" of the AOT and Isopar-L system, which would then provide a means for predicting the charge of other mineral oxides in such a system. Further investigation is needed to determine whether or not this behavior is consistent over a range of surfactants. One would anticipate that as long as the surfactant is amphoteric, both positive and negative surface charges would be observed depending on the relative acidity of the particle to the surfactant. If the surfactant were not amphoteric, the polarity of charge would be dictated by the surfactant; however, the magnitude of surface charge might still be dependent on particle acidity (or basicity). Specifically, with AOT, an acidic surface donates a proton to an adsorbed monomer, while a basic surface adsorbs the sodium ion, as shown schematically in Figure 2.5.

While these results appear to support the mechanism proposed by Fowkes and coworkers, it is far from definitive proof of an all-encompassing mechanism. As mentioned previously, the charge behavior of particles in the presence of AOT has been extensively studied in the past [9,19-21]. Research performed by Smith et al. [9] and Kitahara [20] support the theory that the particle's surface "hydrophobicity" or "hydrophilicity" plays a key role in apolar charging in the

presence of AOT. Both observed that hydrophilic TiO_2 particles obtained a positive charge in apolar systems containing AOT, whereas various hydrophobic particles obtained a negative charge. This was explained by the preferential adsorption of "hydrophilic" Na^+ ions to the bare TiO_2 surface and preferential adsorption of the "hydrophobic sulfosuccinate ions" to the TiO_2 treated with octylsilane. This specific adsorption mechanism is still plausible, but it would appear that the preferential adsorption of ions is driven by acid-base functionality, at least in the case of hydrophilic mineral oxides.

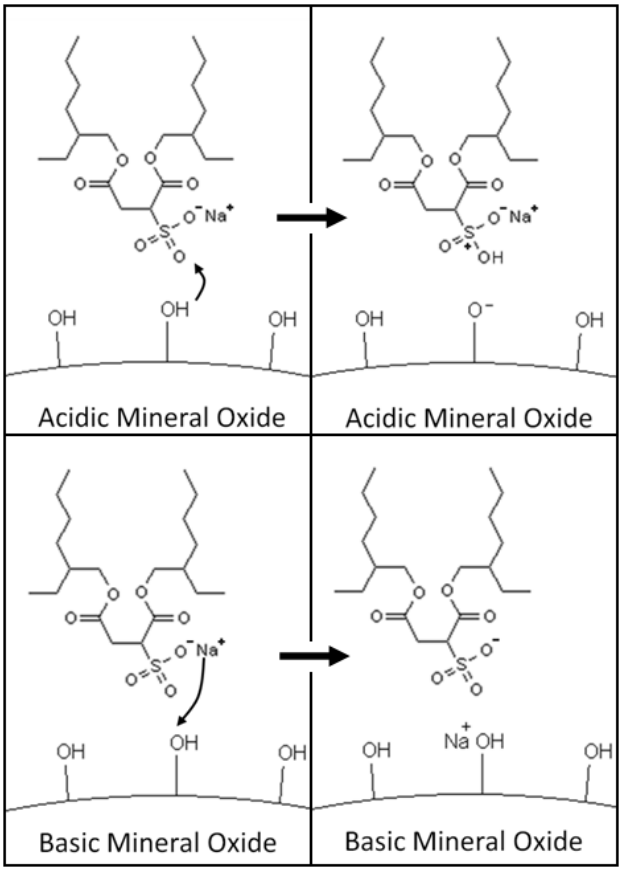

Figure 2.5. Schematic of proposed mineral oxide charging. The above figure illustrates the proposed acid-base charging mechanism that would explain the particle charging behavior observed in solutions of AOT and Isopar-L. In the case of an acidic surface (top), a proton is removed from the surface by an adsorbed monomer. The positively charged monomer is then stabilized in an inverse micelle, leaving a net negative charge on the particle surface. Conversely, a basic surface adsorbs the sodium ion from the AOT monomer, resulting in a positive particle charge.

Another possible explanation is that there exist two completely different mechanisms for hydrophobic and hydrophilic particles, in which hydrophobic particles are charged via specific adsorption and hydrophilic particles engage in an acid-base charge transfer with the polar head groups of the surfactant molecules. Clearly, this is an area of research that warrants more attention.

2.6. Conclusion

The effect of particle acidity (or basicity) on the charging of apolar colloids was examined using a series of mineral oxide particles dispersed in solutions of AOT and Isopar-L. The chosen particles (SiO_2, TiO_2, Al_2O_3, ZnO, and MgO) have PZC's ranging from a pH of approximately 3 to 11. The electrophoretic mobility of each type of particle dispersion was determined using a phase angle light scattering (PALS) device.

The results indicate a correlation between particle acidity and electrophoretic mobility, both in polarity and magnitude. The mobility for the acidic silica particles was -0.056 (μm cm) / (V s). Titania did not exhibit much charging, with a maximum mobility of 0.005 (μm cm) / (V s). The more basic alumina, zinc oxide, and magnesia particles were all positively charged with maximum mobilities of 0.053, 0.067, and 0.073 (μm cm) / (V s), respectively. These results are similar to what one would expect for mineral oxides in an aqueous solution with a pH of 5, and support the acid-base charge transfer mechanism proposed by Fowkes and coworkers [10-12]. This characterization of an "effective pH" of AOT in Isopar-L provides a means for predicting the charging behavior of other mineral oxides based on their aqueous IEP or PZC.

Further investigation should be conducted to determine if this charging behavior is consistent with other surfactants and other mineral oxides. If these results prove to be consistent

across a range of surfactants and particles, then this study represents a viable method for predicting and controlling the charge of mineral oxide particles in apolar systems based on the relative acidity (or basicity) of the particle and surfactant.

2.7. Acknowledgement

This research was supported, in part, by a gift from the Xerox Corporation, and by the University of Washington Center for Surfaces, Polymers, and Colloids. The authors also acknowledge helpful discussions with Dr. Saran Poovarodom.

2.8. References

[1] Morrison, I.D. *Colloids Surf., A* **1993**, *71*, 1-37.

[2] Comiskey, B.; Albert, J.D.; Yoshizawa, H.; Jacobsen, J. *Nature* **1998**, *394*, 253-255.

[3] Roberts, G.S.;Sanchez, R.; Kemp, R.; Wood, T.; Bartlett, P. *Langmuir* **2008**, *24*, 6530-6541.

[4] Hsu, M.F.; Dufresne, E.R.; Weitz, D.A. *Langmuir* **2005**, *21*, 4881-4887.

[5] Van der Minne, J.L.; Hermanie, P.H.J. *J. Colloid Sci.* **1952,** *7(6)*, 600-615.

[6] Koelmans, H.; Overbeek, J.T.G. *Discuss. Faraday Soc.* **1954,** *18*, 52-63.

[7] Dukhin, A.S.; Goetz, P.J. *J. Electroanal. Chem.* **2006**, *588*, 44-50.

[8] Kitahara, A. Nonaqueous Systems. In Surfactant Science Series, *Marcel Dekker: New York*; **1998**; p. 135-150.

[9] Smith, P.G.; Patel, M.N.; Kim, J.; Milner, T.E.; Johnston, K.P. *J. Phys. Chem. C* **2007,** *111*, 840-848.

[10] Pugh, R.J.; Fowkes, F.M. *Colloids Surf.* **1984,** *9*, 33-46.

[11] Pugh, R.J.; Fowkes, F.M. *Colloids Surf.* **1984,** *11*, 423-427.

[12] Riddle, F.L.; Fowkes, F.M. *J. Am. Chem. Soc.* **1990,** *112(9)*, 3259-3264.

[13] Labib, M.E.; Williams, R. *Colloid Polym. Sci.* **1986**, *264*, 533-541.

[14] Labib, M.E.; Williams, R. *J. Colloid Interface Sci.* **1984**, *97, 2*, 356-366.

[15] Labib, M.E. *Colloids Surf.* **1988**, *29*, 293-304.

[16] Mysko, D.D.; Berg, J.C. *Ind. Engr. Chem. Res.* **1993**, *32*, 854.

[17] Poovarodom, S.; Berg, J.C. *J. Colloid Interface Sci.* **2010,** *346*, 370-377.

[18] Ash, M.; Ash, I. Handbook of Green Chemicals (2nd Edition); Synapse Information Resources: Endicott, 2004.

[19] Poovarodom, S.; Berg, J.C. *J. Colloid Interface Sci.* **2011**, *351*, 415-420.

[20] Kitahara, A.; Satoh, T.; Kawasaki, S.; Kon-no, K. *J. Colloid Interface Sci.* **1982**, *86(1)*, 105-110.

[21] Parfitt, G. D.; Peacock, J. Stability of Colloidal Dispersions in Nonaqueous Media. In *Surface and Colloid Science: Volume 10.*; Matijevic, E., Ed.; Surface and Colloid Science; Plenum Press: New York, 1978; pp 163-226.

[22] Kotlarchyk, M.; Huang, J.S.; Chen, S.-H. *J. Phys. Chem.* **1985,** *89*, 4382-4386.

[23] Kosmulski, M. Chemical properties of material surfaces. In *Surfactant Science Series*, *Vol. 102*; Marcel Dekker: New York, 2001.

[24] Kitahara, A.; Amano, M.; Kawasaki, S.; Kon-no, K. *Colloid Polym. Sci.* **1977,** *255*, 1118-1121.

[25] McGown, D.N.L.; Parfitt, G.D; Willis, E. *J. Colloid Sci.* **1965**, *20*, 650-654.

[26] Espinosa, C.E.; Behrens, S.H.; Guo, Q. *Langmuir*, **2010**. *26(22)*. 16941-16948.

Chapter 3

Surfactant mediated acid-base charging of mineral oxide particles dispersed in apolar systems

3.1. Summary

This chapter examines the role of acid-base properties on particle charging in apolar media. Manipulating the polarity and magnitude of charge in such systems is of growing interest to a number of applications. A major hurdle to the implementation of this technology is that the mechanism(s) of particle charging remain a subject of debate. The authors previously conducted a study of the charging of a series of mineral oxide particles dispersed in apolar systems that contained the surfactant AOT. It was observed that there was a correlation between the particle electrophoretic mobility and the acid-base nature of the particle, as characterized by aqueous point of zero charge (PZC), or the isoelectric point (IEP). The current study investigates whether or not a similar correlation is observed with other surfactants, namely the acidic Span 80 and the basic OLOA 11000. This is accomplished by measuring the electrophoretic mobility of a series of mineral oxides that are dispersed in Isopar-L containing various concentrations of either Span 80 or OLOA 11000. The mineral oxides used have PZC values that cover a wide range of pH, providing a systematic study of how particle and surfactant acid-base properties impact particle charge. It was found that the magnitude and polarity of particle surface charge varied linearly with the particle PZC for both surfactants used. In addition, the point at which the polarity of charge reversed for the basic surfactant OLOA 11000 was shifted to a pH of approximately 9,

compared to the previous result of about 5 for AOT. This proves that both surfactant and particle acid-base properties are important, and provides support for the theory of acid-base charging in apolar media.

3.2. Introduction

The ability to impart charge on particles dispersed in apolar media has been of particular interest to researchers since the 1950s, when it was observed that the stability of carbon black particles was greatly enhanced when the particles possessed a sizeable zeta potential [1,2]. Currently, particle charge is an important function in a number of applications involving apolar systems, including motor oil additives [3,4], nonpolar paints and inks [3], and airborne drug delivery [5]. In other applications particles need to be both stable and carry the correct polarity and magnitude of charge, such as electrostatic lithography [3], photoelectrophoresis [3], and electrophoretic displays [6].

The primary challenge with implementing such applications is that particle charging in apolar media is much more difficult and complex than in aqueous systems. The inherently small dielectric constant in apolar systems creates a large energy barrier to overcoming Coulombic forces to create charge separation. This requires the presence of "charge stabilizing agents" such as surfactants that form reverse micelles, or similar structures, to sequester and stabilize charges from recombination. The reverse micelle consists of a polar core containing a local dielectric constant much larger than the surrounding medium, surrounded by a steric barrier made up of long carbon chains. Even though particle charging is actively employed, the mechanism(s) by which the charge arises is actively debated and appears to be largely system dependent [3,7]. The proposed charging mechanisms include: (1) preferential adsorption of charged species [8], (2)

charge dissociation of surface functional groups and subsequent stabilization in inverse micelles [9], and (3) acid-base charge transfer between surface functional groups and adsorbed surfactant molecules [10-12]. The first proposed mechanism implies that the particle charge is controlled by the surfactant, whereas the second mechanism suggests that the particle surface functional groups dictate the polarity and magnitude of charge. The third mechanism is interesting in that it states that the polarity and magnitude of particle charge is dependent on the relative acidity or basicity of both the particle surface functional groups and the surfactant. In principle, this is similar to the charging mechanism for mineral oxide particles in aqueous systems, where the polarity and magnitude of the particle charge is dictated by the inherent acidity or basicity of the particle and the pH of the solution.

A previous study done by this group showed a close correlation between the acid-base properties of mineral oxide particles and the nature of the charge the particles obtained when dispersed in an apolar medium containing the surfactant AOT [13]. It was observed that an acidic particle, as characterized by having an aqueous point of zero charge (PZC) at low pH, exhibited a negative electrophoretic mobility, whereas basic particles obtained a positive charge. Additionally, the magnitude of the particle surface charge had a nearly linear dependence on the particle PZC, indicating that acid-base properties play an important role in how these particles obtain charge in apolar systems. However, it was unclear if this relationship would exist for other surfactant systems. Therefore, the purpose of this study is the continuation of the investigation of acid-base charging in apolar media. The procedure outlined in the previous study is duplicated for apolar systems containing the acidic surfactant Span 80 and the basic surfactant OLOA 11000. The results will provide further indication of whether or not the charging of mineral oxide

particles in apolar systems is dependent on the acid-base properties of both the particle and the surfactant.

3.3. Materials and methods

3.3.1. Materials

The apolar solvent chosen was Isopar-L, a commercial isoparaffinic hydrocarbon supplied by Exxon Mobil Chemical (Houston, TX). It consists of C8 to C15 saturated hydrocarbons, with an aromatic content of only 30 ppm, and a dielectric constant of 2.0. It was used as received.

The two surfactants used in this study were SPAN 80 from Sigma-Aldrich Corp. (St. Louis, MO) and OLOA 11000 from Chevron Oronite (Bellaire, TX). Span 80, sorbitan monooleate, is an acidic surfactant that has been used previously in apolar charging studies [14]. The manufacturer characterizes Span 80's acidity by an acid number that represents the equivalent amount of KOH needed to neutralize it. The acid number for Span 80 is reported to be approximately 8 mg KOH/g. OLOA 11000 is a proprietary compound, and its exact chemical structure is not published. It is known to be a polyisobutylene succinimide compound with a polyamine head group, making it a basic surfactant. The basicity of OLOA 11000 is quantified by the total base number (TBN) which is reported to be equivalent to 80 mg of KOH/g of surfactant. Both of these surfactants are known to act as charge stabilizers in apolar media, and were used as received.

The particles used were a series of mineral oxides: silica (SiO_2) from Fiber Optics Center Inc. (New Bedford, MA), titania (TiO_2) from J.T. Baker Chemical Co. (Phillipsburg, NJ), alumina (Al_2O_3) from Baikalox International Corp. (Charlotte, NC), zinc oxide (ZnO) from MK

Nano (Mississauga, Ontario), and magnesia (MgO) from MTI Corp. (Richmond, CA). The particles ranged in size from 50 to 500 nm and were selected because their aqueous points of zero charge (PZC) are well documented and span a wide pH range. However, each mineral oxide has a range of reported values [15], making it necessary to experimentally determine the PZC and IEP of the oxides used in this study. All particles were supplied in powder form and used as received.

3.3.2. Dispersion preparation

Particles of each type were dried at 175 ^{o}C for 2 hours before being added to surfactant solutions containing a range of surfactant concentrations from 0.01 to 5.0 wt%. Previous research has shown that this is the ideal concentration range to study apolar particle charging for both OLOA 11000 and SPAN 80 [14]. Surfactant concentrations smaller than 0.01 wt% are below the critical micelle concentration and result in little to no particle charging. The particle loading in each of the dispersions was 500 ppm by weight. This was done to prevent inter-particle interactions and multiple scattering during electrophoretic mobility measurements. The dispersions were then sonicated for 3 h and allowed to equilibrate for 24 h. All dispersions were stored in a desiccator, except during sonication and measurement, to regulate the amount of water in each sample. Previous work has shown that oxide charging in apolar media can be affected by the water content in the system [16]. The water content was monitored using a Karl Fischer titrator from Mettler Toledo (Columbus, OH), and was in the range of 5-25 ppm for all samples.

3.3.3. Measurement of electrophoretic mobility

The electrophoretic mobility of the apolar dispersions was measured by dynamic light scattering (DLS) using a Brookhaven Instruments Zeta-PALS (Holtsville, NY). The instrument is theoretically capable of measuring mobilities as low as 0.001 (μm cm)/(s V). The measurements were conducted using a sinusoidal voltage with a frequency of 2 Hz applied across electrodes spaced 0.5 cm apart. To eliminate any effects of field-induced charging, as demonstrated by Behrens and coworkers [17], the electrophoretic mobility of each sample was determined using applied field strengths of 17 – 55 kV/m. These values were then extrapolated back to zero field strength to determine the inherent mobility of the particles.

3.3.4. Aqueous particle charge characterization

The acid-base properties of each type of particle were characterized by determining their aqueous isoelectric point (IEP) and point of zero charge (PZC). The aqueous IEP of each particle was determined by electrokinetic titration. The above mentioned Zeta-PALS instrument was used to measure electrophoretic mobility. The pH was controlled with HNO_3 and KOH, and monitored with an Oakton Instruments 510 series pH/conductivity meter (Vernon Hills, IL). The aqueous PZC of each particle was also determined to verify the obtained IEP values. This was done via potentiometric titration using HNO_3 and KOH for pH control, and KNO_3 was used for the background electrolyte in concentrations of 0.001, 0.01, and 0.1 M. These measurements were carried out and analyzed by the authors in a previous study [13], and the results are duplicated in Table 3.1.

Table 3.1. Mineral oxide IEP and PZC data (in terms of pH)

Oxide	IEP (Exp.)	PZC (Exp.)	PZC (Lit.)
Silica	2.1 + 0.3	3.0 + 0.3	2-3
Titania (rutile)	4.0 + 0.2	3.7 + 0.2	4-6
Alumina	7.1 + 0.3	7.5 + 1.0	8-9
Zinc Oxide	7.5 + 0.5	7.7 + 0.3	9-10
Magnesia	8.5 + 0.5	10.7 + 0.2	10-12

Shown in this table are previously determined experimental values of the IEP and PZC for each type of particle used in the study [13]. The range of reported literature values are shown for comparison [15].

3.4. Results

3.4.1. Determination of maximum mobility.

Before comparing the different particles to one another, it is necessary to determine a metric for this comparison. As previously mentioned, both applied electric field strength and surfactant concentration can greatly affect the particle electrophoretic mobility. Therefore, it was necessary to perform measurements at several different electric field strengths for each surfactant concentration of interest. An example of this is shown for alumina particles dispersed in OLOA 11000 and Isopar-L in Figure 3.1.

In this case, it was observed that the particles obtained a negative charge at all surfactant concentrations and all applied electric field strengths. A significant amount of field-induced charging was observed at the lower surfactant concentrations, and little to no field-induced charging was seen at the larger surfactant concentrations.

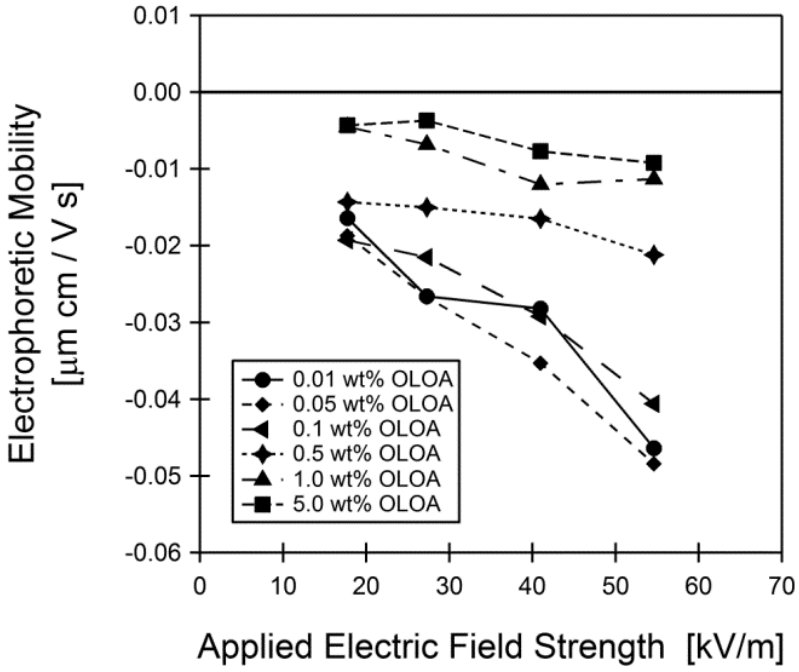

Figure 3.1. The effect of applied electric field strength on measured particle electrophoretic mobility is shown here for alumina particles dispersed in Isopar-L containing various concentrations of OLOA 11000. The lines are intended only to guide the eye. Error bars are derived from four measurements and are approximately the same size as the data markers.

This was true for all particle and surfactant combinations and is consistent with results obtained in previous studies [16,17]. To account for this, the data sets were extrapolated back to zero field strength to eliminate any effects of field-induced charging, and obtain the inherent particle charge at each surfactant concentration. Once this was accomplished, the impact of surfactant concentration on apolar particle charging could be properly analyzed. This is demonstrated in Figure 3.2, where the zero-field electrophoretic mobility values for alumina are plotted against OLOA concentration.

The magnitude of the zero-field electrophoretic mobility was seen to initially increase with increasing surfactant concentration before reaching a maximum of -0.0144 μm cm/V s, and then decrease upon the further addition of surfactant. This trend occurred for all of the particles

tested, with the maximum mobility regularly occurring between 0.1 and 1.0 wt% for both OLOA 11000 and Span 80. The consistent appearance of a maximum mobility as a function of surfactant concentration made it a suitable metric for comparing the charging behavior of the different particle types.

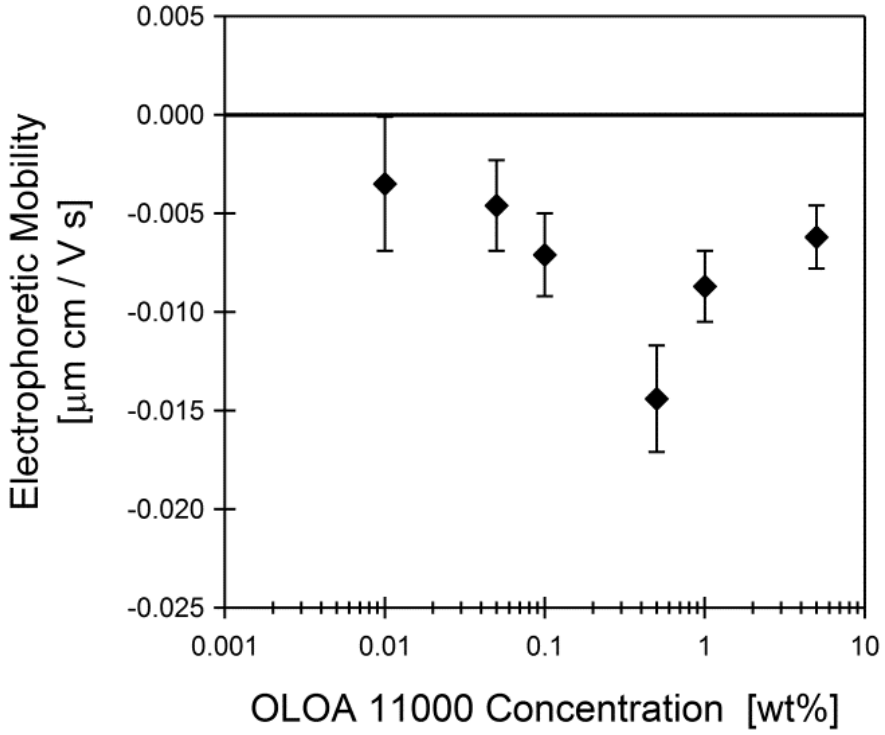

Figure 3.2. The zero-field electrophoretic mobility dependence on surfactant concentration is shown for alumina particles dispersed in Isopar-L with OLOA 11000. The error bars are determined from the extrapolation of data shown in Figure 3.1.

3.4.2 Apolar charging vs. acid-base properties

The final phase of the current investigation consisted of comparing the apolar electrophoretic mobilities of the different particles to their inherent acid-base properties, as characterized by their aqueous PZCs. The maximum observed zero-field electrophoretic mobility

of each particle type is plotted against aqueous particle PZC in Figure 3.3(a) for dispersions containing OLOA 1100 (solid line) and Span 80 (dashed line). The data from the authors' previous study of dispersions containing AOT [13] is reproduced in Figure 3.3(b) for comparison.

A close correlation was observed between the aqueous PZCs and the measured apolar electrophoretic mobilities for all of the surfactant systems used. For dispersions containing the basic surfactant OLOA 11000, the most acidic particle (silica) had the largest negative mobility observed at -0.0592 μm cm/V s. As one moved to increasingly basic particles (titania, alumina, and zinc oxide), the magnitude of the mobility was seen to decrease. Magnesia, the most basic particle, exhibited a positive electrophoretic mobility of 0.0178 μm cm/V s, completing the linear relationship between apolar particle mobility and aqueous PZC. A similar trend was observed for dispersions containing the acidic surfactant SPAN 80, except that every particle tested had a positive mobility. The magnitude of the particle mobility steadily increased with increasing particle basicity from 0.0166 μm cm/V s for silica to 0.0470 μm cm/V s for magnesia. The data for dispersions containing AOT also displayed a direct correlation between apolar particle charge and aqueous PZC, where both positive and negative particle charges were observed. The difference between AOT and OLOA 11000 is that the particle charge reverses polarity at different pH values along the aqueous PZC scale. The polarity reversal occurred at approximately a pH of 5 for AOT and 9 for OLOA 11000.

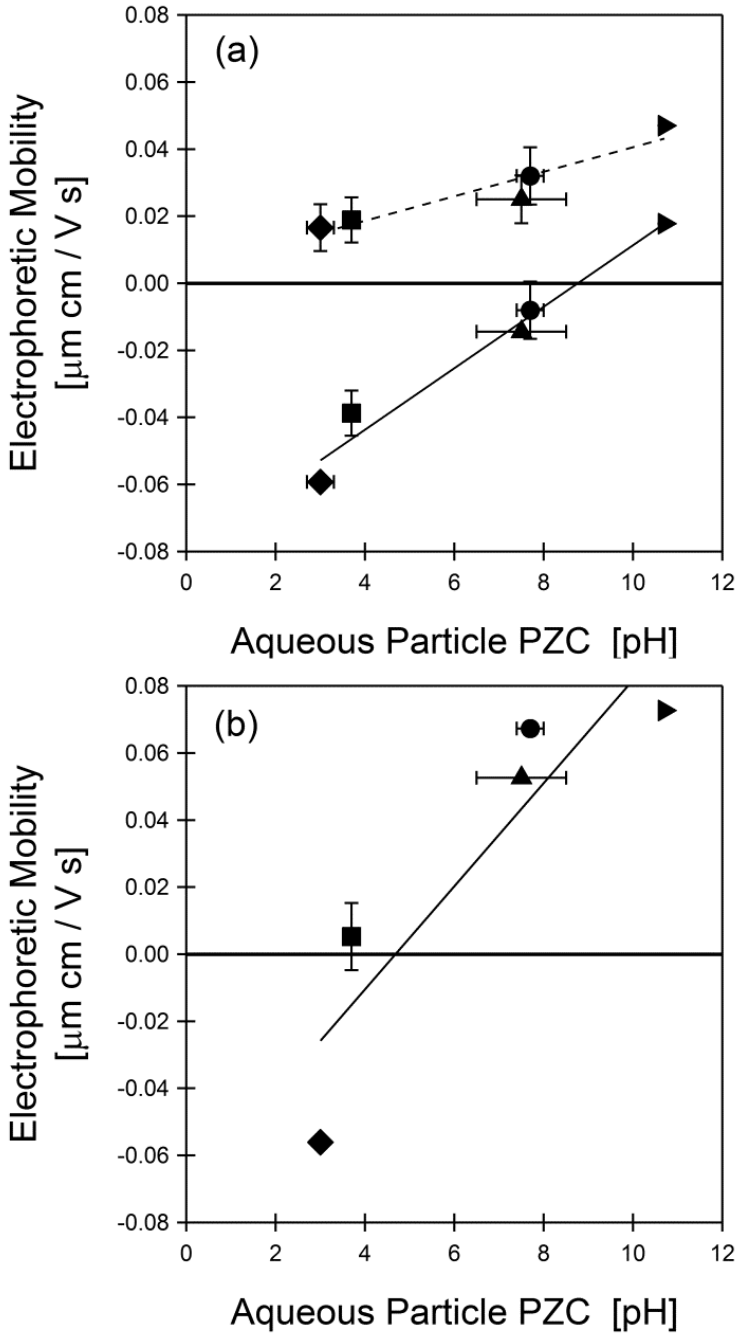

Figure 3.3. The relationship between mineral oxide acid-base character and apolar charging is shown here. The maximum zero-field electrophoretic mobility of silica (♦), titania (■), alumina (▲), zinc oxide (●), and magnesia (►) particles dispersed in Isopar-L are plotted against their aqueous PZCs. In the top figure (a), the solid line represents dispersions containing OLOA 11000 and the dashed line represents dispersions containing Span 80. The data for dispersions containing AOT are shown in the bottom figure (b), and are reproduced from a previous study [13].

3.5. Discussion

3.5.1. Effects of surfactant concentration and electric field strength

It is increasingly apparent that surfactant concentration, applied electric field strength, and water content can significantly impact particle charging in apolar media. Therefore, it is necessary to account for these factors whenever one attempts to characterize charging behavior in such systems or compare data with those in the literature. In the current study, it was found that the magnitude of the zero-field electrophoretic mobility consistently went through a maximum as a function of surfactant concentration, as shown in Figure 3.2 for alumina with OLOA 1100. This behavior has been observed in a number of studies [8,13,14,16]. The common explanation is that at a small surfactant concentration the degree of particle charging is limited by the total number of reverse micelles available to stabilize the counter-charges. Therefore, an increase in surfactant concentration results in an increase in particle charge. At a large surfactant concentration, it is theorized that the number of charged micelles in the bulk solution is large enough to cause electrostatic screening or neutralization of the particle surface charge, leading to a decrease in electrophoretic mobility with a further increase in surfactant concentration.

It was also found that a significant amount of field-induced charging occurred at smaller surfactant concentrations, as demonstrated in Figure 3.1. This resulted in electrophoretic mobility measurements increasing by as much as five times when going from low to high applied field strength. Conversely, at large surfactant concentrations, the particle electrophoretic mobilities are seen to be field independent. Even though this type of behavior has been observed previously, the cause is still somewhat unclear. An interesting observation is that the electric field induced charging tends to subside at approximately the same surfactant concentration as the

maximum mobility, approximately 0.5 wt% OLOA in Figures 3.1 and 3.2. At this point in time, it is not clear whether these two shifts in charging behavior are related, and more research is needed in this area to fully understand the mechanism(s) at work.

3.5.2. Apolar charging vs. aqueous PZC

The primary purpose of this work is the investigation of the validity of surfactant mediated acid-base charging of mineral oxide particles dispersed in apolar systems. The authors previously determined that there was a linear correlation between the aqueous PZCs of various mineral oxides and the electrophoretic mobility of these oxides when they were dispersed in an apolar medium in the presence of the surfactant AOT [13], as shown in Figure 3.3(b). The results from the current work look to extend this to other surfactant systems, namely OLOA 11000 and Span 80. The results in Figure 3.3(a) show that there is a similar linear correlation between apolar particle charge and acid-base properties for these surfactant systems. All of the mineral oxides used in this study obtain a positive charge when dispersed in apolar solutions containing the acidic surfactant Span 80. What is significant is that the more inherently basic particles display larger magnitudes of electrophoretic mobility than the inherently acidic particles. This suggests that the Span 80 monomers will act as proton donors to the surface hydroxide groups of the mineral oxides, and the degree to which this occurs is dependent on how readily the particle surface groups act as proton receivers. This is precisely what is predicted by the proposed acid-base charging mechanism.

In the case of dispersions containing the basic surfactant, OLOA 1100, a majority of the particles obtain a negative charge, with the more acidic particles obtaining larger magnitudes of charge. In this case, the basic OLOA acts as a proton receiver from the hydroxide groups on the

surface of the mineral oxides. Only in the case of the extremely basic magnesia is the particle surface charge positive. The molecular mechanism for this charging remains unclear. The occurrence of a reversal in the polarity of particle charge for systems containing OLOA 11000 and AOT is a significant finding. More important is that the point on the aqueous PZC scale where this charge reversal occurs is different for the two surfactants, at a pH of 9 for OLOA and 5 for AOT. Since OLOA 11000 is more likely to act as a proton receiver than AOT, it is logical that the point of charge reversal would be shifted to more basic particles. This reinforces the conclusions made in the previous study [13] that the polarity and magnitude of the particle charge is dependent on the acid-base properties of both the surfactant and the particle. The reason a charge reversal is not observed with Span 80 may simply be that it is more acidic than any of these mineral oxides, and not capable of receiving a proton from the particle surface groups. Another possible explanation is that some surfactants may only be capable of being either a proton donor or a proton receiver, but not both. In such a case, the magnitude of the electrophoretic mobility would be dependent on the relative acid-base properties of the particles, but the polarity would be dictated entirely by the surfactant.

One aspect that remains a mystery is the origin of the difference in slopes of the linear relationship between the particle mobility and PZC for the different surfactant systems. While the slope for Span 80 has a statistically nonzero value of 0.0036 ± 0.0017 μm cm / V s pH, it is much less pronounced than the slopes for both OLOA 11000 and AOT. It is important to remember that what is being analyzed is the maximum mobility observed as a function of surfactant concentration. This maximum is thought to occur due to a competition between surfactant-particle charging and electrostatic screening or neutralization resulting from a sufficiently large concentration of charged micelles in the bulk solution. It is well documented

that, in addition to stabilizing the counter charges from the particles, reverse micelles will spontaneously become charged in apolar systems, as evidenced by an increase in conductivity with the addition of surfactant. Therefore, it makes sense that the maximum mobility would depend on how readily a particular surfactant is able to impart charge to a particle as well as how readily the surfactant micelles obtain charge on their own. Even though the cause of the difference in slope remains uncertain, we have demonstrated and confirmed a method for establishing a baseline for mineral oxide particle charging in apolar media for a particular surfactant of interest. Such information could then be used to predict the maximum magnitude and polarity of charge for other mineral oxides.

As of now, we have only demonstrated the possible validity of an acid-base charging mechanism for bare mineral oxide particles that have hydroxide surface functionality. It is quite possible that particles other than mineral oxides undergo completely different charging mechanisms. Clearly, more systematic research is needed using other particle systems to determine whether or not similar relationships with acid-base properties exist.

3.6. Conclusion

The purpose of the current work was to investigate the validity of surfactant mediated acid-base charging of mineral oxide particles that are dispersed in apolar systems. This was accomplished by measuring the electrophoretic mobility of different mineral oxide particles (silica, titania, alumina, zinc oxide, and magnesia) dispersed in Isopar-L that contained various concentrations of either OLOA 11000 or Span 80. By eliminating the effects of water content and applied electric field strength, the maximum mobility as a function of surfactant concentration could by isolated for each system. The mineral oxide particle mobilities were then

plotted against their aqueous points of zero charge. It was observed that a linear relationship existed between the maximum particle mobility and the PZCs. In addition, for the system containing the basic surfactant OLOA 11000 a charge reversal was observed at approximately a particle PZC of 9, where oxides more acidic than this became negatively charged and more basic oxides obtained a positive charge. All of this reinforces the theory that acid-base properties of both the particle and the surfactant play an important role in the charging mechanism of mineral oxides. The method employed and results obtained in this study should provide a basis for predicting the polarity and magnitude of charge on mineral oxides in apolar surfactant systems.

3.7. Acknowledgement

This research was supported, in part, by a gift from the Xerox Corporation, and by the University of Washington Center for Surfaces, Polymers, and Colloids.

3.8. References

[1] Van der Minne, J.L.; Hermanie, P.H.J. *J. Colloid Sci.* **1952**, *7*, 600-615.

[2] Van der Minne, J.L.; Hermanie, P.H.J. *J. Colloid Sci.* **1953**, *8*, 38-52.

[3] Morrison, I. *Colloids Surf., A* **1993**, *71*, 1-37.

[4] Pugh, R.J.; Matsunaga, T.; Fowkes, F.M. *Colloids Surf.* **1983**, *7*, 183-207.

[5] Jones, S.A.; Martin, G.P.; Brown, M.B. *J. Pharm. Sci.* **2006**, *95*, 1060-1074.

[6] Comiskey, B.; Albert, J.D.; Yoshizawa, H.; Jacobson, J. *Nature* **1998**, *394*, 253-255.

[7] Lyklema, J. *Adv. Colloidal Interface Sci.* **1968**, *2*, 65-114.

[8] Dukhin, A.S.; Goetz, P.J. *J. Electroanal. Chem.* **2006**, *588*, 44-50.

[9] Smith, P.G.; Patel, M.N.; Kim, J.; Milner, T.E.; Johnston, K.P. *J. Phys. Chem. C* **2007**, *111*, 840-848.

[10] Pugh, R.J.; Fowkes, F.M. *Colloids Surf.* **1984**, *9*, 33-46.

[11] Pugh, R.J.; Fowkes, F.M. *Colloids Surf.* **1984**, *11*, 423-427.

[12] Riddle, F.L.; Fowkes, F.M. *J. Am. Chem. Soc.* **1990**, *112*, 3259-3264.

[13] Gacek, M.; Brooks, G.; Berg, J.C. *Langmuir* **2012**, *28*, 3032-3036.

[14] Poovarodom, S.; Berg, J.C. *J. Colloid Interface Sci.* **2010**, *346*, 370-377.

[15] Kosmulski, M. Chemical properties of material surfaces. In *Surfactant Science Series*; Marcel Dekker: New York, 2001; Vol. 102.

[16] Gacek, M.; Bergsman, D.; Michor, E.; Berg, J.C. *Langmuir* **2012**, *28*, 11633-11638.

[17] Espinosa, C.E.; Behrens, S.H.; Guo, Q. *Langmuir*, **2010,** *26*, 16941-16948.

Chapter 4

Effect of synergists on organic pigment particle charging in apolar media

4.1. Summary

The current chapter investigates the apolar charging behavior of organic pigment particles and the role that synergists play in regard to particle charging. Organic pigments are often used in apolar paints, inks, and most recently electrostatic lithography. For electro-lithography to work the particles must be both stable and possess the correct polarity and magnitude of charge. It is therefore important to better understand the charging behavior and potential charging mechanisms of these particles that have received little or no attention in the literature. Unfortunately these already complex systems are further complicated by the fact that the stability of organic pigments is often improved through the use of synergists. Synergists are designed to enhance the adsorption of steric stabilizers to the particles. However, their effect on particle charging has not been previously published. In this study the particle zeta potential is determined for apolar dispersions of magenta and cyan particles in heptane (with and without synergist present). The particles are dispersed with three different surfactants commonly used in apolar charging studies: Span 80, AOT, and OLOA 11000. Acid-base interactions appear to play an important role, particularly for cyan. However, due to the complexity of these systems, any general rules must be applied with caution as the particle, surfactant, and synergist chemistry all determine the nature of the particle charge.

4.2. Introduction

Particle charging and stabilization in apolar media is a field that has received increased attention in recent years, due to the increasing number of applications that make use of this technology. These include motor oil additives [1,2], airborne drug delivery systems [3], electrophoretic displays [4], and most recently full color electrostatic lithographic printers (http://h20195.www2.hp.com/V2/GetPDF.aspx/4AA3-6493ENW.pdf). The common theme with these examples is that they require the particles to have the proper polarity and magnitude of charge as well as to be stable against aggregation. The difficulty in this lies with the complex nature of particle charging in apolar media. The inherently small dielectric constant in apolar systems means there is a large energy barrier of overcoming coulombic attraction in order to stabilize charge. This usually requires the presence of "charge stabilizing agents" such as surfactant inverse micelles, or similar structures, to sequester and stabilize charges from recombination. A key to this stabilization appears to be the size of the polar core of the inverse micelle [5,6], which has a much higher local dielectric constant than the surrounding medium.

Even though particle charging is actively used in apolar systems, the precise mechanism(s) are actively debated and likely system dependent. Smith and Eastoe published a comprehensive review describing many of the proposed mechanisms [7]; they include (1) acid-base charging [8-12], (2) specific adsorption of ions or charged inverse micelles [13,14], and (3) dissociation of surface ions [15]. These mechanisms have been used to describe the charging behavior of a number of different particles, including mineral oxides, carbon black, and polymer particles. However, very little has been published regarding organic pigment particles, and what has been published does not go into detail on the possible charging mechanism(s) [6]. An additional complication is that organic pigments are notoriously difficult to stabilize and often

require the use of synergists. Synergists are molecules that are designed to strongly adsorb to the particle of interest. They contain functional groups that provide anchoring sites for the adsorption of steric stabilizers. To our knowledge, there have been no studies published that examine how these synergists might affect particle charging in apolar media. The current work is thus a preliminary investigation of the apolar charging of organic pigment particles and the effects of synergists on their charging. To do this we examine the charging behavior of two commonly used organic pigments, magenta and cyan, and their corresponding synergists. The charge stabilizing agents used in this study are the common commercial surfactants Span 80, Aerosol-OT (AOT), and OLOA 11000, all three of which have been used extensively in the past to study apolar charging [16,17].

4.3. Materials and methods

4.3.1. Materials

The apolar solvent chosen was n-heptane supplied by Fisher Scientific (Fair Lawn, NJ). It was chosen because it has a low dielectric constant (1.92) and a low viscosity (0.39 cP), which enhances the electrophoretic mobility of the particles. It was used as received.

The three surfactants used in this study were dioctyl sodium sulfosuccinate (AOT) from Fisher Scientific (Fair Lawn, NJ), Span 80 from Sigma-Aldrich Corp. (St. Louis, MO), and OLOA 11000 from Chevron Oronite (Bellaire, TX). Span 80, sorbitan monooleate, is an acidic surfactant that is characterized by an acid number that represents the equivalent amount of KOH needed to neutralize it. The acid number for Span 80 is reported to be approximately 8 mg KOH/g [11]. OLOA 11000 is a proprietary compound, so its exact chemical structure is not published. It is known, however, to be a polyisobutylene succinimide compound with a

polyamine head group, making it a basic surfactant. The basicity of OLOA 11000 is quantified by the total base number (TBN) reported to be equivalent to 80 mg of KOH/g of surfactant [11]. AOT is a di-tail anionic surfactant that has been extensively used as a "charge control agent" for apolar dispersions [14,16,18]. All three of these surfactants are known to be somewhat hygroscopic; therefore, the raw supply and the subsequent solutions were always stored in a desiccator to prevent any additional uptake of water.

The particles used were two common commercial pigments: cyan and magenta from Clariant (Charlotte, NC). The magenta particles are classified as permanent rubine and fall under the color index name of P.R. 57:1. Chemically, they are beta-oxynapthoic acid (BONA) pigment lakes that make use of calcium as the divalent cation binder [19]. The cyan particles are copper phthalocyanine blue pigments that are classified as P.B. 15:3 in the pigment color index system [19]. The chemical structure of cyan consists of four isoindole units bonded together four nitrogen atoms, forming a planar ring that is coordinated to a central copper atom. The synergists used were Solsperse® synergists 22000L (paired with magenta) and 5000 (paired with cyan) provided by Lubrizol (Wickliffe, OH). The 22000L synergist is a sulfonated derivative of pigment yellow 12, whereas the 5000 synergist is a sulfonated derivative of copper phthalocyanine blue. The particle diameters were determined to be 50 ± 7 nm for cyan and 100 ± 10 nm for magenta using dynamic light scattering using a Brookhaven Instruments Zeta-PALS (Holtsville, NY).

4.3.2. Synergist adsorption isotherms

The first phase of this study was to attempt to determine whether or not the synergists were adsorbing to the particle surface. This is more difficult to achieve than one might expect at

first glance, because the synergists are not readily soluble in heptane. The common practice in commercial applications is to prepare particle dispersions by ball milling the particles, synergist, and surfactant together for 10 to 24 hours. This creates enough intimate contact between the synergist and the particles that a sufficient amount of synergist is applied to the particle surface. However, it is difficult to quantify this in the standard terms of an adsorption isotherm, where the amount of material adsorbed to the surface is dependent on the concentration in the bulk solution. In an attempt to remedy this, adsorption studies were carried out in the presence of the surfactants of interest. The presence of Span 80 helped to solubilize a significant amount of both synergists so that adsorption isotherms could be generated for this case. To carry out the adsorption study, calibration curves were made by correlating spectrophotometer absorbance to synergist concentration for both synergists in solutions of 1 wt% Span 80 in heptane. The spectrophotometer used was a Spectronic 20 from Bausch & Lomb (Rochester, NY), set to a wavelength of 435 nm for the magenta synergist (Solsperse 22000L) and 630 nm for the cyan synergist (Solsperse 5000). Then, an adsorption study was performed by adding pigment particles to solutions of various initial concentrations of synergist, allowing them to sit for 48 hours, and centrifuging out the particles before measuring the absorbance of the supernatant. The concentration of synergist remaining in solution was then determined using the calibration curves. Unfortunately, the surfactants AOT and OLOA 11000 were not as successful at solubilizing the magenta synergist. It was observed that there was no detectable hue change or change in spectrophotometer absorbance upon the addition of magenta synergist to the AOT or OLOA 11000 systems. This was true both without particles present and with particles added and subsequently centrifuged out. In the case of the cyan synergist, there was only a small change in spectrophotometer absorbance upon the addition of synergist to both the AOT and OLOA

solutions. When particles were added and subsequently centrifuged out there was a slight decrease in the spectrophotometer absorbance, indicating some synergist was adsorbed; however full adsorption isotherms were not completed. It is possible that the extended sonication of the particle/surfactant/synergist solutions would cause enough intimate contact that a larger amount of synergist would be adsorbed. However, we could not verify or quantify the existence of adsorbed magenta synergist in the AOT or OLOA 11000 systems due to insufficient synergist in the bulk.

4.3.3. Particle charging

Particles of each type were added to apolar solutions containing a range of surfactant concentrations from 0.01 to 5.0 wt %. Previous research has shown that this is the ideal concentration range to study apolar charging for all three surfactants because the range used is above the surfactant critical micelle concentration. The critical micelle concentrations are approximately 0.001, 0.005, and 0.008 wt % for AOT, OLOA 11000, and Span 80, respectively [11,16]. The particle loading in each case was 300 ppm by weight to prevent inter-particle interactions and multiple scattering during electrophoretic mobility measurements. In the dispersions containing synergist, the synergist loading was 100 ppm by weight. Each dispersion was allowed to equilibrate charge for 24 hours and then it was sonicated before testing. The electrophoretic mobility was measured using a Brookhaven Instruments Zeta-PALS (Holtsville, NY). The measurements were conducted using a sinusoidal voltage with a frequency of 2 Hz applied across electrodes spaced 0.5 cm apart. To eliminate any effects of field-induced charging, as demonstrated by Behrens and co-workers [12], the electrophoretic mobility of each sample was measured using applied field strengths of 17-55 kV/m. These were then extrapolated back to zero applied field strength to obtain the inherent particle charge. The electrophoretic

mobility results were converted to zeta potential using the Hückel equation: $u_e = 2\varepsilon\varepsilon_0\zeta / 3\mu$, where u_e is the electrophoretic mobility, ε is the dielectric constant of the media, ε_0 is the permittivity of vacuum, ζ is the zeta potential, and μ is the viscosity. This is valid over the range of surfactant concentrations used, because the particles are approximately 100 nm in diameter and the Debye length is approximately 2 μm at even the largest surfactant concentration used.

4.4. Results and discussion

4.4.1. Synergist adsorption

In order to determine whether or not the adsorption of synergists to pigment particles would affect their charging it was important to first establish that the synergist would adsorb to the particles. Neither synergist was readily soluble in heptane, so 1 wt % Span 80 was added in all cases to solubilize the synergist. Calibration curves correlating spectrophotometer absorbance with synergist concentration were created and are shown in Figure 4.1(a). These curves were used to determine the synergist concentration in solution during the adsorption study, and the resulting adsorption isotherms were created with knowledge of the specific surface area obtained from the Brunauer-Emmett-Teller (BET) technique. The results are shown in Figure 4.1(b).

To rule out the possibility that the synergist molecules were aggregating in solution and settling out we centrifuged several synergist/Span 80/heptane solutions without the presence of particles. It was observed that the spectrophotometer absorbance did not change upon centrifugation, indicating that the synergist solubilized with the Span 80 was not self-aggregated to the degree that it could be removed from solution via sedimentation. With this in mind, it is clear that the synergists adsorb strongly to their corresponding particles in the presence of Span 80. While adsorption was verified for the cyan synergist with AOT and OLOA 11000, full

adsorption isotherms were not obtained. No adsorption could be verified for the magenta synergist in the presence of AOT or OLOA 11000. Both synergists exhibit Henry adsorption over the entire range of Span 80 concentration.

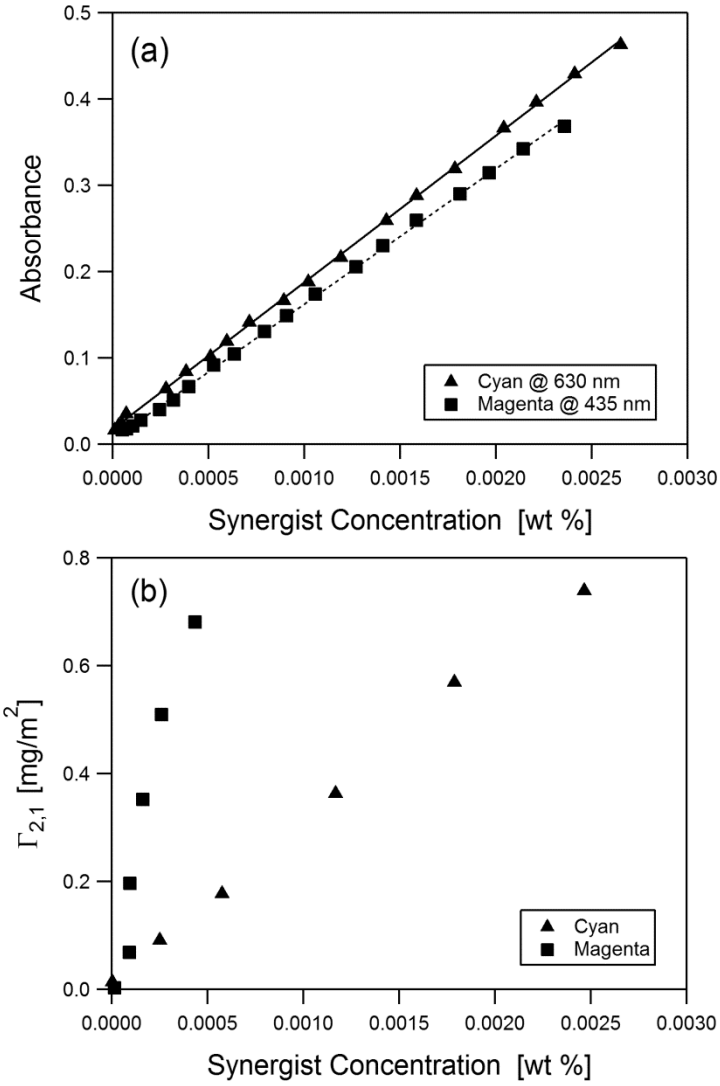

Figure 4.1. A study of synergist adsorption was conducted using spectrophotometer absorbance to determine synergist concentration in solutions containing 1 wt % Span 80 in heptane. Figure (a) shows the calibration curve for the absorbance at wavelengths of 630 and 435 nm for the cyan and magenta synergists, respectively. Figure (b) shows the adsorption isotherms for the two synergists onto their respective pigment particles.

The driving force for synergist adsorption onto the particles is likely co-crystallization, which in this case corresponds to the stacking of conjugated pi-bonds [20]. Due to uncertainty in the degree of sulfonation of these synergists it is difficult to know their exact molecular mass or packing area. However, we can approximate the molar mass by assuming only one or two sulfates are added, and the Van der Waals area of the molecules can be estimated using the molecular software Marvin developed by ChemAxon (Cambridge, MA). Using these two approximations we can state that one adsorbed monolayer of synergist would correspond to approximately 0.7 mg/m^2 for both synergists, which is approximately equal to the maximum adsorption observed in this study.

4.4.2. Pigment particle charging

First, baseline charging values were established for cyan and magenta with the three different surfactants. Figure 4.2 shows the particle zeta potential plotted against the surfactant concentration for (a) Span 80, (b) AOT, and (c) OLOA 11000.

The cyan particles charged positively in both Span 80 and AOT over the entire concentration range with maximum zeta potentials of 23 ± 2 and 39 ± 4 mV, respectively. In dispersions containing OLOA 11000 they charged negatively with a peak zeta potential of -37 ± 3 mV. This charging behavior is consistent with the proposed acid-base charging mechanism observed with mineral oxides [16,17], even though the chemistry of the cyan particle is quite different. The conjugated aromatic pi-bonds in cyan are known to act as a weak base, and it appears that the AOT and Span 80 are able to act as either proton donors or electron receivers, yielding a positive particle surface charge. In the case of OLOA 11000 it appears that the amine head group is a strong enough base that it acts as a proton acceptor or electron donor to the

particle, explaining the negative particle surface charge. It is also worth noting that the magnitude of charge of the cyan particles was smaller, in general, than the charge observed in the study involving mineral oxides. This is consistent with the decreased functionality present on the cyan particles compared to mineral oxides.

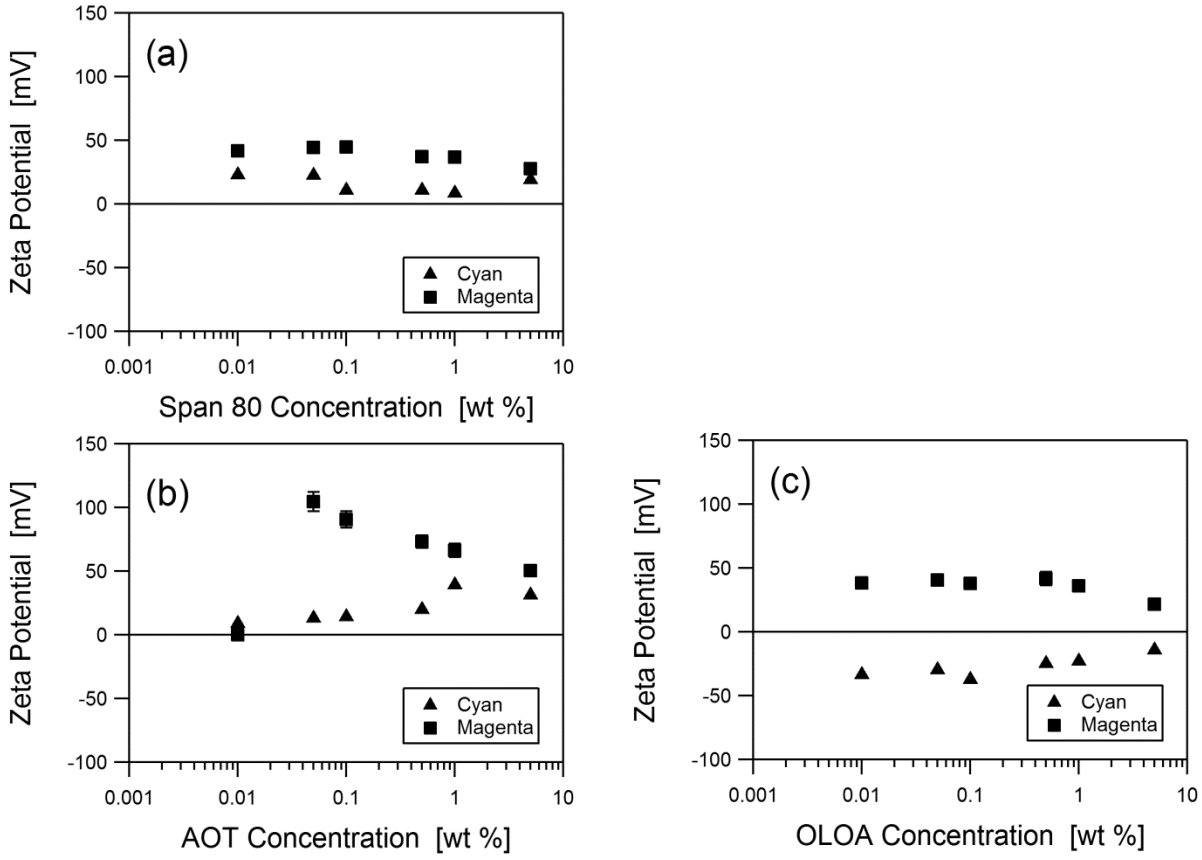

Figure 4.2. The charging behavior of magenta and cyan particles is characterized. The particle zeta potential is plotted as a function of surfactant concentration for dispersions in heptane containing (a) Span 80, (b) AOT, and (c) OLOA 11000. Error bars were determined from 4 different samples of a single dispersion and are smaller than the symbols when not displayed.

In contrast, the magenta particles charged positively with all three surfactants over the entire range of surfactant concentration. The maximum zeta potential was 43 $\pm$ 5 mV for both Span 80 and OLOA 11000, whereas in AOT the particles exhibited a maximum zeta potential of

105 ± 7 mV. The likely explanation for this is the presence of carbonyl and sulfonyl groups on the magenta surface that will act as electron donor sites. It is postulated that these basic groups would be able to form acid-base adducts with the adsorbed surfactant monomers, and when these adducts are separated, there is a positive charge left on the particle surface. There may also be some residual chlorine left over from the particle synthesis, and this could be dissociated and stabilized in the inverse micelles. Until this is investigated further, it remains purely speculation.

4.4.3. Effect of synergist on magenta charging

Once baselines for charging in the absence of synergist were established, the next phase was to repeat the testing with synergist present in the system. As mentioned previously, the adsorption, if any, of these synergists onto the particle surface would impart some sulfonate functionality. What remains to be seen is what effect this has on particle charging. For magenta, Figure 4.3 shows the charging behavior with and without synergist for (a) Span 80, (b) AOT, and (c) OLOA 11000 (it should be noted that in order to properly compare the change in particle charge upon the addition of synergist the y-axis ranges are different than those shown in Figure 4.2).

In dispersions containing Span 80, where we verified that synergist adsorption is taking place, the addition of synergist resulted in a dramatic reduction of the positive particle charge, inducing severe aggregation of the particles at low surfactant concentrations. There was little or no aggregation of particles at higher surfactant concentrations, but the particle charge remained lower than without synergist, achieving a maximum zeta potential of only 23 ± 4 mV. It is likely that the addition of the acidic synergist to the particle surface was covering up the sites that would normally allow the acidic surfactant to adsorb to the particle. This would diminish the

amount of charging events that occur at the particle surface as well as remove the steric stabilization that the surfactant provides. The fact that the effect diminished at higher surfactant concentration indicates that there was likely competitive adsorption between the surfactant and synergist onto the particle surface.

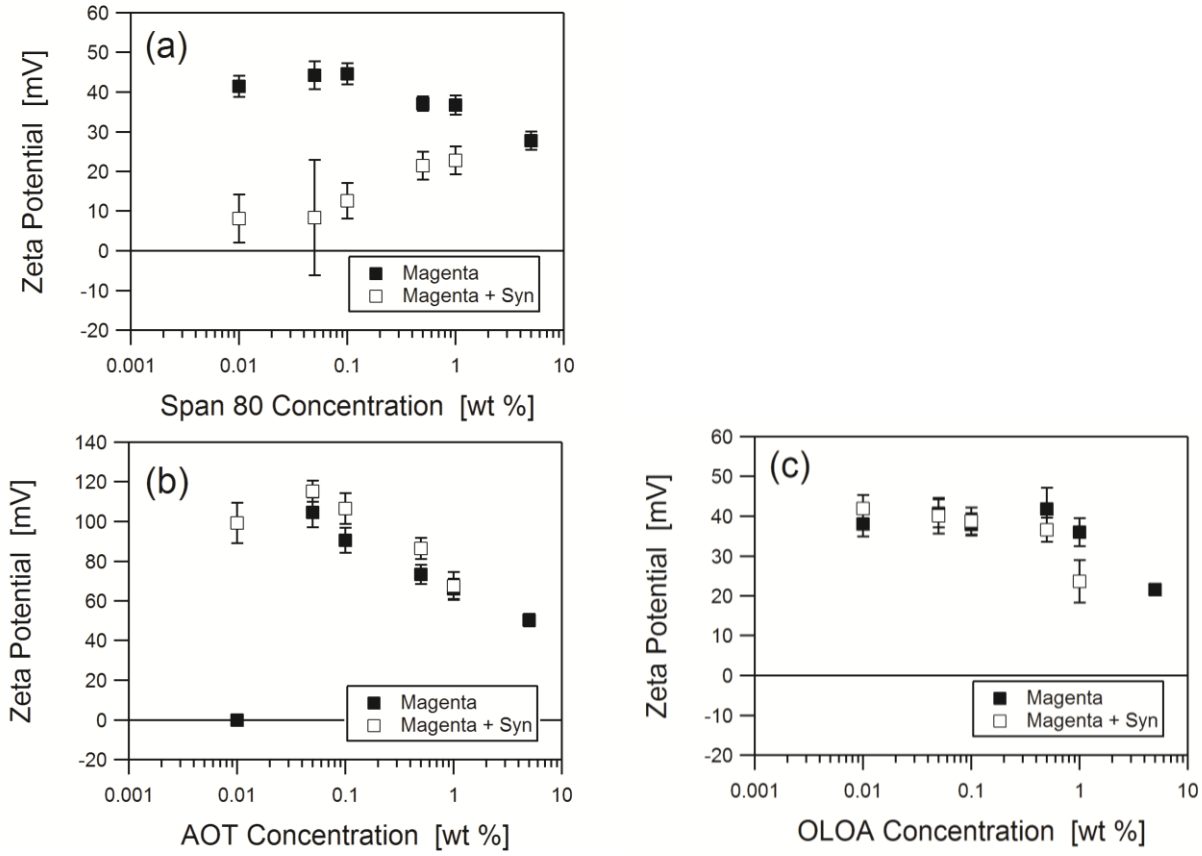

Figure 4.3. The charging results of magenta particles are shown with (empty symbols) and without (filled symbols) synergist present. The zeta potential is plotted against surfactant concentration for (a) Span 80, (b) AOT, and (c) OLOA 11000. Error bars were determined from 4 different samples of a single dispersion and are smaller than the symbols when not displayed.

This represents an important example of how the addition of synergist can degrade the stability of the dispersion if it is not paired with the appropriate surfactant. When synergist was added to dispersions containing AOT and OLOA 11000, no significant change in magenta

particle charge was observed. This appears to indicate that, as suspected, the technique of sonicating the samples was not enough to drive sufficient synergist to the magenta surface. If synergist had been present on the particle surface, we would expect to see a similar change in particle charge as was observed with Span 80.

4.4.4. Effect of synergist on cyan charging

The final phase of this study was to examine the effects of adding synergist to the cyan pigment dispersion. Figure 4.4 shows the charging behavior of cyan with and without synergist for (a) Span 80, (b) AOT, and (c) OLOA 11000 (as with Figure 4.3, the y-axis ranges are different than those shown in Figure 4.2).

It is initially clear that there were no universal trends across the three systems, so it is best to analyze them one at a time. In the case of Span 80, the addition of synergist did not change the particle charging in a statistically significant way; the particles charge marginally positive in both cases. A likely explanation for this is that the acidic sulfonate groups added to the particle surface do not interact in a significant way with the acidic surfactant. This is consistent with previous data showing that even acidic particles do not charge negatively in the presence of Span 80 [16]. As the adsorption study showed, the cyan synergist does not adsorb as well as the magenta synergist. This means there are likely still exposed areas of the particle where the Span 80 can adsorb, explaining why the cyan particles did not aggregate, as was seen with the magenta dispersions.

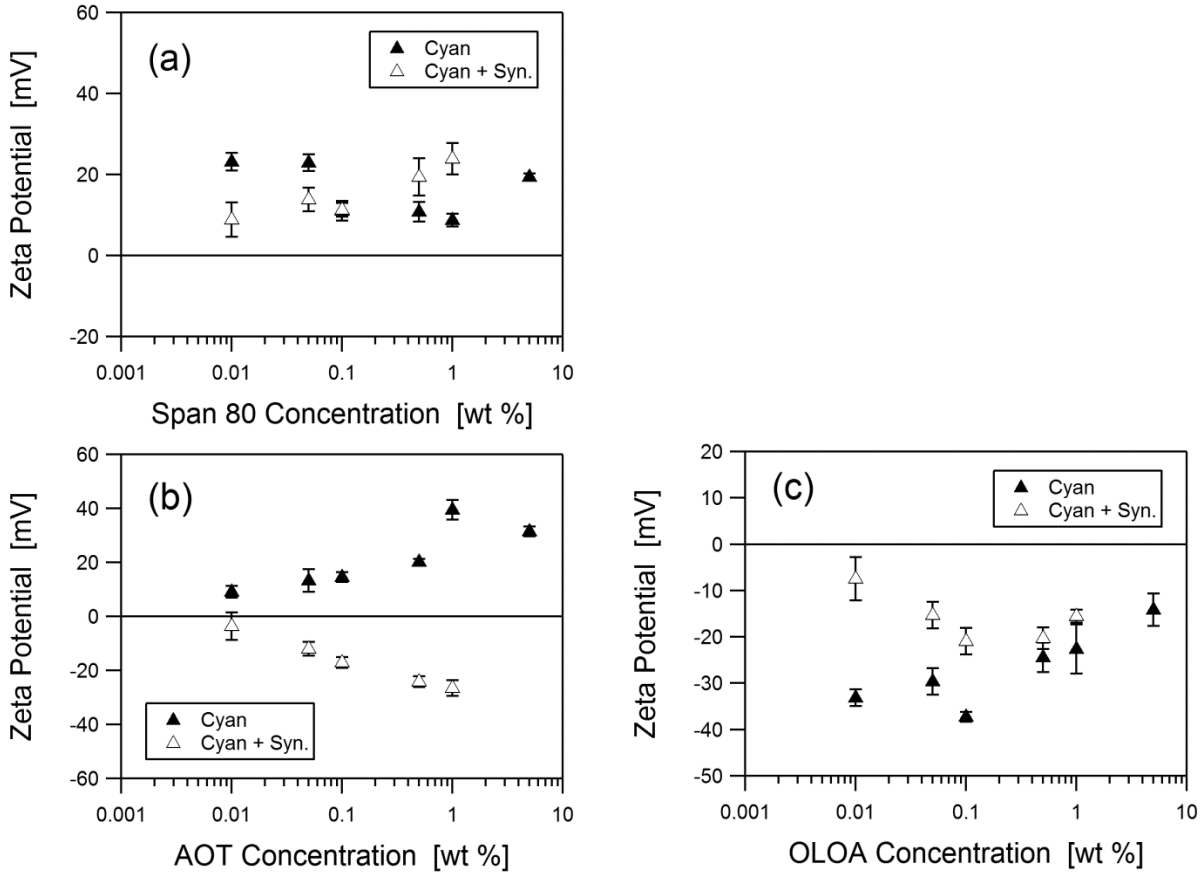

Figure 4.4. The charging results of cyan particles are shown with (empty symbols) and without (filled symbols) synergist present. The zeta potential is plotted against surfactant concentration for (a) Span 80, (b) AOT, and (c) OLOA 11000. Error bars were determined from 4 different samples of a single dispersion and are smaller than the symbols when not displayed.

Conversely, when the synergist is added to the AOT system there was a significant result. The particle charge reversed sign from positive without synergist to negative with synergist, exhibiting a maximum negative zeta potential of -27 $\pm$ 3 mV. The most likely explanation for this is that, unlike the magenta synergist, a sufficient amount of cyan synergist was able to adsorb to the particle surface, and the sulfonate groups of the adsorbed synergist gave the particle acidic surface functionality. This allowed the particle to act as a proton donor or electron acceptor when interacting with the adsorbed AOT. Lastly, when synergist was introduced to the

OLOA 11000 system the particles became less negatively charged, particularly at low surfactant concentration. This is the opposite effect that one would expect by making the particles more acidic. We speculate that what was occurring in this case was that the basic OLOA 11000 formed an acid-base adduct with the synergist in solution. This would essentially make the surfactant head group more acidic or less basic, diminishing the acid-base charge transfer with the particle surface. This also explains why the effect was more pronounced at low surfactant concentrations. As more surfactant was added to the system there was a smaller percentage of surfactant bound to synergist and the effect of the added synergist was diminished.

Clearly, these results demonstrate the potential for synergists to affect the charge of apolar particle dispersions. It appears that the formation of acid-base adducts plays the dominant role in the charging behavior of these systems. This is true for both acid-base interactions at the particle surface, with or without synergist, and for synergist and surfactant interactions in the bulk solution.

4.5. Conclusion

The current study set out to investigate the potential effects of the use of synergists on the apolar charging of organic pigment particles. We observed that when synergist was added to cyan dispersions containing Span 80, there was no significant change in particle charge. This is because cyan particles in the presence of Span 80 already charge marginally positive, and making the surfaces more acidic does not significantly affect the particle charge as Span 80 appears to be unable to charge particles negatively. When synergist is added to dispersions of cyan particles containing AOT, the particle charge reversed polarity from positive to negative. This occurs because AOT is able to charge particles both positively and negatively, and the

addition of sulfonic acid groups makes the cyan particle sufficiently acidic to charge it negatively. In dispersions of cyan containing OLOA 11000 the addition of synergist caused the magnitude of negative charge to decrease, particularly at low surfactant concentrations. The explanation for this is that the basic OLOA 11000 will aggressively bind with the acidic synergist in solution, rendering them incapable of exchanging charge with the surface of the cyan particle.

When synergist was added to magenta dispersions containing Span 80 it was observed that the magnitude of the positive charge was greatly diminished. This appears to again be a result of the addition of sulfonic acid to the particle surface, making it more acidic. Finally, we were not able to properly examine the effects of synergist in magenta dispersions containing AOT and OLOA 11000 because there was not a sufficient amount of synergist adsorbed to the magenta.

Based on these results, it appears that the dominant mechanism for particle charging is acid-base interactions. The addition of synergist to these systems changes the nature of the acid-base interactions by introducing addition sulfonic acid groups to the system.

4.6. Acknowledgement

This research was supported, in part, by a gift from the Xerox Corporation and by the University of Washington Center for Surfaces, Polymers, and Colloids. The authors would like to thank undergraduate researcher Benjamin Ponto for his assistance in conducting this research.

4.7. References

[1] Morrison, I., *Colloids Surf., A* **1993**, *71*, 1-37.

[2] Pugh, R.J.; Matsunaga, T.; Fowkes, F.M.; *Colloids Surf.* **1983**, *7*, 183-207.

[3] Jones, S.A.; Martin, G.P.; Brown, M.B.; *J. Pharm. Sci.*, **2006**, *95*, 1060-1074.

[4] Comiskey, B.; Albert, J.D.; Yoshizawa, H.; Jacobson, J.; *Nature* **1998**, *394*, 253-255.

[5] Guo, Q.; Singh, V.; Behrens, S.H.; *Langmuir* **2010**, *26*, 3203-3207.

[6] Parent, M.E.; Yang, J.; Jeon, Y.; Toney, M.F.; Zhou, Z.L.; Henze, D.; *Langmuir* **2011**, *27*, 11845-11851.

[7] Smith, G.N.; Eastoe, J.; *Phys. Chem. Chem. Phys.* **2013**, *15*, 424-439.

[8] Pugh, R.J.; Fowkes, F.M.; *Colloids Surf.* **1984**, *9*, 33-46.

[9] Pugh, R.J.; Fowkes, F.M.; *Colloids Surf.* **1984**, *11*, 423-427.

[10] Riddle, F.L.; Fowkes, F.M.; *J. Am. Chem. Soc.* **1990**, *112*, 3259-3264.

[11] Poovarodom, S.; Berg, J.C.; *J. Colloid Interface Sci.* **2010**, *346*, 370-377.

[12] Espinosa, C.E.; Behrens, S.H.; Guo, Q.; *Langmuir* **2010**, *26*, 16941-16948.

[13] Dukhin, A.S.; Goetz, P.J.; *J. Electroanal. Chem.* **2006**, *588*, 44-50.

[14] Roberts, G. S.; Sanchez, R.; Kemp, R.; Wood, T.; Bartlett, P.; *Langmuir* **2008**, *24*, 6530-6541.

[15] Smith, P.G.; Patel, M.N.; Kim, J.; Milner, T.E.; Johnston, K.P.; *J. Phys. Chem. C* **2007**, *111*, 840-848.

[16] Gacek, M.; Brooks, G.; Berg, J.C; *Langmuir* **2012**, *28*, 3032-3036.

[17] Gacek, M.M.; Berg, J.C.; *Langmuir* **2012**, *28*, 17841-17845.

[18] Hsu, M.F.; Dufresne, E.R.; Weitz, D.A.; *Langmuir* **2005**, *21*, 4881-4887.

[19] Herbst, W.; Hunger, K.; *Industrial Organic Pigments*, Wiley-VCH, Weinheim **2004**.

[20] Sinnokrot, M.O.; Sherrill, C.D.; *J. Phys. Chem. A* **2006**, *110 (37)*, 10656-10668.

Chapter 5

Effects of Trace Water on Charging of Silica Particles Dispersed in Apolar Media

5.1. Summary

This paper presents an investigation of the effects of trace water on the charging of silica (SiO_2) particles dispersed in a nonpolar medium. There are a growing number of applications that seek to use electrostatic effects in apolar media to control particle movement and aggregation stability in such systems. One factor that is often overlooked in the preparation of nonpolar colloidal dispersions is the amount of water that is introduced to the system by hygroscopic particles and surfactants. The amount and location of this water can have significant effects on the electrical properties of these systems. For nonpolar surfactant solutions it has been shown that water can affect the conductivity, and it has been speculated that this is due to swelling of the polar cores of inverse micelles, increasing the fraction of them that are charged. Some studies have suggested that particle surface charging may also be sensitive to water content, but a clear mechanism for the process has not been fully developed. The situation with particles is further complicated by the fact that it is often unclear whether the water resides on the particle surfaces or in the polar cores of inverse micelles. The current work explores not only the effect of water content on reverse micelle and particle charging, but seeks to differentiate between water bound to the particles and water located in the micelles. This is accomplished by measuring the solution conductivity and the electrophoretic mobility of silicon dioxide particles

dispersed in solutions of Isopar-L and OLOA 11000. The water content is determined for both the dispersion and the supernatant after centrifuging the particles out. It is found that at equilibrium the majority of the water in the system adsorbs to the surface of the hygroscopic silica particles. In addition, the effect of water on particle electrophoretic mobility is found to be dependent on surfactant concentration. At small OLOA concentrations, additional water results in an increase in particle mobility due to increased particle charging. However, at large OLOA concentrations, additional water leads to a decrease in particle mobility, presumably as a result of increased electrostatic screening or neutralization. Thus particle charging and electrophoretic mobility in an apolar surfactant solution are found to be highly sensitive to both the total water content in the system and to its concentration relative to the amount of surfactant present.

5.2. Introduction

The manipulation of charge in nonpolar liquids originated with the petroleum industry's desire to prevent electrokinetic explosions by increasing their conductivity [1]. It has since expanded to encompass a number of applications in which particles are stabilized electrostatically, including motor oil additives and nonpolar paints and inks [1,2]. Most recently, charged particles have been used in electrophoretic displays [3], such as the Amazon Kindle®, in which the particle electrophoretic mobility is a critical parameter for achieving a high refresh rate. It has been previously found that particle type, surfactant type, and surfactant concentration all play a vital role in achieving the ideal amount of charge in these systems. It now appears that water content must also be considered if these systems are to be efficiently designed and optimized.

Charge stabilization in nonpolar systems is inherently more difficult than in aqueous systems. This is due to the large amount of energy required to separate charges in a low dielectric medium. Therefore, it is often necessary to employ surfactants that form reverse micelles in such systems. These reverse micelles have a polar core surrounded by a steric barrier that sequesters and stabilizes the charges from recombination. However, the mechanism by which charge separation occurs is actively debated and appears to be largely system dependent [1]. In addition, it is often difficult to draw any meaningful conclusions, because the presence of trace water is not rigorously controlled. Morrison's 1993 review highlights experimental evidence that demonstrates the various observed effects that water can have on charging in these systems [1]. The current work aims to contribute to the understanding of how water impacts the stabilization of charge in nonpolar media, and in particular, how it affects particle charging in such systems.

In this study we investigate the effects of water on the charging of 250 nm silica particles dispersed in solutions of the commercial surfactant OLOA 11000 in the nonpolar fluid Isopar-L. Silica is an acidic mineral oxide, and OLOA 11000 is a nonionic, polyisobutylene succinimide (PIBS) surfactant with a polyamine head group, making it basic in nature. OLOA 11000 is also commonly used as a charge stabilizer in nonpolar media. Previous research [4,5] has shown that mineral oxides will engage in acid-base charge transfer with compatible surfactants, and the basic OLOA is a prime example of this. The objective of this study is to vary, systematically, the trace water content in dispersions with various concentrations of surfactant. By simultaneously measuring the electrophoretic mobility, conductivity, and water content of these dispersions, we hope to answer several questions, including: where does the water reside (on the particle surfaces or in the polar core of the reverse micelles)? and, what is the ultimate effect of water on the particle electrophoretic mobility?

5.3. Materials and methods

5.3.1. Materials

The nonpolar solvent used in these experiments was Isopar-L, a commercial isoparaffinic hydrocarbon supplied by Exxon Mobile Chemical (Houston, TX). It consists of C11 to C15 saturated hydrocarbons, giving it a very low dielectric constant of 2.0. It was used as received.

The particles used were 250 nm silica (SiO_2) particles from Fiber Optics Center Inc. (New Bedford, MA). The particles are spherical, monodisperse, hygroscopic, and inherently acidic in nature, as evidenced by their low aqueous point of zero charge (PZC) [4]. The particles were received in powder form and used as is. All dispersions in this study contained 0.35 wt% particles.

The surfactant of interest was OLOA 11000, a polyisobutylene succinimide with a polyamine head group [6] from Chevron Oronite (Bellaire, TX). This makes it a basic surfactant that is somewhat hygroscopic. The OLOA series of surfactants have been used frequently as charge control agents in nonpolar media [5-8].

5.3.2. Conductivity investigation

The first stage of the current work was to establish a baseline for micelle charging without the presence of particles. To accomplish this, we prepared solutions with a range of OLOA 11000 concentrations in Isopar-L. In addition, for each concentration of OLOA we varied the water content by either storing them in a desiccator with molecular sieves or by exposing them to air at various levels of relative humidity. Each solution was allowed to come to equilibrium over 24 hours, and then the conductivity and water content were determined. The

conductivity measurements were carried out with a DT-700 Non-aqueous Conductivity Probe from Dispersion Technology, Inc. (Bedford Hills, NY), and the water content was determined with a C20 Coulometric Karl Fischer Titrator from Mettler Toledo (Columbus, OH). The DT-700 automatically set the frequency of the applied sine wave voltage to 1 Hz for every conductivity measurement in this work.

After this baseline was established, we prepared similar solutions of OLOA and Isopar that now contained silica particles that had been dried in an oven for 2 hours at 250 ^{o}C and dispersed in the solvent via sonication. These dispersions were also allowed to come to equilibrium for 24 hours before measuring their conductivity. Particle electrophoretic mobility was measured using a ZetaPALS Zeta Potential Analyzer from Brookhaven Instruments Corporation (Holtsville, NY). The mobility measurements were carried out with a sinusoidal voltage at a frequency of 2 Hz using field strengths ranging from 10 – 50 kV/m. The measured mobilities were then extrapolated back to zero electric field to eliminate any effects of electric field induced charging, as demonstrated by Behrens and coworkers [9]. Next, the particles were centrifuged out, and the water content was measured as before. This allowed comparison of the conductivity before and after adding the silica particles while adjusting for water content variations.

5.3.3. Trace water effects on particle electrophoretic mobility

The second phase of research was to determine where the water resided in these systems, and the ultimate effect of the trace water on the electrophoretic mobility of the silica particles. The first step of the experiment was carried out by independently pretreating both the silica particles and the nonpolar solutions containing various concentrations of OLOA 11000 with

varying amounts of moisture. The silica was either dried for 4 hours at 250 ^{o}C (dry) or exposed to 80% humidity air for 48 hours (wet). The OLOA solutions were either stored in a desiccator with molecular sieves for 48 hours (dry) or exposed to 80% humidity air for 48 hours (wet). These were then combined in the 4 possible permutations, sealed in airtight containers, sonicated, and allowed to equilibrate for 24 hours. Next, the electrophoretic mobility, conductivity, and water content were measured in the same manner as in the previous section. Finally, the particles were centrifuged out, and the water content was measured again. This enabled the determination of the total water content as well as the fraction of water that ended up on the silica particles for each sample.

5.4. Results

5.4.1. Conductivity investigation

As previously mentioned, the first phase of the experiment was to determine how water affected micelle charging without the presence of particles. Figure 5.1 shows the effect of water content on conductivity for a number of OLOA concentrations. The conductivity is seen to increase dramatically with the addition of water for every concentration studied. In many cases, the conductivity increases a full order of magnitude by going from very dry to nearly saturated (without forming microemulsions). This is consistent with previous results found in the literature [10].

By maintaining a consistent ratio of water to OLOA, we are able to determine how the system conductivity changes as a function of OLOA concentration with and without the presence of particles. The data for a molar water/OLOA ratio of roughly 0.5 are shown in Figure 5.2(a). Without the presence of particles, the conductivity exhibits a dramatic linear rise above

approximately 0.01 wt% OLOA, corresponding to the critical micelle concentration (CMC), as reported previously [5,8]. Below this concentration, the conductivity is very small, and the uncertainty often approaches the instrument limit of 0.1 pS/m.

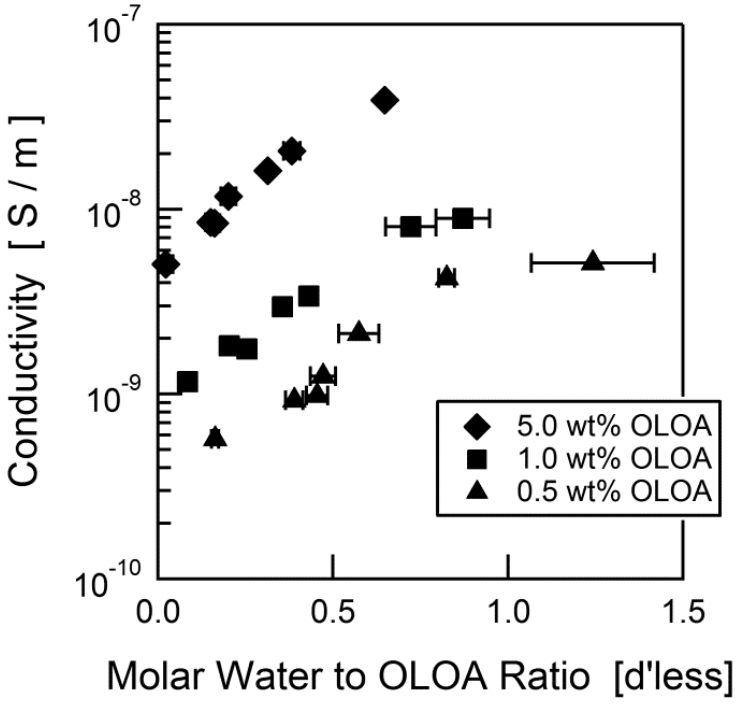

Figure 5.1. Effect of water on the conductivity of OLOA 11000 solutions in Isopar-L. Conductivity data for Isopar-L solutions containing various OLOA 11000 concentrations are plotted as a function of the molar ratio of water to OLOA. Error bars are derived from 3 measurements and are often smaller than the data markers.

With particles present in the system, we again observed little charging below the CMC, as evidenced by electrophoretic mobility measurements. However, at OLOA concentrations above the CMC, the conductivity was larger than that corresponding to the particle-free system. It was also apparent in Figure 5.2(a) that the relative difference between conductivities with and without particles reached a maximum at approximately 0.1 wt% OLOA. This is seen to be about the same concentration yielding the maximum in particle electrophoretic mobility, shown in Figure 5.2(b).

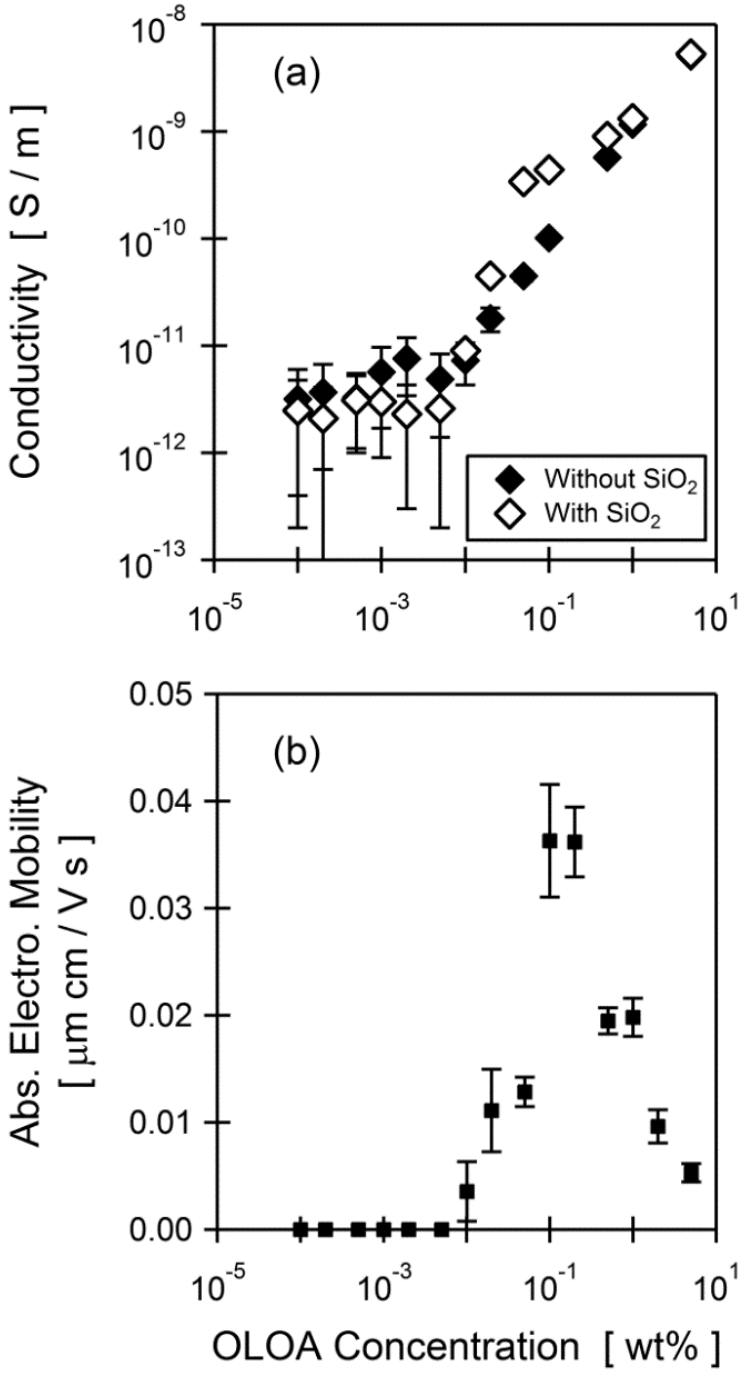

Figure 5.2. Silica particle charging in solutions of Isopar-L and OLOA 11000. (a) The top figure shows conductivity data plotted as a function of OLOA concentration, where the open symbols are samples without silica particles and the closed symbols represent samples with dispersed silica particles. Error bars were derived from 10 measurements, and are often smaller than the markers. (b) The bottom figure shows the magnitude of the particle electrophoretic mobility plotted as a function of OLOA concentration. It should be noted that in all cases the sign of the mobility was negative.

It should be noted that the polarity of the silica surface charge was negative for every sample in this work, and for convenience, the magnitude of the mobility is plotted in all graphs. It was observed that below the CMC, no significant particle charging occurred, while above the CMC, the mobility increased with increasing OLOA concentration until a maximum was reached, after which the mobility decreased with increasing OLOA.

5.4.2. Trace water effects on particle charging

Since both the silica particles and the OLOA 11000 are hygroscopic, it is important to understand where the water ultimately resides in these systems. The fraction of the total water that was adsorbed on the silica particles as a function of the total water content in the system is plotted in Figure 5.3. This was done for the various mixtures of "wet" and "dry" pretreatments of the silica particles and OLOA/Isopar solutions. It should be noted that the "dry" OLOA and "dry" silica combination is not shown in Figure 5.3 because the total water contents were under 15 ppm water and often approached the instrument limit of approximately 5 ppm. As a result, the uncertainty of these data approached 100%.

It was observed that roughly 80 – 90% of the water present was adsorbed at the silica surface once equilibrium had been reached. This was true regardless of whether the water was introduced to the system with the particles or with the surfactant solution, and held true for all but the largest total water contents. This indicated that there is a natural balance of water scavenging that occurs between the more hygroscopic particles and less hygroscopic surfactant micelles. The percent of water associated with the particles dropped dramatically at high water contents because the water on the particles never exceeded 275 ppm. This maximum value seemed to suggest that the particles became saturated with water, and any additional water added

to the system was taken up by the surfactant micelles. The saturation limit for the silica particles was calculated to be approximately 20 monolayers of water.

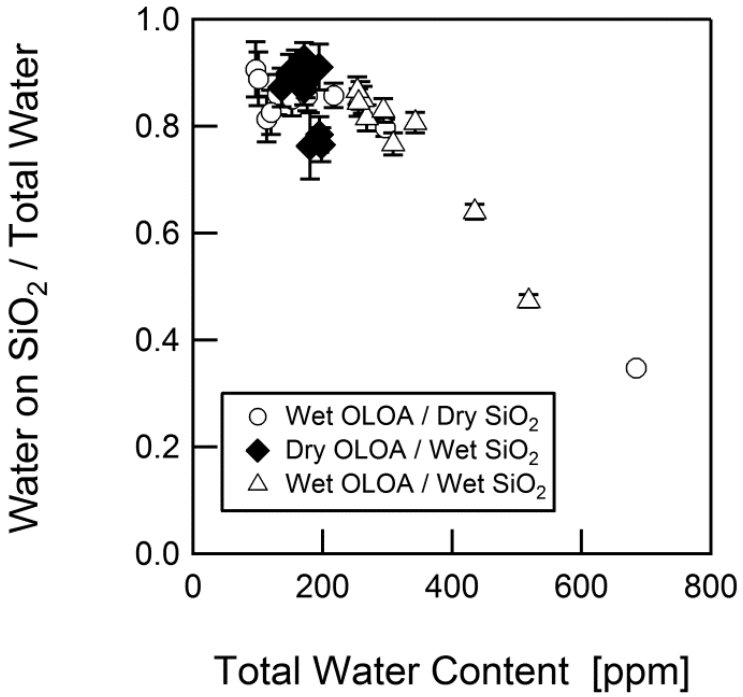

Figure 5.3. Equilibrium location of water. The fraction of the total water that was adsorbed to the particle surface at equilibrium is plotted against the total water content in each sample. Each form of pretreatment (represented by the different markers) represents a series of OLOA concentrations ranging from 0.01 to 5 wt%. Error bars were derived from three measurements.

The final set of results deals with the effects of water on the particle electrophoretic mobility. In Figure 5.4 the magnitude of the particle electrophoretic mobility is plotted against the total water content for (a) small OLOA concentrations, (b) intermediate OLOA concentrations, and (c) large OLOA concentrations. As previously mentioned, the polarity of the particle charge was negative in every sample. The nature of the dependence of particle electrophoretic mobility on water content is seen to depend dramatically on the surfactant concentration level.

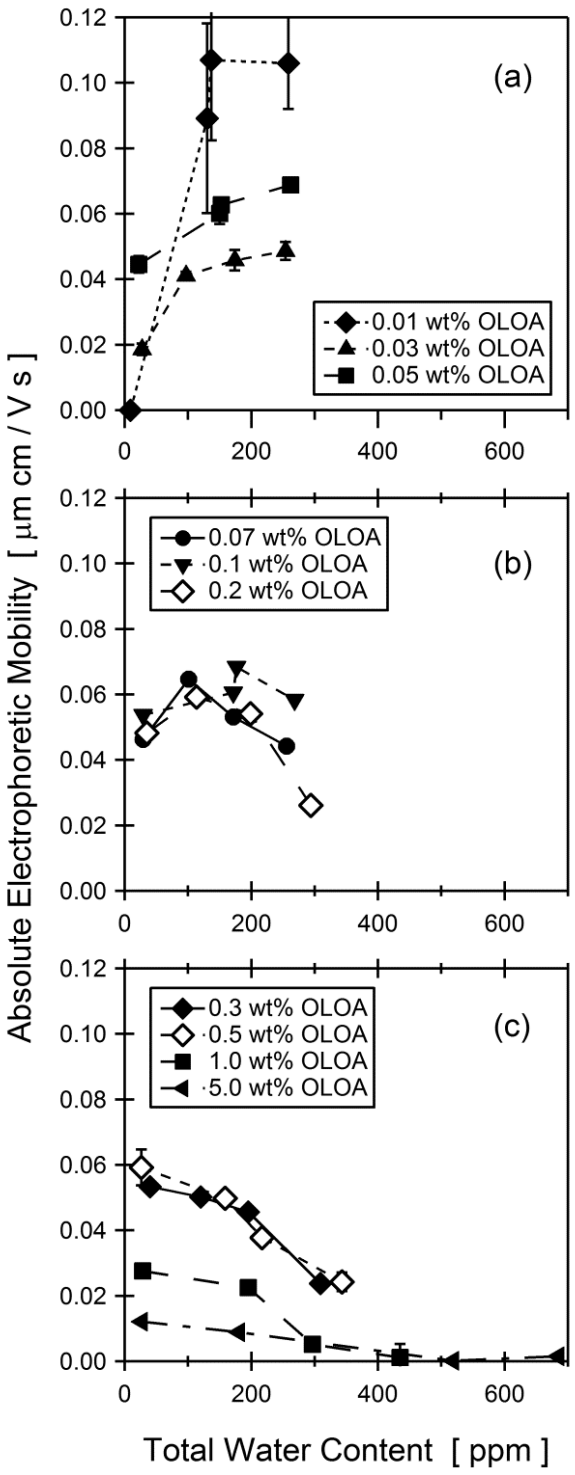

Figure 5.4. Silica particle charging dependence on water content. The magnitude of the particle electrophoretic mobility is plotted as a function of total water content for (a) small, (b) intermediate, and (c) large OLOA 11000 concentrations. Error bars are derived from three measurements, and are often smaller than the markers.

At small OLOA concentrations the particle mobility increased with increasing water content. This trend was particularly apparent when the OLOA concentration was very near the CMC of 0.01 wt%. At this point, the driest samples exhibited negligible charging, while the "wet" samples had the largest mobilities observed in this study under any conditions. However, particle charging so near the threshold of micelle formation (i.e. low surfactant concentration) made these samples somewhat unstable with respect to aggregation, and a large error in measured electrophoretic mobility was observed. For samples containing 0.01 wt% OLOA the average particle diameter, as determined by the ZetaPALS two hours following sonication, was 1063 ± 428 nm. At every other OLOA concentration in this work the average particle size was roughly 300 nm, indicating minimal aggregation. The samples near the CMC were also the only ones to exhibit any dependence on applied electric field strength, and the extrapolation back to zero field strength added to the uncertainty of these values. Another observation of note is that the particle mobilities for 0.05 wt% OLOA were generally larger than those for 0.025 wt%.

At large OLOA concentrations, the opposite trend was observed. The particle mobility decreased with increasing water content. In addition, the mobility decreased with increasing OLOA concentration. At intermediate OLOA concentrations a transition between the two extremes can be observed, exhibited by a maximum mobility at intermediate water contents.

5.5. Discussion

5.5.1 Effect of water on conductivity

The increase in conductivity with additional water shown in Figure 5.1 can be explained by micelle swelling resulting in a larger fraction of micelles becoming charged. This reasoning can be justified by evaluating the work needed to place an ion in the polar core of a reverse

micelle. The system may be represented by a series of spherical capacitors where the innermost sphere is the ion, the second sphere is the edge of the high dielectric polar core of the reverse micelle, and the outer edge extends into the low dielectric medium to infinity [11.12]. Therefore, the energy required to place an ion in a reverse micelle is represented by

$$E = \frac{e^2}{8\pi\varepsilon_0\varepsilon_{np}r_c} + \frac{e^2}{8\pi\varepsilon_0\varepsilon_p}\left(\frac{1}{r_i} - \frac{1}{r_c}\right) \tag{5.1}$$

where e is the elementary charge, ε_0 is the permittivity of free space, r_c is the radius of the polar core of the reverse micelle, r_i is the radius of the ion, and ε_{np} and ε_p are the dielectric constants of the nonpolar external medium and the polar core, respectively. It is often assumed that the dielectric constant of the polar core is large enough compared to the nonpolar medium that the second term may be considered negligible. However, it should be noted that this assumption holds true only if the ion radius is rather large. For elemental ions, the second term may contribute a significant amount of energy, and leads us to believe that either water or some other large ionizable impurity is the likely source of charge in the reverse micelles. This would also explain why the use of a 0.1M NaCl aqueous solution as the swelling agent yielded exactly the same conductivity as pure DI water in Behrens and coworkers' previous work [10]. The micelle ionization energy from equation (5.1) is then used in a Boltzmann relation to represent the fraction of total micelles that are charged at equilibrium [10,13].

$$C_{\pm Z} = C_0 \exp\left(\frac{-Z^2\lambda_B}{2r_c}\right) \tag{5.2}$$

where $C_{\pm Z}$ is the concentration of charged micelles of valence Z, C_0 is the concentration of neutral micelles, and $\lambda_B = e^2/4\pi\varepsilon_0\varepsilon_{np}k_BT$ is the Bjerrum length of the nonpolar medium. For systems with dielectric constants as low as those of our system, the probability of a micelle

containing more than a single charge is negligible, and Z is therefore assumed to be ± 1. It is clear from this equation that the larger the polar micelle core, the more energetically favorable it is for the micelle to obtain charge. As previously mentioned, the water to OLOA ratio was kept low enough to prevent the formation of water-in-oil emulsions. However, if one did force more water into the system and emulsions or microemulsions were formed, then the analysis of such structures could be considerably more complicated [14,15].

5.5.2. Charging mechanisms

The linear relationship between conductivity and OLOA concentration above the CMC shown in Figure 5.2(a) suggests a two-micelle interaction based on the law of mass action. Therefore, disproportionation, where two neutral micelles interact to form two oppositely charged micelles, is the common mechanistic explanation by which OLOA and other surfactant reverse micelles obtain charge. If the mechanism were dissociation, where a single micelle could eject an ion, one would observe a square root relationship between conductivity and surfactant concentration. Disproportionation is also the energetically more favorable mechanism. In consideration of equation (5.1), the work of creating one charged micelle and one ion requires roughly five times more energy than two oppositely charged micelles (assuming r_c = 2.5 nm and r_i = 0.2 nm) [6].

Before analyzing the observed change in conductivity upon the addition of silica particles, one must account for the fact that OLOA 11000 monomers will adsorb to the surfaces of the particles. There is some concern that this could change the concentration of OLOA in the bulk solution, complicating any direct comparison of the conductivity. A previous study involving OLOA 11000 analogues showed that the maximum packing density of an adsorbed

monolayer on carbon black particles dispersed in hexane is roughly $18x10^{-8}$ mol/m^2 [16]. Applying this number to the total surface area in our system reveals that the maximum amount of OLOA that could be removed from solution is 0.0015wt%, a full order of magnitude less than the smallest OLOA concentration used in this study. Therefore, in the following analysis the concentration of surfactant in the bulk solution is assumed to be the same before and after the silica particles are added.

The increase in conductivity with the addition of particles indicates that there is a specific interaction between the surfactant and the particle that is separate from the micelle-micelle disproportionation mechanism. It is possible that this increase in conductivity is due to charges being generated at the particle surfaces when the system is in the presence of the electric field generated by the conductivity meter. However, the field produced by the DT-700 conductivity meter is only 5 kV/m. Since we observed no particle electrophoretic mobility dependence on electric field strengths of 10-50 kV/m for nearly all of the OLOA concentrations tested, it seems to provide circumstantial evidence that the charge is spontaneously generated upon addition of the particles. Regardless of the possible implications of field-generated charges, the negative surface charge on the silica is consistent with the mechanism of acid-base interaction in which the acidic silica donates a proton to a basic OLOA monomer that is adsorbed at the surface. This positively charged monomer is then incorporated into a nearby micelle, leaving a negative charge on the silica surface. Another interesting observation is that as the relative difference in conductivity decreases, the particle mobility also decreases. This supports the idea that once the micelle concentration reaches a certain level, the total charge in the bulk solution is large enough to engage in either electrostatic screening or charge neutralization. This screening effect has been observed in a number of different systems [5,6,9,17,18].

5.5.3. Effect of water on particle electrophoretic mobility

The observation that the water in the system achieved a consistent equilibrated balance between particles and micelles is not altogether surprising given their relative hygroscopic natures. However, it does mean that we were unable to completely separate the effects of water at the particle surface from water in the micelles, and could only study the effects of total water content. Therefore, the following analysis of the different particle electrophoretic mobility trends is largely speculative.

As Figure 5.4(a) shows, at OLOA concentrations of 0.01, 0.025, and 0.05 wt% we observed an increase in particle electrophoretic mobility with increasing water. There are several possible explanations for this behavior. The first is that, as others have speculated [1], additional water at the particle surface could serve to "loosen" surface ions, allowing them to dissociate more freely. This is consistent with the fact that the proton conductivity in a water layer at a silica surface can be much greater (several orders of magnitude) than in bulk water. In this nonpolar system, the ions of interest are the surface protons that would dissociate from the surface hydroxyl groups of the silica and become bound to the OLOA monomers. Previous research has also shown that as mineral oxides are progressively dried, they lose their acid-base character, indicating that water is necessary for facilitating acid-base interactions [19].

Another contributing explanation is that the additional water would swell the micelles, allowing them to more readily stabilize the countercharges. Returning to equation (5.1), if the inner spherical capacitor radius (representing the radius of the ion) is replaced by the radius of the particle, one can approximate the energy required to place an ion at the particle surface. For this system, it is found that it takes roughly 1/50 the energy to place a single ion at the particle

surface as it does to stabilize one in a reverse micelle. This would suggest that micelle charging is the limiting step in the particle charging mechanism, and explains why multiple charges are able to accumulate on the particle surface, whereas each micelle can only stabilize a single charge. It would also suggest that while the acid-base interaction between OLOA and silica dominates the polarity of the particle's charge, the micelle size and concentration strongly influences the magnitude of charge. At these small surfactant concentrations, there are not enough micelles in solution to produce a significant amount of micelle-micelle charging events, and electrostatic screening or neutralization effects are minimal. Using this logic, it makes sense that the particle mobilities at 0.05 wt% OLOA are slightly larger than at 0.025 wt%. However, it is somewhat peculiar that the largest particle mobilities occurred at the lowest OLOA concentration of 0.01 wt%. The fact is that these values had the most variability from sample to sample and exhibited the most electric field strength dependence. Therefore, we speculate that when the surfactant concentration is very near the CMC, micelles or premicellar structures may form right at the water-rich particle surface. Clearly, more investigation is required at these small surfactant concentrations. The use of a less viscous medium than Isopar-L might be needed to allow electrophoretic mobility measurements to be successfully performed at lower field strengths than those used in this study.

At large OLOA concentrations, shown in Figure 5.4(c), we observe the opposite trend. As either water content or OLOA concentration increases the particle electrophoretic mobility decreases. The most probable explanation for this is that at these surfactant concentrations micelle-micelle charging and electrostatic screening/neutralization dominate the particle mobility. Therefore, increasing either the micelle concentration or swelling the micelles results in more charge in the bulk solution, enhancing these screening effects. One could speculate that if

the water content were small enough, it would begin to inhibit the particle charging. However, due to the hygroscopic nature of the particles we never reached such a critically low level of water. At intermediate OLOA concentrations, shown in Figure 5.4(b), the transition between the dominance of micelle-particle charging and micelle-micelle charging is manifested by a maximum in particle mobility as a function of water content. This transition is further evidenced in Figure 5.2(b) by a maximum observed electrophoretic mobility as a function of OLOA concentration at roughly 0.1 wt%.

5.6. Conclusion

The current work investigates the effects of trace water on particle charging in the nonpolar system consisting of untreated silica particles and the nonionic surfactant OLOA 11000 in Isopar-L. It is found that trace water has a large impact on both micelle and particle charging:

- In OLOA and Isopar solutions containing no particles, the addition of water greatly enhances reverse micelle charging, as evidenced by conductivity measurements. This can be explained by the swelling of the polar cores of the reverse micelles, making it energetically more favorable for a charge to reside there.
- When particles are added to the system, the conductivity is seen to increase even though the water content remains constant. This is indicative of a charge-generating interaction between the particles and the surfactant molecules that is separate from micelle-micelle charging. The negative charge obtained by the silica particles supports the theory of acid-base charge transfer as a dominant charging mechanism for mineral oxides.

The effect of water on the particle electrophoretic mobility can be separated into two regimes that are dependent on surfactant concentration:

- At OLOA concentrations ranging from 0.01 to 0.05 wt% an increase in particle electrophoretic mobility with increasing water content is observed. This suggests that additional water increases the occurrence of micelle-particle charging events, resulting in a larger particle surface charge.
- At large OLOA concentrations of 0.3 wt% or more the particle electrophoretic mobility decreases with increasing water content. This suggests that at large surfactant concentrations micelle-micelle charging, leading to electrostatic screening or neutralization, has a large influence on particle mobility. The increase in micelle-micelle charging from additional water in the micelle cores only enhances these effects.

In summary, particle electrophoretic mobility in nonpolar systems is highly dependent on surfactant concentration and water content, and one must optimize both if the maximum mobility is to be achieved.

5.7. Acknowledgement

This research was supported, in part, by a gift from the Xerox Corporation, and by the University of Washington Center for Surfaces, Polymers, and Colloids.

5.8. References

[1] Morrison, I.D.; *Colloids Surf., A* **1993**, *71*, 1-37.

[2] Pugh, R.J.; Matsunaga, T.; Fowkes, F.M.; *Colloids Surf.* **1983**, *7*, 183-207.

[3] Comiskey, B.; Albert, J.D.; Yoshizawa, H.; Jacobsen, J.; *Nature* **1998**, *394*, 253-255.

[4] Gacek, M.; Brooks, G.; Berg, J.C.; *Langmuir* **2012**, *28*, 3032-3036.

[5] Poovarodom, S.; Berg, J.C.; *J. Colloid Interface Sci.* **2010**, *346*, 370-377.

[6] Parent, M.E.; Yang, J.; Jeon, Y.; Toney, M.F.; Zhou, Z.; Henze, D.; *Langmuir* **2011**, *27*, 11845-11851.

[7] Prieve, D.C.; Hoggard, J.D.; Fu, R.; Sides, P.J.; Bethea, R.; *Langmuir* **2008**, *24*, 1120-1132.

[8] Strubbe, F.; Verschueren, A.R.M.; Schlangen, L.J.M.; Beunis, F.; Neyts, K.; *J. Colloid Interface Sci.* 2006, *300 (1)*, 396-403.

[9] Espinosa, C.E.; Behrens, S.H.; Guo, Q.; *Langmuir* **2010**, *26*, 16941-16948.

[10] Guo, Q.; Singh, V.; Behrens, S.H.; *Langmuir* **2010**, *26*, 3203-3207.

[11] Parsegian, A.; *Nature* **1969**, *221*, 844-846.

[12] Smythe, W.R. *Static and Dynamic Electricity*, 3rd Edition; McGraw-Hill: New York, **1967**; 27-30.

[13] Hall, D.G.; *J. Phys. Chem.* **1990**, *94*, 429-430.

[14] Wines, T.H.; Dukhin, A.S.; Somasundaran, P.; *J. Colloid Interface Sci.* **1999**, *216 (2)*, 303-308.

[15] Dukhin, A.; Goetz, P.; *Colloids Surf., A* **2005**, *253*, 51-64.

[16] Shen, Y.; Duhamel, J.; *Langmuir* **2008**, *24*, 10665-10673.

[17] Dukhin, A.S.; Goetz, P.J.; *J. Electroanal. Chem.* **2006**, *588*, 44-50.

[18] Hsu, M.F.; Dufresne, E.R.; Weitz, D.A.; *Langmuir* **2005**, *21*, 4881-4887.

[19] Sun, C.; Berg, J.C.; *J. Chromatogr. A* **2002**, *969*, 59-72.

Chapter 6

Effect of surfactant hydrophile-lipophile balance (HLB) value on mineral oxide charging in apolar media

6.1. Summary

The current work examines the role of surfactant hydrophile-lipophile balance (HLB) on the ability for surfactant reverse micelles to impart charge to particles dispersed in an apolar medium, a study motivated by a number of applications that seek to maximize particle charge in such systems. Previous investigations have shown that relative acid-base properties of the particles and surfactants, as well as surfactant concentration and trace water content, all play a major role in the particle charge obtained. However, the ability of a surfactant to stabilize charge in reverse micelles is also an important aspect of creating charge on a particle surface. It has been previously shown that surfactant HLB value is an important parameter in assessing the size of the polar core of the reverse micelles, thereby impacting the total charge that is generated in the bulk solution as determined by conductivity. In the current study, this theory is extended to investigate the impact on particle charging. To accomplish this, the electrophoretic mobility is determined for a series of mineral oxides dispersed in Isopar-L with either Span 20, Span 80, or Span 85. These three surfactants all have the same head group chemistry, but their HLB value ranges from 1.8 to 8.6. It is found that the maximum observed particle electrophoretic mobility does scale directly with the HLB of the accompanying surfactant. This indicates that there is a direct correlation between a surfactant's ability to stabilize charge and its ability to impart charge

to a particle. However, the largest HLB surfactant, Span 20, also exhibited a large amount of charge screening or neutralization at larger surfactant concentrations. This highlights the competition between particle charging and micelle-micelle charging that remains one of the largest obstacles to maximizing particle charge in apolar systems.

6.2. Introduction

The study of stabilizing and manipulating charge in apolar liquids is an area that has seen increased interest in recent years. This is due in large part to the development of a number of commercial applications that make use of charged particles stabilized in such systems. Traditionally, charge was used simply for stabilizing particles in motor oil and apolar paints and inks [1,2]. More recently, charge has been implemented to drive the transport of particles in a desired manner. Examples of this include the Amazon Kindle Paperwhite ® electronic reader and Indigo ® electrophoretic ink by Hewlett-Packard. Research in this area has been centered on better understanding what factors influence particle charge in apolar media. The difficulty in understanding these systems stems from the inherent complexity involved in stabilizing charge in low dielectric fluids. It has been well documented that charge-stabilizing surfactants must be present in the system for charging to occur, and these surfactants must be present in a sufficient concentration to form reverse micelles or similar aggregate structures. A reverse micelle consists of a polar core, often containing some moisture, surrounded by a nonpolar shell. It is believed that the polar core is responsible for stabilizing charge.

Particle charging occurs when the surfactant interacts with the particle surface, generating a charge transfer event that results in charge residing on the particle surface and a corresponding counter charge stabilized in a reverse micelle. Significant evidence has been published in the literature indicating that the charging of mineral oxides dispersed in apolar media is dominated

by an acid-base mechanism [3-8]. The current theory is that the relative magnitude and polarity of particle charge can be explained by the relative acidity or basicity of the particle surface functional groups to the surfactant head group chemistry. Therefore, implementing a series of mineral oxides is a convenient technique for analyzing the performance of a particular surfactant of interest [5-7]. By plotting the apolar particle electrophoretic mobility as a function of aqueous particle PZC it is possible to classify the acidity or basicity of the surfactant by determining the point on the PZC scale where the particle charge crosses from positive to negative (or by extrapolation if no intersect occurs). One aspect of these plots that has remained somewhat unclear to date is the slope of the particle charge vs aqueous PZC line. In order to obtain a truly predictive model for particle charge in apolar media, a greater understanding of what influences this slope is necessary. One possible explanation may be the HLB value of the surfactant.

Changing the HLB value of the surfactant has been shown to influence the size of the polar core of the reverse micelles formed [9], which has a direct relationship with the micelle's ability to stabilize charge [9-12]. However, the effect this has on particle charging remains unclear. In a previous study, Parent and coworkers observed that magenta particle zeta potential decreased with increasing surfactant HLB value for a series of synthesized PIBS surfactants [9]. However, this study was conducted at only one surfactant concentration that was well above the surfactant CMC. It is possible that this study only revealed the effect of increased charge screening due to increased micelle-micelle charging in the bulk solution. Therefore, the purpose of the current work is to investigate the effects of surfactant HLB value on particle charging for a range of particles and a range of surfactant concentrations. This was accomplished by preparing dispersions of a series of mineral oxides in Isopar-L with a series of Span surfactants over a range of surfactant concentrations. The Span surfactants used were Span 20, Span 80, and Span

85, with HLB values of 8.6, 4.3, and 1.8, respectively. Span 40 (with an HLB of 6.7) could not be used as it is only sparingly soluble in Isopar-L at room temperature. The electrophoretic mobility and conductivity of the dispersions were measured to determine the particle charge and to track micelle charging.

6.3. Materials and methods

6.3.1. Materials

The surfactants used in this study were Span 20, Span 80, and Span 85 from Sigma-Aldrich Corp. (St. Louis, MO). All three surfactants are made up of a sorbitan head group paired with various nonpolar tail groups. The different tail groups shift the ratio of polar to nonpolar components of the surfactant, as defined by the hydrophile-lipophile balance (HLB) value. Span 80 (sorbitan monooleate) has an HLB value of 4.3 and is commonly used in apolar charging studies [4,6,7]. Span 20 (sorbitan monolaurate) and Span 85 (sorbitan trioleate) have HLB values of 8.6 and 1.8, respectively. All three surfactants were used as received.

The apolar solvent chosen was Isopar-L, a commercial isoparaffinic hydrocarbon supplied by Exxon Mobil Chemical (Houston, TX). It consists of C8 to C15 saturated hydrocarbons, with an aromatic content of only 30 ppm, and a dielectric constant of 2.0. It was used as received.

The particles used were a series of mineral oxides: silica (SiO_2) from Fiber Optics Center Inc. (New Bedford, MA), titania (TiO_2) from J.T. Baker Chemical Co. (Phillipsburg, NJ), alumina (Al_2O_3) from Baikalox International Corp. (Charlotte, NC), zinc oxide (ZnO) from MK Nano (Mississauga, Ontario), and magnesia (MgO) from MTI Corp. (Richmond, CA). The particles ranged in size from 50 to 500 nm and were selected because their aqueous points of

zero charge (PZC) are well documented and span a wide pH range. However, each mineral oxide has a range of reported values [13], making it necessary to experimentally determine the PZC and IEP of the oxides used in this study. All particles were supplied in powder form and used as received.

6.3.2. Dispersion preparation

Particles of each type were dried at 175 ^{o}C for two hours before being added to surfactant solutions containing a range of surfactant concentrations from 0.0001 to 2.5 wt%. The particle loading in each of the dispersions was 500 ppm by weight. This was done to prevent inter-particle interactions and multiple scattering during electrophoretic mobility measurements. The dispersions were then sonicated for 20 minutes and allowed to equilibrate for 24 h. All dispersions were stored in a desiccator, except during sonication and measurement, to regulate the amount of water in each sample. Previous work has shown that oxide charging in apolar media can be affected by the water content in the system [14]. This was monitored using a Karl Fischer titrator from Mettler Toledo (Columbus, OH), and was in the range of 5 - 45 ppm for all samples.

6.3.3. Measurement of electrophoretic mobility

The electrophoretic mobility of the apolar dispersions was measured by dynamic light scattering (DLS) using a Brookhaven Instruments Zeta-PALS (Holtsville, NY). The instrument is theoretically capable of measuring mobilities as low as 0.001 (μm cm)/(s V). The measurements were conducted using a sinusoidal voltage with a frequency of 2 Hz applied across electrodes spaced 0.5 cm apart. To eliminate any effects of field-induced charging, as demonstrated by Espinosa and coworkers [15], the electrophoretic mobility of each sample was

determined using applied field strengths of 17 – 55 kV/m. These values were then extrapolated back to zero field strength to determine the inherent mobility of the particles.

6.3.4. Conductivity measurements

The conductivity of every dispersion was measured using a DT-700 nonaqueous conductivity probe from Dispersion Technology, Inc. (Bedford Hills, NY). This was done to track micelle charging in the bulk solution as a function of surfactant concentration. The critical micelle concentration (CMC) of the different Span surfactants can be approximated from these data since below the CMC, little to no charging will occur.

6.3.5. Aqueous particle charge characterization

The acid-base properties of each type of particle were characterized by determining its aqueous isoelectric point (IEP) and point of zero charge (PZC). The aqueous IEP of each particle was determined by electrokinetic titration. The above mentioned Zeta-PALS instrument was used to measure the particle electrophoretic mobility. The pH was controlled with HNO_3 and KOH, and monitored with an Oakton Instruments 510 series pH/conductivity meter (Vernon Hills, IL). The aqueous PZC of each particle was also determined to verify the obtained IEP values. This was accomplished via potentiometric titration using HNO_3 and KOH for pH control, and KNO_3 was used for the background electrolyte in concentrations of 0.001, 0.01, and 0.1 M. These measurements were carried out and analyzed by the authors in a previous study [5], and the results are duplicated in Table 6.1. It should be noted that the experimental values obtained by this group are slightly lower than the average values reported in literature, especially for alumina, zinc oxide, and magnesia. However, IEP and PZC values have been shown to vary significantly from one supplier to another, and these values are within the reported range.

Regardless of this, the mineral oxides used represent a wide range of acidity or basicity for this study.

Table 6.1. Mineral oxide IEP and PZC data (in terms of pH)

Oxide	IEP (Exp.)	PZC (Exp.)	PZC (Lit.)
Silica	2.1 + 0.3	3.0 + 0.3	2-3
Titania (rutile)	4.0 + 0.2	3.7 + 0.2	4-6
Alumina	7.1 + 0.3	7.5 + 1.0	8-9
Zinc Oxide	7.5 + 0.5	7.7 + 0.3	9-10
Magnesia	8.5 + 0.5	10.7 + 0.2	10-12

Previously determined experimental values of the IEP and PZC are listed for each type of particle used in the study [5]. The ranges of average reported literature values are shown for comparison [13].

6.4. Results and discussion

6.4.1. Conductivity series

Conductivity is often used to track the charging of reverse micelles and to determine the critical micelle concentration (CMC) in apolar solutions [14]. This is relevant to the current study because the presence of reverse micelles or similar aggregate structures is typically necessary to facilitate particle charging. Figure 6.1 shows the conductivity of the different Span solutions as a function of surfactant concentration.

It is clear that each surfactant series exhibits little to no charging at low Span concentrations. Above a certain concentration, presumably the CMC, the conductivity increases with increasing surfactant concentration. This is likely due to charge disproportionation that occurs when two uncharged micelles collide, exchange charge, and result in a positively and

negatively charged micelle [14,16-18]. There is a clear correlation between the conductivity and the surfactant HLB value, and the values obtained are consistent with the study conducted by Dukhin and Goetz [12]. The CMC was observed to be approximately 0.001 – 0.005 wt. % for all three Span surfactants. This observation is somewhat unexpected, because surfactants with intermediate HLB value tend to form micelles or reverse micelles with less curvature. The lack of packing constraint typically allows these micelles to form at smaller concentrations. It should be noted that the conductivities at low surfactant concentration shown in Figure 6.1 are close to the instrument limit of the DT-700 conductivity meter.

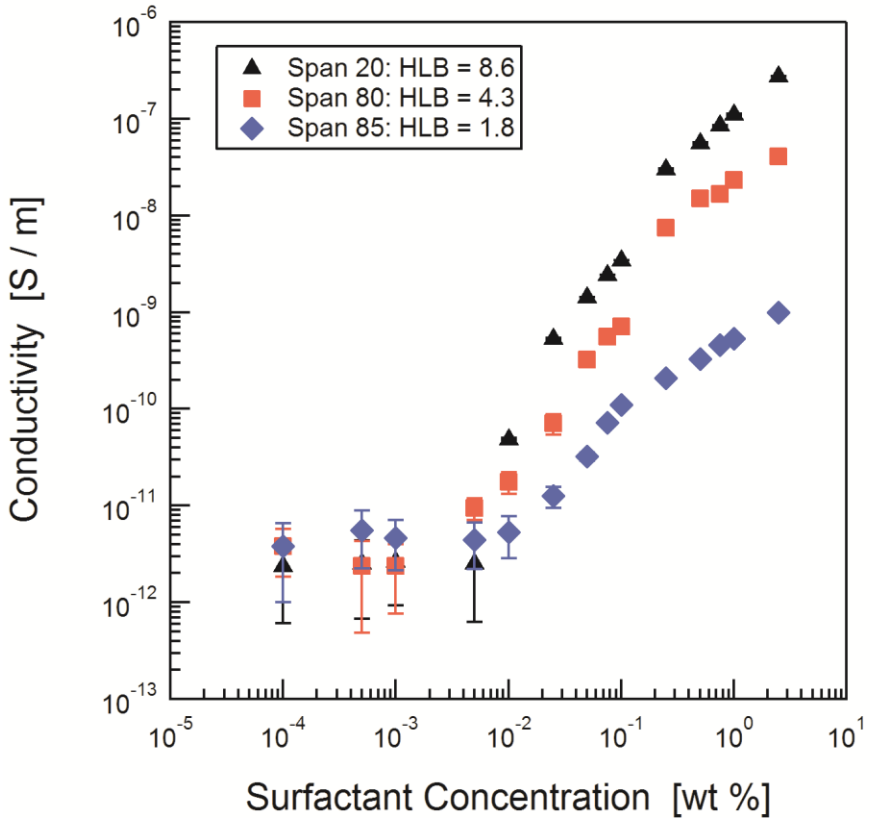

Figure 6.1. Span solution conductivity. Conductivity of Isopar-L solutions are plotted as a function of surfactant concentration for Span 20 (▲), Span 80 (■), and Span 85 (♦). Error bars are determined from 20 measurements and are equal to or smaller than the data marker when not shown.

Therefore, it is possible that micelles or pre-micellar aggregates begin to form at smaller concentrations than are reported here. However, the purpose of this study is to examine how reverse micelle charge stabilization affects particle charging. The increase in conductivity indicates that there are micelles that are capable of stabilizing charge, and it is logical that this is near the CMC. It is expected that particle charging can occur at or above this concentration, as reverse micelles exist to stabilize the counter charges from the particle surface.

6.4.2. Determination of maximum mobility

It has been extensively shown that particle charge in apolar media is strongly dependent on surfactant concentration [4-7,12,19]. Typically, below a certain concentration there is no particle charging due to a lack of micelles or similar structures that can stabilize the counter charges from the particle surface. Above this point, there is typically a maximum in particle charge as a function of surfactant concentration as there is a competition between micelle-particle charging and micelle-micelle charging resulting in charge screening or neutralization. This behavior has been widely observed using both electrophoretic and electroacoustic techniques [4-7,12]. As expected, a maximum in electrophoretic mobility as a function of surfactant concentration was observed in all of the dispersions prepared in this study. To demonstrate this, Figures 6.2(a), 6.2(b), and 6.2(c) show the electrophoretic mobility of magnesium oxide particles dispersed with Span 20, Span 80, and Span 85, respectively.

It was observed that the magnitude of charge as well as the surfactant concentration at the maximum electrophoretic mobility changes with the surfactant used. Span 20 exhibited a sharp rise and fall in particle charge with a maximum occurring at a surfactant concentration of 0.001 – 0.005 wt. % for all particles used. With Span 80 the particle charge increased and decreased more gradually, reaching a maximum at 0.01 – 0.05 wt. % for all particles. Span 85 showed only

modest charging with all particles, with the maximum particle charge occurring at 0.5 – 1.0 wt. % surfactant. Similar results were observed for all of the particles tested, and these plots can be found in the supplemental information online. Since the electrophoretic mobility exhibits a peak at different surfactant concentrations, it is necessary to determine a metric for comparing the performance of different surfactants. The maximum observed mobility is a logical choice as it depicts the peak performance of that particle for a given surfactant.

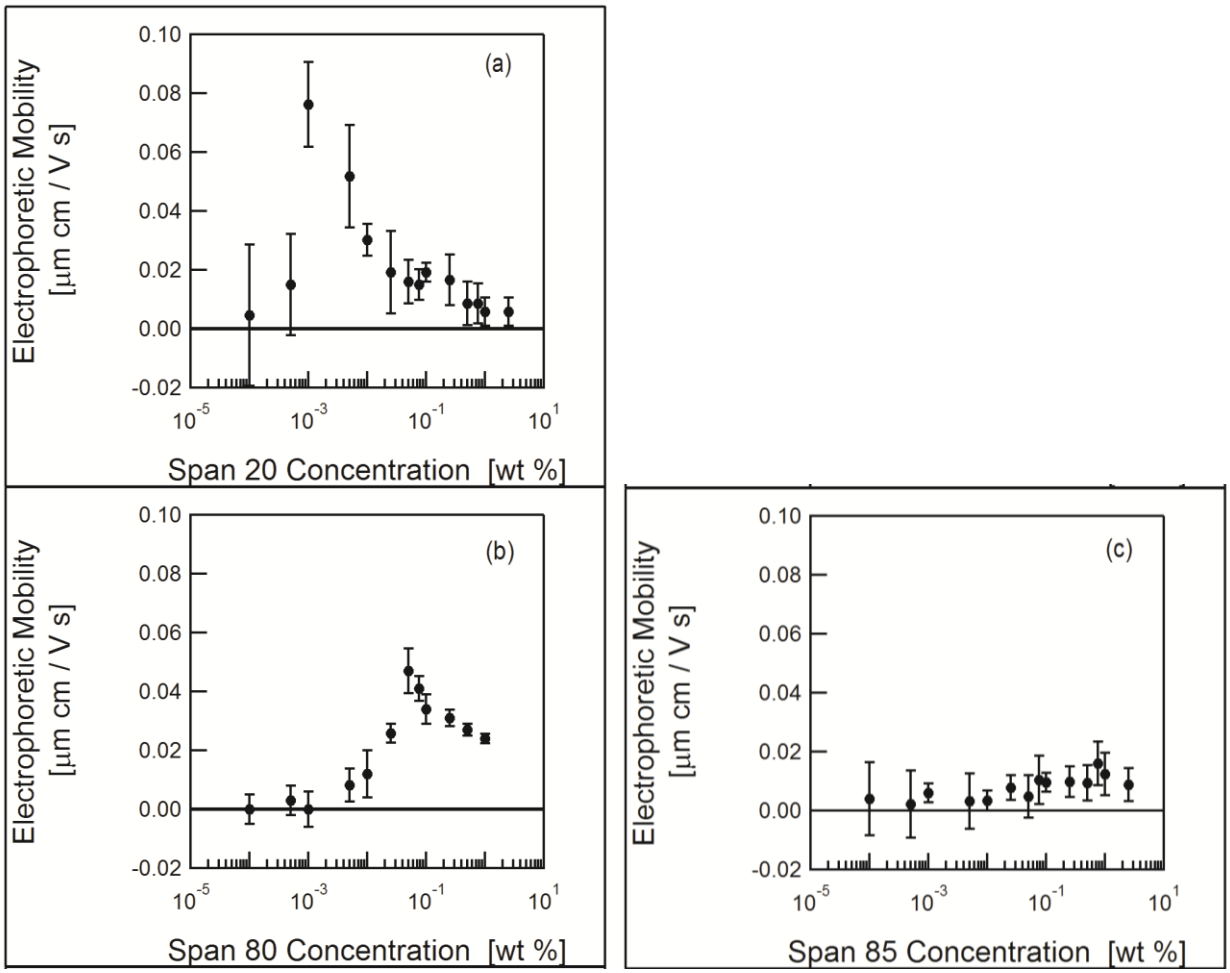

Figure 6.2. Magnesium oxide charging. Particle electrophoretic mobility of magnesium oxide dispersed in Isopar-L is plotted as a function of surfactant concentration for a) Span 20, b) Span 80, and c) Span 85. Error bars shown represent the uncertainty in the extrapolation of the electrophoretic mobility to zero applied electric field strength.

6.4.3. Effect of surfactant on mineral oxide charging

The final phase of this study is to compare the charging behavior of the mineral oxide series for the different Span surfactants. As shown in previous studies [5,6], the particle electrophoretic mobility is expected to vary as a function of the mineral oxide's aqueous point of zero charge (PZC). It is theorized that this is due to the charging mechanism being dominated by acid-base charge transfer between the surface functional groups and the polar head group of adsorbed surfactant molecules. This behavior is demonstrated in Figure 6.3, which shows the maximum electrophoretic mobility of the apolar dispersions as a function of the particle PZC.

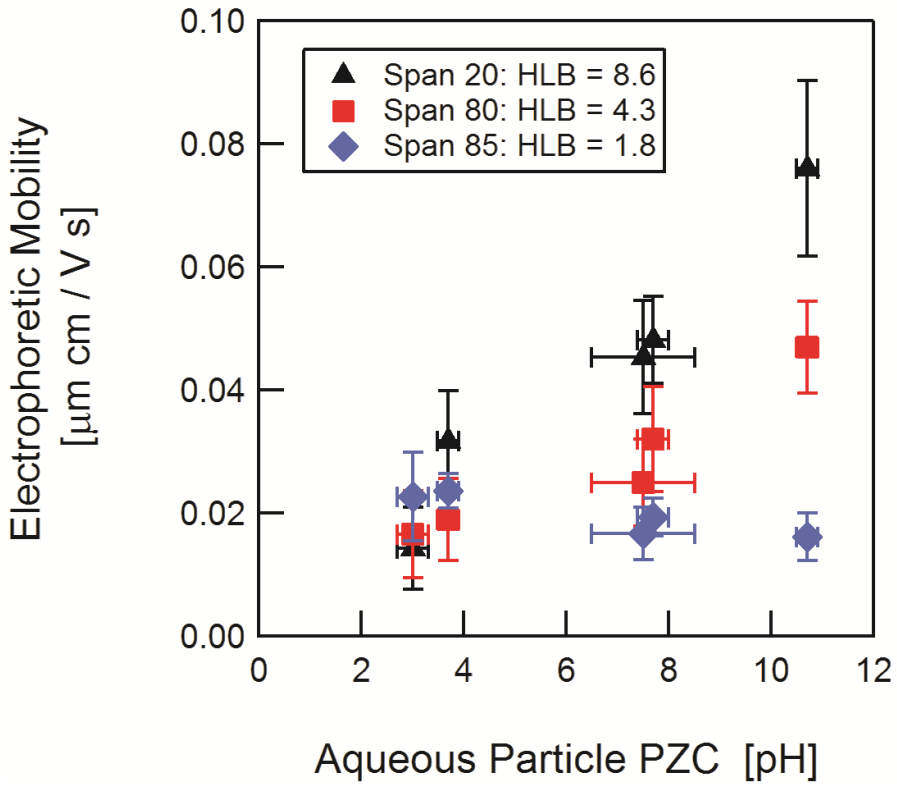

Figure 6.3. Effect of surfactant HLB on mineral oxide charging in apolar media. The maximum zero-field electrophoretic mobility of silica, titania, alumina, zinc oxide, and magnesia particles dispersed in Isopar-L are plotted against their aqueous PZCs. The particles were dispersed with Span 20 (▲), Span 80 (■), and Span 85 (♦).

All three surfactants charged the silica and titania particles minimally with maximum electrophoretic mobilities in the range of 0.014 – 0.032 μm-cm/V-s. Span 85 also charged alumina, zinc oxide, and magnesia in the same range. Span 80 charged alumina and zinc oxide marginally more than this. The largest charge for Span 80 occurred with the magnesia particles, exhibiting a maximum mobility of 0.047 ± 0.008 μm-cm/V-s. Span 20 exhibited even more maximum charging than Span 80. Aluimina and zinc oxide both had a maximum electrophoretic mobility of approximately 0.046 ± 0.009 μm-cm/V-s, and magnesia exhibited the largest maximum mobility in the study with a value of 0.076 ± 0.014 μm-cm/V-s.

6.4.4. Surfactant concentration impacts

It is important to keep in mind in the following analysis that the HLB value of a surfactant is not the direct cause of the observed charging behavior; it is an indicator of the size of the reverse micelles that are formed. In particular, a larger HLB value will logically produce reverse micelles that possess a larger polar core due to both a shift in the packing parameter of the surfactant as well as the amount of water that the surfactant introduces to the system. It has been previously shown that the size of the polar core has a direct impact on a reverse micelle's ability to house charge. According to the charge fluctuation model, the fraction of reverse micelles that obtain charge, χ, can be accurately predicted by Eq. (6.1), shown below [10].

$$\chi = 2\exp\left\{\frac{-1}{8\pi\varepsilon_0 kT}\left[\frac{e^2}{\varepsilon_{hc}a}+\frac{e^2}{\varepsilon_w}\left(\frac{1}{b}-\frac{1}{a}\right)\right]\right\} \tag{6.1}$$

Where ε_0 is the permittivity of free space, k is the Boltsmann constant, T is the absolute temperature, e is the elementary charge, ε_{hc} is the dielectric constant of the apolar medium, ε_w is the dielectric constant of the water filled reverse micelle core, a is the radius of the polar reverse micelle core, and b is the radius of the ion housed in the reverse micelle core. As equation (6.1) illustrates, the probability that a micelle becomes charged is related to the exponential of the

negative inverse of the micelle core radius. This means that as the micelle core becomes larger, the probability of that micelle housing a charge increases. This has been demonstrated by either swelling the cores with moisture [10,11,14] or changing the surfactant head group chemistry [9,12]. The conductivity results shown in Figure 6.1 provide further support for this theory. The CMCs for all three surfactants appear to be in the same range of 0.001 – 0.005 wt. % surfactant, and the conductivity of the solution is directly related to the surfactant HLB value above this concentration.

The main question at the heart of this study is whether or not this correlates to increased particle charging. Figure 6.2 highlights the complexity of answering this question. Span 85 has a low HLB value of only 1.8 and appears to produce reverse micelles that are unable to stabilize charge as well as the other surfactants. The result is a relatively modest amount of particle charge, with the maximum charge occurring at a rather large surfactant concentration of approximately 1 wt. %. The likely cause of this is that the small polar core of the Span 85 reverse micelles necessitates a large number of micelles be present in the system for particle charging to occur, and the lack of significant micelle-micelle charging minimizes the charge screening and neutralization that typically occurs at large surfactant concentrations. On the other end of the HLB spectrum lies Span 20 with a value of 8.6. For particles dispersed with Span 20 it was observed that the electrophoretic mobility exhibited a sharp rise at or near the CMC, followed by a relatively quick decrease in measured electrophoretic mobility at surfactant concentrations above this point. This behavior appears to be a result of the larger polar cores that are expected to form with this surfactant, causing the reverse micelles to readily exchange charge with the particle surface. At larger surfactant concentrations it is suspected that there is a significant amount of micelle-micelle charging that leads to a large degree of screening or neutralization of

the particle surface charge. A similar effect was observed in a previous study where OLOA 11000 micelles were swelled with water [14]. For the case of a water saturated system, where the reverse micelle cores were the largest, the particle electrophoretic mobility was the largest in a narrow surfactant concentration range right near the CMC. Dispersions prepared with Span 80 fell in between these two extremes. The particle electrophoretic mobility was seen to increase gradually above the CMC before reaching a maximum at approximately 0.05 to 0.1 wt. % surfactant. Above this concentration there was a moderate amount of charge screening as the electrophoretic mobility decreased with increasing surfactant concentration. In the case of Span 80 it appears that the reverse micelles with medium sized polar cores are capable of exchanging charge with the particle surface without having the same degree of charge screening observed with Span 20 at larger surfactant concentrations.

6.4.5. Effect of HLB on charging of mineral oxide series

The main purpose of this study is to determine if surfactant HLB value impacted the charging behavior of mineral oxides dispersed in an apolar medium. By plotting the apolar electrophoretic mobility against the particle aqueous PZC value, Figure 6.3, it is possible to evaluate a number of important characteristics. Firstly, the fact that the Span series of surfactants are acidic in nature is reinforced by the fact that all of the particles obtained a positive charge with all three surfactants used. Secondly, there was a linear correlation between the maximum apolar particle charge and the aqueous PZC, with the more basic particles achieving a larger surface charge for Span 20 and Span 80. This behavior is consistent with the acid-base charging mechanism that has been proposed previously. Finally, the slope of the mineral oxide charging vs aqueous PZC line directly correlated with the HLB value of the surfactant. This can be extended to a previous study conducted with Aerosol-OT (with an HLB of 10.2), where it was

found that the slope of the mineral oxide charging vs aqueous PZC line was even greater than the Span surfactants in this study. The logical indication is that the surfactant that forms reverse micelles most capable of stabilizing charge is best suited to stabilize a large amount of charge on a particle surface. Therefore, if the desire is to maximize particle surface charge, the ideal surfactant should be selected to have the proper acid-base characteristics and have a large HLB value. In the case of magnesia particles, for instance, the best Span surfactant for maximizing electrophoretic mobility is Span 20. However, as discussed previously, the maximum particle charge spans a narrow range of surfactant concentration, and there is a larger standard deviation in the surface charge. In addition, the maximum particle charge occurs at a small surfactant concentration where the total number of micelles present in the system is relatively small, meaning it may not be suitable for generating charge on dispersions containing a larger particle loading. With these factors in mind, in industrial applications one might describe Span 80 as the most robust surfactant for generating particle charge in apolar media. With its intermediate HLB value, Span 80 is capable of generating a significant amount of particle charge over a much larger range of surfactant concentrations because charge screening does not play as significant of a role. It appears that promoting particle charging while minimizing the effects of charge screening or neutralization is one of the primary obstacles for maximizing particle electrophoretic mobility in apolar systems.

6.5. Conclusions

This study examines the effects of surfactant HLB value on particle charging in apolar media. It has been previously determined that using a surfactant with a large HLB value dramatically increases the charging of reverse micelles, but it is unclear how it might affect particle charging in such systems. To examine this, the electrophoretic mobility of a series of

mineral oxides (silica, titania, alumina, zinc oxide, and magnesia) was measured for dispersions in Isopar-L using a series of Span surfactants (Span 20, Span 80, and Span 85) for charge stabilization. The following major effects were observed:

- There was a linear relationship between the particle's aqueous PZC and the maximum particle electrophoretic mobility, indicating an acid-base charge transfer is likely the mechanism for particle charge
- The maximum electrophoretic mobility of all particles scaled directly with the HLB value of the stabilizing surfactant.
- The surfactant concentration at which the maximum particle electrophoretic mobility occurs shifts as a function of the HLB value. The larger the surfactant HLB value, the smaller the surfactant concentration of the maximum particle charge.

The direct correlation between maximum particle electrophoretic mobility and surfactant HLB is thought to occur because the reverse micelles formed from large HLB surfactants have larger polar cores, making them more capable of housing the counter charges that are generated at the particle surface. However, reverse micelles with large polar cores are also capable of engaging in more micelle-micelle charging that can lead to increased screening or neutralization at larger surfactant concentrations, reducing the particle electrophoretic mobility. Therefore, when optimizing particle charge in apolar systems it is important to select a surfactant that has the appropriate acid-base characteristics as well as an appropriate HLB value.

6.6. Acknowledgement

This research was supported by the University of Washington Center for Surfaces, Polymers, and Colloids.

6.7. References

[1] Morrison, I.; *Colloids Surf., A* **1993**, *71*, 1-37.

[2] Pugh, R.J.; Matsunaga, T.; Fowkes, F.M.; *Colloids Surf.* **1983**, *7*, 183-207.

[3] Pugh, R.J.; Fowkes, F.M.; *Colloids Surf.* **1984**, *11*, 423-427.

[4] Poovarodom, S.; Berg, J.C.; *J. Colloid Interface Sci.* **2010**, *346*, 370-377.

[5] Gacek, M.; Brooks, G.; Berg, J.C.; *Langmuir* **2012**, *28*, 3032-3036.

[6] Gacek, M.M.; Berg, J.C.; *Langmuir* **2012**, *28*, 17841-17845.

[7] Gacek, M.M.; Berg, J.C.; *Electrophoresis* **2014**, *35*, 1766-1772.

[8] Guo, Q.; Lee, J.; Singh, V.; Behrens, S.H.; *J. Colloid Interf. Sci.* **2013**, *392*, 83-89.

[9] Parent, M.E.; Yang, J.; Jeon, Y.; Toney, M.F.; Zhou, Z.-L.; Henze, D.; *Langmuir* **2011**, *27*, 11845-11851.

[10] Michor, E.L.; Berg, J.C.; *Langmuir* **2012**, *28*, 15751-15755.

[11] Guo, Q.; Singh, V.; Behrens, S.H.; *Langmuir* **2010**, *26*, 3203-3207.

[12] Dukhin, A.S.; Goetz, P.J.; *J. Electroanal. Chem.* **2006**, *588*, 44-50.

[13] Kosmulski, M. Chemical properties of material surfaces. In Surfactant Science Series; Marcel Dekker: New York, **2001**; Vol. 102.

[14] Gacek, M.; Bergsman, D.; Michor, E.; Berg, J.C.; *Langmuir* **2012**, *28*, 11633-11638.

[15] Espinosa, C.E.; Behrens, S.H.; Guo, Q.; *Langmuir* **2010**, *26*, 16941-16948.

[16] Hsu, M.F.; Dufresne, E.R.; Weitz, D.A.; *Langmuir* **2005**, *21*, 4881-4887.

[17] Beunis, F.; Strubbe, F.; Karvar, M.; Drobchak, O.; Brans, T.; Neyts, K.; *Curr. Opin. Colloid In.* **2013**, *18*, 129-136.

[18] Karvar, M.; Strubbe, F.; Beunis, F.; Kemp, R.; Smith, A.; Goulding, M.; Neyts, K.; *Langmuir* **2011**, *27*, 10386-10391.

[19] Smith, P.J.; Patel, M.N.; Kim, J.; Milner, T.E.; Johnston, K.P.; *J. Phys. Chem. C* **2007**, *111*, 840-848.

Bibliography

Alexandridis, P.; Andersson, K.; J Phys Chem B 1997, 101, 8103–8111.

Arrhenius, S.Z.; Phys. Chem. 1887, 1, 631.

Ash, M.; Ash, I. Handbook of Green Chemicals (2nd Edition); Synapse Information Resources: Endicott, 2004.

ASTM D2896-11; Standard Test Method for Base Number of Petroleum Products by Potentiometric Perchloric Acid Titration, ASTM International; 2011. DOI: 10.1520/D2896-11

ASTM D664-11a; Standard Test Method for Acid Number of Petroleum Products by Potentiometric Titration, ASTM International; 2011. DOI: 10.1520/D0664-11A

Auroux, A.; Gervasini, A.; J. Phys. Chem. 1990, 94, 6371–6379.

Barz, D.P.J.; Vogel, M.J.; Steen, P.H.; Langmuir 2010, 26, 3126–3133.

Basch, A.; Horn, R.; Besenhard, J.O.; Colloids Surf. Physicochem. Eng. Asp. 2005, 253, 155–161.

Basu, S.; Colloid Polym. Sci. 1998, 276, 420–426.

Bazant, M.Z.; Squires, T.M.; Curr. Opin. Colloid Interface Sci. 2010, 15, 203–213.

Berg, J.C.; An introduction to interfaces & colloids: the bridge to nanoscience, World Scientific; 2010.

Berg, J.C.; Wettability, CRC Press; 1993.

Bert, T.; Beunis, F.; Smet, H.; Neyts, K.; Displays 2006, 27, 35–38.

Beunis, F.; Strubbe, F.; Karvar, M.; Drobchak, O.; Brans, T.; Neyts, K.; Curr. Opin. Colloid In. 2013, 18, 129-136.

Briscoe, W.H.; Horn, R.G.; Langmuir 2002, 18, 3945–3956.

Bronsted, J.N.; Recl. Trav. Chim. Pays-Bas 1923, 42, 718–728.

Cady, H.P.; Baldwin, E.J.; J. Am. Chem. Soc. 1921, 43, 646–651.

Cady, H.P.; Lichtenwalter, H.O.; J. Am. Chem. Soc. 1913, 35, 1434–1440.

Cao, H.Y.; Cheng, Y.J.; Huang, P.W.; Qi, M.; Nanotechnology 2011, 22, 445709.

Chen, Y.; Au, J.; Kazlas, P.; Ritenour, A.; Gates, H.; McCreary, M.; Nature 2003, 423, 136–136.

Comiskey, B.; Albert, J.D.; Yoshizawa, H.; Jacobsen, J. Nature 1998, 394, 253-255.

Delamar, M.; J. Electron Spectrosc. Relat. Phenom. 1990, 53, C11–C14.

Drago, R.; Wayland, B.; J. Am. Chem. Soc. 1965, 87, 3571.

Dukhin, A.; Goetz, P.; Colloids Surf., A 2005, 253, 51-64.

Dukhin, A.S.; Goetz, P.J. J. Electroanal. Chem. 2006, 588, 44-50.

Edwards, J.O.; J. Am. Chem. Soc. 1954, 76, 1540–1547.

Eicke, H.-F.; Christen, H.; Helv. Chim. Acta 1978, 61, 2258–2263.

Eicke, H.-F.; Top. Curr. Chem. 1980, 87, 85–145.

Espinosa, C.E.; Behrens, S.H.; Guo, Q. Langmuir, 2010, 26, 16941-16948.

Fowkes, F. M. et al. Acid-base complexes of polymers. POL J. Polym. Sci. Polym. Chem. Ed. 22, 547–566 (1984).

Fowkes, F.M.; Pugh, R.J.; ACS Symp. Ser. 1984, 240, 331-354.

Gacek, M.; Bergsman, D.; Michor, E.; Berg, J.C. Langmuir 2012, 28, 11633-11638.

Gacek, M.; Brooks, G.; Berg, J.C. Langmuir 2012, 28, 3032-3036.

Gacek, M.M.; Berg, J.C.; Electrophor. 2014, 35, 1766–1772.

Gacek, M.M.; Berg, J.C.; J. Colloid Interface Sci. 2014. doi: http://dx.doi.org/10.1016/j.jcis.2014.11.075

Gacek, M.M.; Berg, J.C.; Langmuir 2012, 28, 17841-17845.

Guo, Q.; Lee, J.; Singh, V.; Behrens, S.H.; J. Colloid Interf. Sci. 2013, 392, 83-89.

Guo, Q.; Singh, V.; Behrens, S.H.; Langmuir 2010, 26, 3203-3207.

Gutmann, V.; Steining, A.; Wychera, E.; Monatshefte Chem. Verwandte Teile Anderer Wiss. 1966, 97, 460.

Gutmann, V.; The donor-acceptor approach to molecular interactions, Plenum Press; 1978.

Hall, D.G.; J. Phys. Chem. 1990, 94, 429-430.

Herbst, W.; Hunger, K.; Industrial Organic Pigments, Wiley-VCH, Weinheim 2004.

Hsu, M.F.; Dufresne, E.R.; Weitz, D.A. Langmuir 2005, 21, 4881-4887.

Jensen, W.B.; The Lewis acid-base concepts: an overview, Wiley; 1979.

Jeon, Y.; Kornilovitch, P.; Beck, P.; Zhou, Z.L.; Henze, R.; Koch, T.; J. Soc. Inf. Disp. 2011, 19, 614–619.

Jones, S.A.; Martin, G.P.; Brown, M.B. J. Pharm. Sci. 2006, 95, 1060-1074.

Kahlenberg, L.; Ruhoff, O.E.; J. Phys. Chem. 1902, 7, 254–258.

Karvar, M.; Strubbe, F.; Beunis, F.; Kemp, R.; Smith, A.; Goulding, M.; Neyts, K.; Langmuir 2011, 27, 10386-10391.

Keir, R.; Quinn, A.; Jenkins, P.; Thomas, J.C.; Ivanova, O.; J. Imaging Sci. Technol. 2000, 44, 528–533.

Keir, R.; Suparno; Thomas, J.C.; Langmuir 2002, 18, 1463–1465.

Kemp, R.; Sanchez, R.; Mutch, K.J.; Bartlett, P.; Langmuir 2010, 26, 6967–6976.

Kim, J.; Anderson, J.L.; Garoff, S.; Schlangen, L.J.M.; Langmuir 2005, 21, 8620–8629.

Kitahara, A. Nonaqueous Systems. In Surfactant Science Series, Marcel Dekker: New York; 1998; p. 135-150.

Kitahara, A.; Amano, M.; Kawasaki, S.; Kon-no, K. Colloid Polym. Sci. 1977, 255, 1118-1121.

Kitahara, A.; Satoh, T.; Kawasaki, S.; Kon-no, K. J. Colloid Interface Sci. 1982, 86(1), 105-110.

Klinkenberg, A.; van der Minne, J.L.; Electrostatics in the petroleum industry: the prevention of explosion hazards; a Royal Dutch/Shell research and development report, Elsevier; 1958.

Koelmans, H.; Overbeek, J.T.G. Discuss. Faraday Soc. 1954, 18, 52-63.

Kornilovitch, P.; Jeon, Y.; J. Appl. Phys. 2011, 109, 064509.

Kosmulski, M. Chemical properties of material surfaces. In Surfactant Science Series, Vol. 102; Marcel Dekker: New York, 2001.

Kosmulski, M.; Colloids Surf. Physicochem. Eng. Asp. 1999, 159, 277–281.

Kosmulski, M.; Electrical Interfacial Layer in Nonaqueous Solvents, Surfactant Sci. Ser.; 2000.

Kosmulski, M.; J. Colloid Interface Sci. 2011, 353, 1–15.

Kotlarchyk, M.; Huang, J.S.; Chen, S.-H. J. Phys. Chem. 1985, 89, 4382-4386.

Kreuzer, H.J.; Wang, R.L.C.; Grunze, M.; J. Am. Chem. Soc. 2003, 125, 8384–8389.

Kwok, D.Y.; Colloids Surf. Physicochem. Eng. Asp. 1999, 156, 191–200.

Labib, M.E. Colloids Surf. 1988, 29, 293-304.

Labib, M.E.; Williams, R.; Colloid Polym. Sci. 1986, 264, 533-541.

Labib, M.E.; Williams, R.; J. Colloid Interface Sci. 2984, 97, 356–357.

Leunissen, M.E.; van Blaaderen, A.; Hollingsworth, A.D.; Sullivan, M.T.; Chaikin, P.M.; Proc. Natl. Acad. Sci. U.S.A. 2007, 104, 2585–2590.

Lewis, G.N.; Valence and the structure of atoms and molecules, The Chemical Catalog Company, Inc.; 1923.

Lewis, K.E.; Parfitt, G.D.; Trans. Faraday Soc. 1966, 62, 1652–1661.

Lowry, T.M.; J. Soc. Chem. Ind. 1923, 42, 43–47.

Lyklema, J.; Adv. Colloid Interface Sci. 1968, 2, 67–114.

Lyklema, J.; Fundamental of Interface and Colloid Science IV. Particulate Colloids, Elsevier; 2005.

Lyklema, J.; Fundamentals of Interface and Colloid Science.: Volume II: Solid-Liquid Interfaces, Academic Press; 1995.

Malbrel, C.; Somasundaran, P.; J. Colloid Interface Sci. 1989, 133, 404–408.

Malbrel, C.; Somasundaran, P.; Langmuir 1992, 8, 1285–1290.

Marinova, K.G.; Alargova, R.G.; Denkov, N.D.; Velev, O.D.; Petsev, D.N.; Ivanov, I.B.; Borwankar, R.P.; Langmuir 1996, 12, 2045–2051.

Mayer, U.; Gutmann, V.; Gerger, W.; Monatshefte Chem. 1975, 106, 1235–1257.

McGown, D.N.L.; Parfitt, G.D.; Willis, E.; J. Colloid Sci. 1965, 20, 650–664.

Michor, E.L.; Berg, J.C.; Langmuir 2012, 28, 15751-15755.

Morrison, I.D.; Colloids Surf., A 1993, 71, 1-37.

Morrison, I.D.; Langmuir 1991, 7, 192–1922.

Mulliken, R.; J. Phys. Chem. 1952, 56, 801–822.

Mullins, W.; Averbach, B.; Surf. Sci. 1988, 206, 41–51.

Murau, P.; Singer, B.; J. Appl. Phys. 1978, 49, 4820–4829.

Mysko, D.D.; Berg, J.C.; Ind. Eng. Chem. Res. 1993, 32, 854–858.

Ohshima, H.; Furusawa, K.; Electrical phenomena at interfaces: fundamentals, measurements, and applications, M. Dekker; 1998.

Parent, M.E.; Yang, J.; Jeon, Y.; Toney, M.F.; Zhou, Z.L.; Henze, D.; Langmuir 2011, 27, 11845-11851.

Parfitt, G. D.; Peacock, J. Stability of Colloidal Dispersions in Nonaqueous Media. In Surface and Colloid Science: Volume 10.; Matijevic, E., Ed.; Surface and Colloid Science; Plenum Press: New York, 1978; pp 163-226.

Parsegian, A.; Nature 1969, 221, 844-846.

Patel, M.N.; Smith, P.G.; Kim, J.; Milner, T.E.; Johnston, K.P.; J. Colloid Interface Sci. 2010, 345, 194–199.

Pearson, R.G.; Hard and soft acids and bases, Dowden, Hutchinson & Ross; 1973.

Pontiga, F.; Castellanos, A.; IEEE Trans. Ind. Appl. 1996, 32, 816–824.

Poovarodom, S.; Berg, J.C.; J. Colloid Interface Sci. 2010, 346, 370–377.

Poovarodom, S.; Berg, J.C.; J. Colloid Interface Sci. 2011, 351, 415–420.

Prieve, D.C.; Hoggard, J.D.; Fu, R.; Sides, P.J.; Bethea, R.; Langmuir 2008, 24, 1120-1132

Pugh, R.J.; Fowkes, F.M.; Colloids Surf. 1984, 11, 423–427.

Pugh, R.J.; Fowkes, F.M.; Colloids Surf. 1984, 9, 33-46.

Pugh, R.J.; Matsunaga, T.; Fowkes, F.M.; Colloids Surf. 1983, 7, 183–207.

Riddle, F.L.; Fowkes, F.M.; J. Am. Chem. Soc. 1990, 112, 3259–3264.

Roberts, G.S.; Sanchez, R.; Kemp, R.; Wood, T.; Barlett, P.; Langmuir 2008, 24, 6530–6541.

Rossotti, F.J.C.; Rossotti, H.; The determination of stability constants: and other equilibrium constants in solution. McGraw-Hill; 1961.

Ruckenstein, E.; Nagarajan, R.; J. Phys. Chem. 1980, 84, 1349–1358.

Sainis, S.K.; Germain, V.; Mejean, C.O.; Dufresne, E.R.; Langmuir 2008, 24, 1160–1164.

Sainis, S.K.; Merrill, J.W.; Dufresne, E.R.; Langmuir 2008, 24, 13334–13337.

Shen, Y.; Duhamel, J.; Langmuir 2008, 24, 10665-10673.

Shrestha, L.K.; Sato, T.; Aramaki, K.; Langmuir 2007, 23, 6606–6613.

Siffert, B.; Eleli-Letsango, J.; Jada, A.; Papirer, E.; Colloids Surf. Physicochem. Eng. Asp. 1994, 92, 107.

Sinnokrot, M.O.; Sherrill, C.D.; J. Phys. Chem. A 2006, 110 (37), 10656-10668.

Smith, G.N.; Eastoe, J.; Phys. Chem. Chem. Phys. 2013, 15, 424-439.

Smith, P.G.; Patel, M.N.; Kim, J.; Milner, T.E.; Johnston, K.P.; J. Phys. Chem. C 2007, 111, 840–848.

Smythe, W.R. Static and Dynamic Electricity, 3rd Edition; McGraw-Hill: New York, 1967; 27-30.

Strubbe, F.; Beunis, F.; Marescaux, M.; Neyts, K.; Phys. Rev. E 2007, 75, 031405.

Strubbe, F.; Verschueren, A.R.M.; Schlangen, L.J.M.; Beunis, F.; Neyts, K.; J. Colloid Interface Sci. 2006, 300, 396–403.

Sun, C.; Berg, J.C.; Adv. Colloid Interface Sci. 2003, 105, 151–175.

Sun, C.; Berg, J.C.; J. Chromatogr. A 2002, 969, 59-72.

Vacha, R.; Zangi, R.; Engberts, J.B.F.N.; Jungwirth, P.; J. Phys. Chem. C 2008, 112, 7689–7692.

Van der Minne, J.L.; Hermanie, P.H.J. J. Colloid Sci. 1952, 7, 600-615.

Van der Minne, J.L.; Hermanie, P.H.J. J. Colloid Sci. 1953, 8, 38-52.

Vanoss, C.; Chaudhury, M.; Good, R.; Adv. Colloid Interface Sci. 1987, 28, 35–64.

Verwey, E.J.W.; Recl. Trav. Chim. Pays-Bas 1941, 60, 625–633.

Watts, J.; Chehimi, M.; J. Adhes. 1993, 41, 81–91.

Wines, T.H.; Dukhin, A.S.; Somasundaran, P.; J. Colloid Interface Sci. 1999, 216 (2), 303-308.